NITROUS OXIDE PRODUCTION AND CONSUMPTION IN SEAWATER

by

Stephen Punshon

Submitted in partial fulfillment of the requirements
for the degree of Doctor of Philosophy

at

Dalhousie University
Halifax, Nova Scotia
April, 2004

Your file Votre référence
ISBN: 0-612-89813-X
Our file Notre référence
ISBN: 0-612-89813-X

DALHOUSIE UNIVERSITY

To comply with the Canadian Privacy Act the National Library of Canada has requested that the following pages be removed from this copy of the thesis:

Preliminary Pages

Examiners Signature Page (pii)

Dalhousie Library Copyright Agreement (piii)

Appendices

Copyright Releases (if applicable)

To Liz, Cathy and Lois

And in memory of

Josephine Punshon

Table of Contents

List of Figures

List of Tables

Abstract

Nitrous oxide (N_2O) is a biogenic trace gas that contributes to climate warming and stratospheric ozone destruction. The coastal ocean is a globally important source of N_2O, the magnitude of which could potentially be affected by human influence. Nitrification is known to yield N_2O as a by-product, and denitrification can act as both a source and sink for N_2O, yet the relative importance of these microbial pathways remains poorly understood. This study seeks to resolve the role of these processes in coastal marine N_2O production and consumption, particularly in response to changes in oxygen concentration.

A stable isotope technique was developed for measuring N_2O production and consumption rates in seawater. Samples were incubated with the appropriate ^{15}N-labelled substrate ($^{15}NH_4^+$, $^{15}NO_3^-$ and $^{15}N_2O$), and the concentration of $^{15}N_2O$ was monitored by purge-and-trap gas-chromatography/mass-spectrometry. A novel internal standard ($^{15}N_2{}^{18}O$) was employed to maintain a high level of analytical precision. Some trial measurements were made in the Labrador Sea during the spring bloom. This region was found to be slightly supersaturated in N_2O at the time of the study (mean: 105%) with nitrification a contributing factor

An 18 month long study of the Bedford Basin, Halifax Harbour, showed that nitrification was the predominant N_2O production mechanism, with rates ranging from undetectable up to 1.6 nmol N_2O L^{-1} d^{-1} (about 8% d^{-1}). The yield of N_2O from ammonium oxidation (mol N_2O:mol NH_4^+) displayed an inverse non-linear relationship with dissolved oxygen, varying from 0.01–0.11% over the range 27-290 μmol O_2 L^{-1}. N_2O production from denitrification (range 20-40 pmols N_2O L^{-1} d^{-1}) was detectable on only two occasions coinciding with oxygen minima, and N_2O loss was only observed at an oxygen level of 2.5 μmol O_2 L^{-1}. These measurements were supplemented by a series of laboratory experiments investigating denitrification processes. Net $^{15}N_2O$ production from nitrate reduction was restricted to ~ 7 – 3 μmol O_2 L^{-1}. Consumption predominated at lower oxygen concentrations, resulting in net N_2O loss rates of up to 10% d^{-1}. These findings suggest that the increasing incidence of eutrophication, and oxygen depletion, in the coastal margin may have important implications for N_2O cycling.

List of Abbreviations and Symbols Used

μ	kinematic viscosity
σ	standard deviation
μg	microgram (1μg = 10^{-6} gram)
μL	microlitre (1μL = 10^{-6} litre)
μm	micrometre (1μm = 10^{-6} metre)
μmol	micromole (1 μmol = 10^{-6} mole)
AOU	apparent oxygen utilisation
atm	atmosphere (1 atmosphere = 760 Torrs)
AVHRR	advanced very high resolution radiometer
C	carbon
C_a	concentration in air
CCG	Canadian Coast Guard
cm	centimetres (1 cm = 10^{-2} metres)
CTD	conductivity, temperature and depth
C_w	concentration in water
d	day
D	diffusion coefficient
ECD	electron capture detector
EI	electron ionisation
eq	equilibrium
F	flux
F	solubility coefficient

g	gram
GC	gas chromatography
GWP	global warming potential
h	hour
i.d.	inside diameter
K	temperature in kelvins
kg	kilogram
kJ	kilojoules
K_s	half-saturation constant
k_w	transfer velocity (cm h^{-1})
L	litre (1L = $1dm^3$)
m	metre
m/z	mass to charge ratio
mbar	millibar (1 mbar = 10^{-3} bars)
min	minute
mL	millilitre (1mL = 10^{-3} litres)
MS	mass spectrometry
N	nitrogen
N_2O	nitrous oxide
NOAA	National Oceanic and Atmospheric Administration
o.d.	outside diameter
PLOT	porous layer open tube
pmol	picomole (1pmol =10^{12} moles)

ppbv	parts per billion by volume (10^{-9})
ppmv	parts per million by volume (10^{-6})
PVC	poly vinyl chloride
RSD	relative standard deviation $(100 \cdot \sigma/\bar{x})$
S	salinity (parts per thousand, ‰)
s	second
sat	saturation
Sc	Schmidt number
SST	sea surface temperature
T	temperature in degrees Celsius
TCD	thermal conductivity detector
Tg	tera gram (1 Tg = 10^{12} grams)
U	windspeed
u	windspeed at 10 metres altitude
UHP	ultra high purity (99.999%)
UV	ultra violet
y	year

Acknowledgements

I wish to thank Robert Moore for his thoughtful supervision and support. I am also grateful to my other committee members for their helpful advice and comments, and to Ryszard Tokarczyk for his technical assistance. Many thanks are also due to: John Batt and the Aquatron staff for their co-operation; Paul Dickie and Bill Li for providing CTD data; Lloyd Baker for his stoical help with sampling in the Bedford Basin; Glen Harrison and other scientists and staff aboard the CCGS *Hudson*. I am indebted to Claire Hughes for the many light-hearted moments shared over cups of tea.

This work was funded by a grant from the Canadian Foundation for Climate and Atmospheric Sciences, and by an Izaak Walton Killam Memorial Scholarship and a Dalhousie University Graduate Scholarship.

Finally, very special thanks are due to Liz for her encouragement and unwavering confidence in me.

Chapter 1

Introduction

1.1. Atmospheric nitrous oxide

Nitrous oxide (N_2O) is the second most abundant atmospheric nitrogen compound after dinitrogen. The atmospheric mixing ratio of N_2O has increased dramatically over the last ~100 years (Figure 1.1), from a pre-industrial level of around 285 ppbv (10^{-9}), inferred from ice core and firn ice data (Khalil and Rasmussen, 1992; Dibb *et al.*, 1993; Machida *et al.*, 1995; Battle *et al.*, 1996; Khalil *et al.*, 2002), to a 1996 average of 314 ppbv in the Northern Hemisphere (Khalil *et al.*, 2002). This latter value is unprecedented in ice core data spanning the last ~ 45,000 years (Leuenberger and Siegenthaler, 1992). The annual rate of increase of atmospheric nitrous oxide from 1981 to 1996 was in the range 0.2 – 0.3% or about 0.7 ppbv (Khalil and Rasmussen, 1992, Khalil *et al.*, 2002) corresponding to about 3.9 Tg N_2O y^{-1}. If this trend continues, atmospheric levels of N_2O are expected to exceed 480 ppbv by the year 2100, 70% higher than pre-industrial levels (Kroeze, 1994; Nevison and Holland, 1997). The low reactivity of N_2O in the troposphere results in a relatively long atmospheric lifetime estimated at about 120 years (Prather *et al.*, 1995). As a result, tropospheric N_2O is well-mixed, although there is a small interhemispheric concentration gradient, with about 0.7 ppbv more in the Northern Hemisphere (Khalil *et al.*, 2002).

The increasing tropospheric abundance of N_2O presents a cause for concern as it can potentially affect the Earth's climate in two ways. First, N_2O is classified as a radiatively-

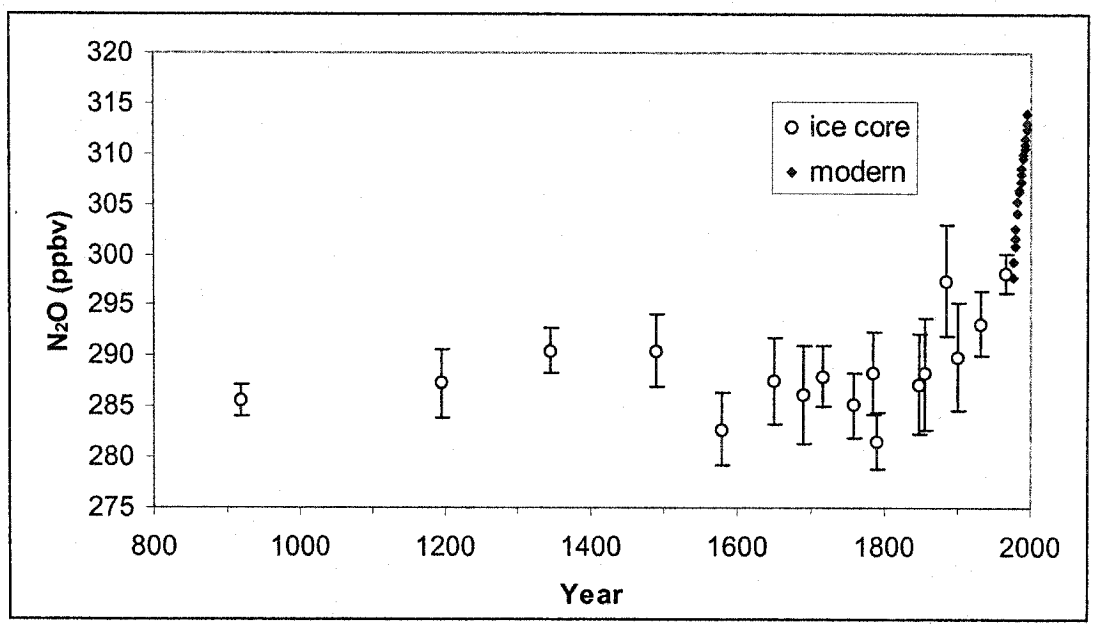

Figure 1.1. Atmospheric nitrous oxide mixing ratios derived from ice cores and modern atmospheric measurements, redrawn from data collated and smoothed by Khalil *et al.*, 2002. The ice core data points represent 10 point averages of data collected by Etheridge *et al.*, (1988), Khalil and Rasmussen, (1988), Zardini *et al.*, (1989), Leuenberger and Siegenthaler, (1992), Machida *et al.*, (1995), Battle *et al.*, (1996) and Flückiger *et al.*, (1999). Error bars represent 90% confidence intervals. The modern measurements are from the studies of Khalil and Rasmussen, (1988) and Khalil *et al.*, (2002), extending from 1976-1996.

active, or "greenhouse" gas because it absorbs and re-radiates energy in the infrared spectrum. An increase in its atmospheric concentration therefore perturbs the balance between incoming radiation from the sun, and outgoing radiation reflected or re-emitted from the Earth. Nitrous oxide is a potent greenhouse gas, currently accounting for 5–6% of the change in the average net radiation at the tropopause (radiative forcing) caused by the total greenhouse gas effect (Lashof and Ahuja, 1990). The concept of Global Warming Potential (GWP) was introduced to assess the future contribution to global warming from present day emissions (IPPC, 1990). Global Warming Potential is defined as: "The cumulative radiative forcing between the present and some chosen later time horizon caused by a unit mass of gas emitted now, expressed relative to that of some reference gas." This term is not necessarily a precise scale as it may encompass some terms which are uncertain, such as atmospheric lifetime and radiative properties. Nonetheless, N_2O has been assigned a GWP of 296 relative to CO_2 on a molecule per molecule basis (IPCC, 2001) This number reflects the long atmospheric half-life of N_2O, implying that effects on the climate caused by present day emissions may persist for many decades, even if those emissions are reduced or curtailed in the near future.

The second way in which N_2O may affect the climate is by exerting a control on stratospheric ozone, also a greenhouse gas. Not only does stratospheric ozone directly influence radiative forcing through the regulation of infrared radiation (Solomon and Srinivasan, 1995), it is also an important control on the level of ultraviolet radiation reaching the troposphere. In the stratosphere, N_2O is susceptible to photo-dissociation by UV radiation. This reaction constitutes the major global sink for this compound.

(R1) $$N_2O + h\nu \rightarrow N_2 + 1/2O_2$$

Smaller amounts are removed by reaction with electronically excited oxygen atoms ($O(^1D)$) produced by ozone photolysis.

(R2) $O_3 + h\nu \rightarrow O_2 + O(^1D)$

(R3) $N_2O + O(^1D) \rightarrow N_2 + O_2$ (42%)

(R4) $N_2O + O(^1D) \rightarrow NO + NO$ (58%)

The latter pathway is the chief source of stratospheric NO*x* (NO and NO_2) implicated in ozone destruction (McElroy and McConnell, 1971).

(R5) $NO + O_3 \rightarrow NO_2 + O_2$

(R6) $NO_2 + O(^1D) \rightarrow NO + O_2$

1.2. Sources of N_2O to the atmosphere

While the increase in atmospheric N_2O over the last ~30 years is well documented by direct measurements, it has proven more difficult to account for the imbalance in N_2O sources and sinks that has given rise to this phenomenon. The strength of the stratospheric N_2O sink is presumed not to change over human timescales. Likewise, too little is known of "natural" terrestrial and ocean sources to assume anything other than a steady state over decadal time scales. Up to the late 1980's, industrial fossil fuel combustion was thought to be the major anthropogenic source of N_2O, conveniently balancing the N_2O budget and explaining the similarity in trends shown by levels of atmospheric CO_2 and N_2O since the industrial revolution. However it was later discovered that most of the N_2O found in industrial flue gases was an artifact of the flask sampling method in use at that time (Muzio and Kramlich, 1988; Muzio *et al.*, 1989),

overestimating the fossil fuel source by an order of magnitude. This interesting revelation demanded a complete re-evaluation of N_2O sources, and by the mid 1990's, the perceived budget gap was balanced by a range of minor anthropogenic sources including fossil fuel and biomass burning, industrial adipic acid production for nylon manufacture and emissions resulting from farming practices and other anthropogenic effects on microbial cycles. These sources total about 4.3 Tg N yr^{-1} (Table 1), but the uncertainties are generally very high or unknown.

More recently it has been suggested that most of the observed atmospheric increase of N_2O can be explained by a terrestrial source of about 3.5 Tg N yr^{-1} associated with anthropogenic nitrogen fixation, principally through the use of artificial fertilisers (Nevison and Holland, 1997). The development of the Haber process and subsequent widespread introduction of nitrogen fertilisers during the 20th Century has resulted in severe anthropogenic influence on the global nitrogen cycle. The rate of anthropogenic nitrogen fixation (~140 Tg N yr^{-1}) now rivals or exceeds the estimated 90-130 Tg N yr^{-1} fixed by terrestrial plants (Galloway *et al.*, 1995). This scale of human intervention in global biogeochemical cycles has prompted the use of the term *Anthropocene* in reference to the present geological era (Crutzen and Ramanathan, 2000; Falkowski *et al.*, 2000; Codispoti *et al.*, 2001). Future growth in the rate of anthropogenic N fixation seems certain, as crop production will need to keep pace with the expected doubling of the global population to around 12 billion by the year 2050 (Pimentel *et al.*, 1994).

Source	Annual emission	Range
	Anthropogenic sources	
Biomass burning [a]	0.2	0.1 – 0.3
Nylon manufacture [b]	0.3	0.2 – 0.4
Nitrogen fertiliser [c]	1.0	Not known
Sewage [d]	0.1	Not known
Cattle/agriculture [e]	0.3	0.2 – 0.7
Aquifers/irrigation [f]	0.8	0.5 – 1.1
Fossil fuel [g]	0.7	0.3 – 0.9
Global warming [d]	0.4	Not known
Fuelwood burning [h]	0.1	0 – 0.5
Land use change [b]	0.4	Not known
Total	**4.3**	**3.2 – 5.8**
	Natural sources	
Soils under natural vegetation [b]	7.0	6.6 – 7.0
Ocean [j]	4.0	1.2 – 6.8
Total	**11.0**	**7.8 – 13.8**

[a] *Crutzen and Andreae* (1990)
[b] *Bouwman et al.*, (1995)
[c] *Bouwman* (1994)
[d] *Kroeze* (1994)
[e] *Khalil and Rasmussen* (1992)
[f] *Ronen et al.* (1988)
[g] *Houghton et al.* (1992)
[h] *De Vries et al.* (1994)
[j] *Nevison et al.*, (1995)

Table 1.1 Natural and Anthropogenic Sources of N_2O (Tg N yr^{-1})

1.3. The ocean

The ocean provides a natural source of N_2O estimated at about 4 ± 2.8 Tg N yr^{-1} (Nevison *et al.*, 1995). The surface ocean is mostly close to atmospheric equilibrium with a global mean saturation of 103% (Butler *et al.*, 1989), but much higher levels can be found in nutrient-rich regions of high productivity. For example, a maximum surface saturation of 8,250% was found in the western Indian continental shelf (Naqvi *et al.*, 2000). Bange *et al.*, (1996a) examined N_2O data from coastal seas including upwelling and estuarine waters and concluded that these regions, although occupying only about 18% of the total ocean area, contributed more than half the total ocean/air flux.

Two lines of evidence also suggest that the coastal margin is likely to become an increasingly important source of N_2O to the atmosphere. First, N_2O emissions from estuaries are apparently related to nitrogen loading (Seitzinger and Kroeze, 1998). A substantial proportion of industrially-fixed nitrogen ultimately enters the sea via land run-off, aerial deposition, groundwater and human waste discharges, causing hypereutrophication of coastal waters surrounding populated regions (Howarth *et al.*, 1996; Kennish, 1997; Livingston, 2001), and the amount of fixed nitrogen transported annually from land to the coastal ocean is forecast to double over the next fifty years (Kroeze and Seitzinger, 1998). Second, N_2O production appears to be enhanced at low oxygen concentrations (de Bie *et al.*, 2002), and oxygen depletion in sub-surface water is symptomatic of eutrophication in coastal regions (Livingston, 2001). The further development or intensification of shelf hypoxia through increasing nutrient run-off may therefore lead to a syzygial increase in marine N_2O emissions (Naqvi *et al.*, 2000). In order to predict the effects of such large-scale nitrogen cycle perturbation on coastal N_2O

emissions, a clear understanding of N_2O production and consumption mechanisms and their sensitivity to environmental factors, particularly substrate availability and dissolved oxygen, is required.

1.4. Production and consumption pathways for N_2O in the water column

Two microbial pathways identified as being important sources of marine N_2O are: (1) the first stage of nitrification i.e. the oxidation of ammonium to nitrite, in which N_2O is emitted as a by-product, and (2) denitrification, the anaerobic sequential reduction pathway of nitrate to nitrogen gas in which N_2O is an intermediate. These processes may also be coupled by the transfer of common intermediates e.g. nitric oxide (NO) and nitrite (NO_2^-) across oxic/suboxic boundaries (Naqvi and Noronha, 1991; Yoshinari *et al.*, 1997). In addition to these established pathways, it has also been speculated that assimilative nitrate reduction by phytoplankton may produce N_2O, thus explaining unusual patterns of distribution in the euphotic zone (Elkins *et al.*, 1978; Pierotti and Rasmussen, 1980; Oudot *et al.*, 1990). The production of N_2O by this process remains to be demonstrated. Aqueous N_2O can also be consumed by bacteria. Several studies have found undersaturated levels of N_2O in anoxic zones coinciding with evidence of denitrification (e.g. Cohen and Gordon, 1978; Elkins *et al.*, 1978) where N_2O is presumably being reduced to dinitrogen. N_2O may also be reduced to N_2 in the process of nitrogen fixation as it is a substrate for nitrogenase-catalysed reduction (Rivera-Ortiz and Burris, 1975; Jensen and Burris, 1986). This pathway is probably of little importance as not only is the abundance of dissolved N_2O in the surface ocean a great deal lower than N_2, but the affinity of nitrogenase for N_2O is around 1000 times less than for dinitrogen (Rivera-Ortiz and Burris, 1975). This study therefore focuses on the well-

established aquatic sources and sink for N_2O, nitrification and denitrification. Figure 1.2 summarises the major pathways of nitrogen cycling in the perturbed coastal margin, and their relevance to nitrous oxide production and consumption.

1.5. Nitrification

Nitrification refers to the microbial oxidation of ammonium to nitrate. For a comprehensive review of marine nitrification see Ward (2000). This two-stage process provides an energy source for two functionally distinct groups of chemolithotrophic bacteria that are capable of converting carbon dioxide to organic carbon. In the first stage, ammonium is oxidised to nitrite via the intermediate hydroxylamine (NH_2OH) chiefly by *Nitrosomonas* and *Nitrosococcus* species.

(R7) $$NH_4^+ + 1/2O_2 \rightarrow NH_2OH + H^+$$

The oxidation of hydroxylamine proceeds via an enzyme-bound [HNO] intermediate

(R8) $$NH_2OH \rightarrow [HNO] + 2e^- + 2H^+$$

(R9) $$[HNO] + 2e^- + 2H^+ + O_2 \rightarrow NO_2^- + H^+ + H_2O$$

In the second stage, nitrite is oxidised to nitrate by *Nitrobacter* and *Nitrococcus* species.

(R10) $$NO_2^- + 1/2O_2 \rightarrow NO_3^-$$

It is the first step of nitrification that is relevant to this study, as nitrous oxide is released as a by-product. The exact biochemical pathway of N_2O formation has yet to be clarified, but the reduction of hydroxylamine has been proposed as a likely mechanism (Kim and Craig, 1990; Ostrom *et al.*, 2000). However it has also been noted that nitric oxide (NO) concentration maxima coincide with those of N_2O in suboxic regions (Ward

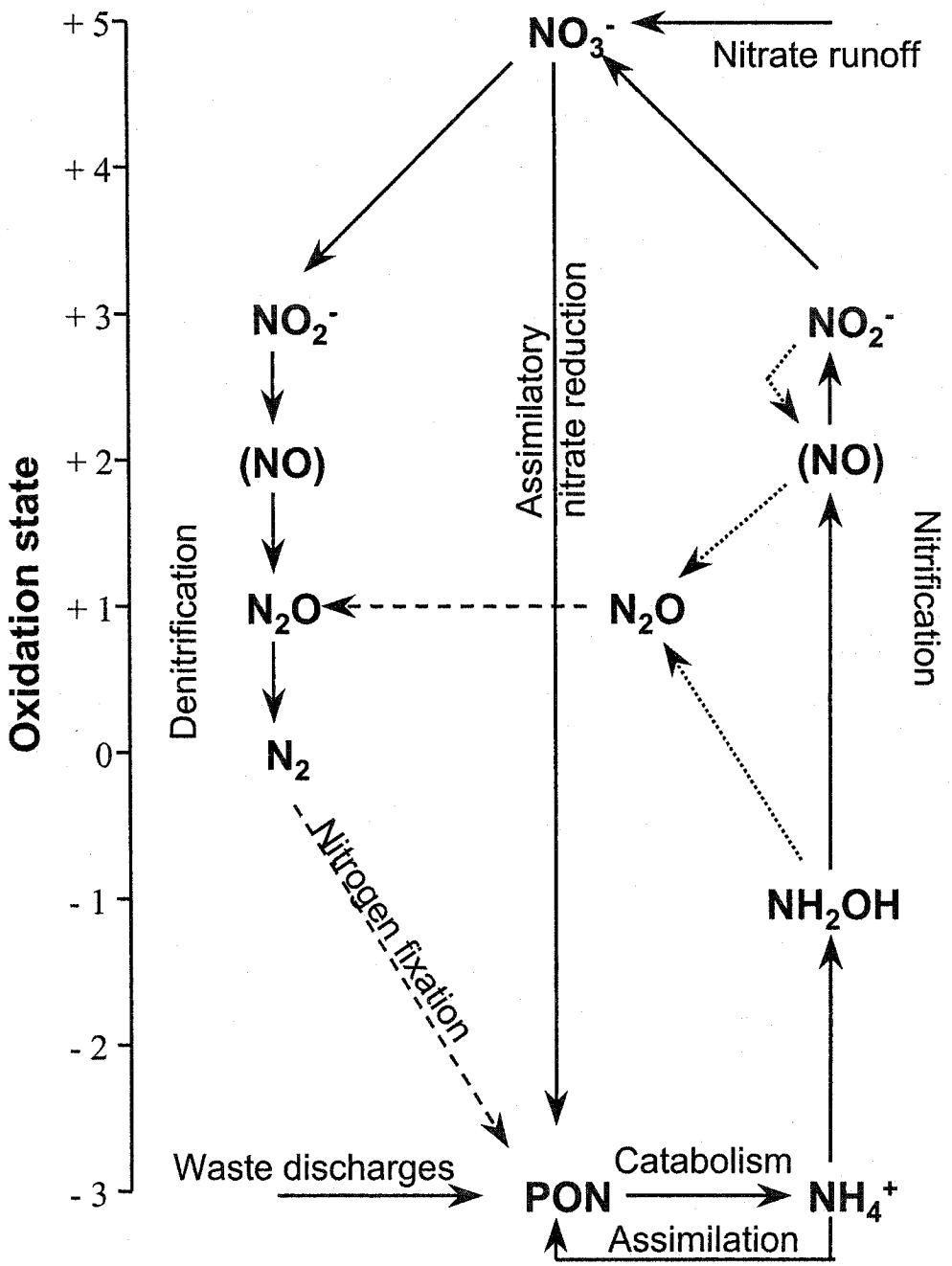

Figure 1.2. A much simplified schematic diagram of coastal microbial nitrogen cycling adapted from Codispoti *et al.*, (2001), indicating sources and sinks of nitrous oxide. The proposed pathways leading to N_2O production from nitrification are uncertain and shown as dashed lines. Nitrogen fixation is represented by a dashed line as it is probably of very minor importance compared to other sources of biologically available nitrogen, and the uptake of N_2O by denitrification may similarly be insignificant.

and Zafiriou, 1988), and it is possible that free NO, produced by nitrification under low oxygen conditions, may also be a precurser to N_2O.

Nitrification is now considered to be the primary N_2O production mechanism in the open ocean. The evidence to support this view has come from observations accrued over the last ~30 years showing positive linear correlations between ΔN_2O ($[N_2O]_{measured}$-$[N_2O]_{saturation}$) and AOU, indicating a production mechanism based on the oxidative decomposition of organic matter (e.g. Yoshinari, 1976; Cohen and Gordon, 1979; Butler *et al.,* 1989). More recently, dual isotope measurements of N_2O in the North Pacific surface ocean show ^{15}N and ^{18}O depletion relative to the tropospheric composition (Dore *et al.*, 1998), consistent with the large negative isotopic fractionation associated with nitrification (Yoshida, 1988).

1.5.1. Important factors controlling nitrification

It is logical to suppose that factors which control nitrification rates in the ocean will consequently, to a greater or lesser degree, also influence the rate of nitrous oxide formation. The environmental variables that are known, or are at least suspected, to affect marine nitrification rates and distribution have been reviewed by Ward (2000) and include light, substrate concentration, temperature, inhibitory compounds, and oxygen concentration. Relatively little is known of the last three of these factors, although some attention will be devoted to the effects of low temperatures on marine nitrification rates later in this text. At this stage it is pertinent to briefly review what is known of perhaps the most important environmental factors influencing marine nitrification: light intensity and substrate concentration.

1.5.2. Light

It is now well established that nitrifying activity is inhibited by exposure to light. The photoinhibition of pure *Nitrosomonas* and *Nitrobacter* cultures was first reported by Müller-Neuglück and Engel (1961), and the likely mechanism, photo-oxidation of cytochrome c oxidase in the presence of oxygen was first proposed by Bock (1965). Olson (1981) showed photoinhibition in natural populations of marine nitrifying bacteria at less than 1% of surface irradiance, and formed the now widely accepted hypothesis that the primary nitrite maximum frequently observed in the lower reaches of the euphotic zone results from differential photoinhibition of ammonium-oxidising and nitrite-oxidising bacteria. Horrigan *et al.*, (1981) demonstrated photoinhibition of ammonium oxidation, in enriched cultures of marine nitrifying bacteria, when subjected to a moderate level of irradiance from a fluorescent light source. Dark recovery was possible over a day/night cycle, sufficient to allow net nitrification to take place. Guerrero and Jones (1996a;b) further pursued the subject of dark recovery in nitrifying cultures, revealing that the time required for both ammonium oxidising and nitrite oxidising activity to be regained following light exposure is related to light intensity, exposure time and wavelength. They also discovered that nitrite oxidising bateria are more susceptible to permanent damage following light exposure. Following 2 hours exposure to full sunlight, ammonium oxidisers were found to require 24 hours to recover only 3% of their original activity, whereas nitrite oxidising bacteria never recovered.

Photoinhibition is therefore considered to be an important factor contributing to the generally very low rates of nitrification observed in the surface ocean. As nitrification is also thought to be the only autochthonous source of N_2O in well oxygenated water,

conceptual and numerical models of oceanic N_2O processes have assumed that production is insignificant in the euphotic zone/upper mixed layer (Nevison *et al.*, 1995; Suntharalingam and Sarmiento, 2000). This may not be strictly true, as quite substantial nitrification rates up to 137 nmols N L^{-1} d^{-1} have been measured in the lower euphotic zone (100-175 m) of the North Pacific (Dore and Karl, 1996). Nevertheless in this study, water samples for incubation experiments were generally obtained from below the euphotic zone to avoid the further complication of photoinhibition during attempts to unravel the important factors controlling N_2O production

1.5.3. Substrate concentration

As nitrification rates are frequently observed to be very high in rivers and coastal regions with high nitrogen loading, and very low in oligotrophic ocean regions, one would reasonably expect nitrification rates to be first-order dependent on ammonium concentration. This is indeed often seen to be the case in cultures of ammonium oxidising bacteria. Stehr *et al.,* (1995) isolated and enriched seven *Nitrosomonas* species from the lower River Elbe, a eutrophic estuary. Ammonium oxidation rates displayed first-order kinetics, but with half-saturation constants (K_s) ranging widely between 30 μmol L^{-1} to 3.3 mmol L^{-1}. However, in the case of open ocean marine populations of ammonium oxidising bacteria, such a clear dependence of nitrifying activity on substrate concentration is rarely observed. Oceanic nitrification rates have been found to be zero-order with respect to ambient ammonium concentration at levels above 0.1 μmol NH_4^+ L^{-1} (Hashimoto *et al.*, 1983; Ward and Kilpatrick, 1990), suggesting that *in situ* natural assemblages of ammonium oxidising bacteria have an extremely high affinity for ammonium. On the other hand, ammonium availability appears to act as a control on

N_2O production associated with nitrification in eutrophic estuaries (de Wilde and de Bie, 2000; de Bie *et al.*, 2002). This contradictary evidence may be interpreted as a species-level adaptation to differing nitrogen regimes. Thus an estuarine environment would favour a community structure dominated by ammonium-oxidisers with high K_s values, able to grow rapidly in high nitrogen loading, whereas an oligotrophic environment would select in favour of slower growing, but more efficient species.

1.5.4 N_2O yield from nitrification

The efficiency of NH_4^+ conversion to N_2O (mol N_2O per mol NH_4^+), or N_2O yield, is potentially an important factor in parameterising N_2O production, yet remains poorly understood. Indirect estimates of N_2O yields have been based on observed oceanic ΔN_2O/AOU relationships combined with the Redfield model for nitrogen regeneration. These estimates are typically in the range 0.1-0.5% (Elkins *et al.*, 1978; Kaplan and Wofsy, 1985; de Wilde and Helder, 1997). However these values are water column integrated and may be influenced by factors such as mixing, variations in the C:N composition of POM, and localised sources and sinks of N_2O. Clearly, better estimates of N_2O yields can be obtained by directly measuring both nitrification rates and N_2O production rates in a particular water mass. Such an approach was taken in the study of Yoshida *et al.*, (1989) in the North Pacific Ocean, in which they measured the production rates of $^{15}N_2O$ and $^{15}NO_3^-$ in water samples incubated with ^{15}N-labelled ammonium. Their calculated yields were suprisingly low, in the range 0.004-0.027 %. Dissolved oxygen may play an important role in governing yields. Goreau *et al.*, (1980) found that the molar N_2O yield from cultures of marine nitrifying bacteria increased from 0.2 to 10 % as the oxygen was decreased. De Bie *et al.*, (2002) incubated water from the Schelde

estuary and saw enhanced N_2O production at oxygen levels below 5 μmol L^{-1}. In contrast, de Wilde and de Bie (2000) obtained N_2O yields of 0.07-0.42 % in the Schelde based on the ratio of estimated N_2O fluxes to measured nitrification rates, but in this case the highest yield was associated with relatively well-oxygenated water.

1.6. Denitrification

The term denitrification is used here to mean dissimilatory nitrate reduction, sometimes called respiratory denitrification (For a review of dissimilatory nitrate reduction see Tiedje, 1988). Denitrifiers are generally a diverse group of aerobic heterotrophic bacteria that are able to utilise oxides of nitrogen as alternative electron acceptors when the supply of oxygen becomes limiting. The complete denitrification pathway can be described as the sequential reduction of nitrate to nitrogen by way of the intermediate species nitrite, nitric oxide and nitrous oxide. Nitrous oxide is an intermediate in this pathway and therefore can potentially be either released to, or consumed from the surrounding environment according to the relative rates of nitric oxide reduction and nitrous oxide reduction.

1.6.1. Regulation of denitrification by dissolved oxygen

The major environmental factor governing the distribution of denitrification in the ocean appears to be the supply of oxygen, and the concept of a threshold oxygen concentration that permits denitrification has become well established. A number of such oxygen threshold values have been reported in the literature, derived variously by comparing profiles of nitrogen oxides and oxygen concentrations (Cohen, 1978; Cohen and Gordon, 1978; Ronner, 1983), measuring $^{15}N_2$ production in $^{15}NO_3^-$ treated samples (Goering, 1968; Chan and Cambell, 1980), and from laboratory chemostat cultures

(Hochstein *et al.*, 1984). Unfortunately there have also been a wide range of different units used to report oxygen concentration in these studies, including mL L^{-1}, mg L^{-1}, μg-atoms L^{-1}, % saturation and μmol L^{-1}. Some of these units require a knowledge of the original temperature and salinity to facilitate interconversion, making direct comparisons difficult. Also, the standard Winkler method used in many of these studies can overestimate dissolved oxygen concentration in near-anoxic water (Broenkow and Cline, 1969; Cline and Richards, 1972). With these limitations in mind, the studies mentioned above point to an oxygen threshold for the onset of denitrification of no greater than about 10 μmol L^{-1}, and possibly a good deal less. It would therefore appear that pelagic denitrification is limited to suboxic zones comprising only about 0.1% of the total ocean volume (Codispoti *et al.*, 2001).

A number of studies have measured N_2O concentrations in the persistent suboxic zones of the Peruvian upwelling, the eastern tropical North Pacific and the north west Indian Ocean (Elkins *et al.*, 1978; Cohen and Gordon, 1978; Law and Owens, 1990; Naqvi and Noronha, 1991; Upstill-Goddard *et al.*, 1999), as well as intermittently anoxic coastal inlets (Elkins *et al.*, 1978; Cohen, 1978). The results frequently show characteristic steep gradients in N_2O concentration varying from undersaturated or even undetectable in the anoxic region, to highly supersaturated in the peripheral suboxic zone. This N_2O distribution pattern is often considered diagnostic of denitrification zones, and implies that net production of N_2O can shift to net consumption over a small oxygen gradient. In the context of the coastal margin, this is an important observation suggesting that water bodies subjected to oxygen depletion through increased eutrophication could

provide enhanced sources of N_2O or localised sinks depending on the degree of oxygen removal.

For many years, denitrification was thought to be the only important ocean sink for inorganic fixed nitrogen. Recently, studies of anoxic waters of Golfo Dulce, Costa Rica, and the Black Sea, have highlighted the importance of anaerobic ammonium oxidation – the 'anammox' reaction (Dalsgaard *et al.*, 2003; Kuypers *et al.*, 2003). Anammox bacteria directly oxidise ammonium to dinitrogen using nitrite as an electron acceptor.

R11 $$NH_4^+ + NO_2^- \rightarrow N_2 + 2H_2O$$

This reaction may be responsible for up to 29% of total N_2 production in denitrifying zones (Dalsgaard *et al.*, 2003), and therefore is potentially a globally important component of the marine nitrogen cycle. The significance of the anammox reaction in marine N_2O cycling has not yet been assessed, but the implications for denitrification and nitrification in sub-oxic zones are immediately apparent. First, the anammox reaction represents a leak for nitrite, which may otherwise be reduced to nitrous oxide. Second, ammonium liberated from organic matter by denitrification may be consumed *in situ*, rather than diffusing out of the anoxic zone and fuelling nitrification in surrounding sub-oxic water. In each case, the potential for N_2O production could be reduced by the anammox reaction.

1.7. 'Enigmatic' N_2O production

While a number of studies have reported positive linear correlations between ΔN_2O and AOU, other investigators have reported non-linear relationships, such that N_2O production appears to be enhanced under low oxygen conditions. In the northwest Indian Ocean, Law and Owens (1990) found that two linear regressions provided the best

statistical fit to their data with an increase in the gradient at 197 μmol L^{-1} AOU. In the same region, Upstill-Goddard *et al.* (1999) found the ΔN_2O/AOU relationship was best represented by a first-order polynomial regression, with the ΔN_2O:AOU ratio progressively increasing with depth towards the N_2O maximum/O_2 minimum and progressively decreasing with depth below it. These observations have been explained by two possible scenarios. In the first scenario, marine N_2O is produced by one mechanism, i.e. nitrification, and the efficiency of this process increases with declining oxygen concentration. This view is supported by the laboratory studies of Goreau *et al.*, (1980) who found that the yield of N_2O from cultures of marine *Nitrosomonas* was highest in those cultures grown under low oxygen conditions. In the second scenario, N_2O is produced only by nitrification at high oxygen levels, but denitrification makes an increasing contribution as oxygen declines, until it predominates in suboxic water. A troubling inconsistency in this second explanation is that much of the range in oxygen concentrations over which N_2O production appears to be enhanced lies well above the generally accepted threshold for the onset of marine denitrification. In support of the second scenario, Law and Owens (1990) and Upstill-Goddard *et al.*(1999) hypothesize denitrification in sub-oxic microzones within suspended organic particles. Ostrom *et al.* (2000) also invoke the "anoxic microniche" hypothesis to explain isotopically enriched N_2O in oxic waters of the North Pacific. While this hypothesis is certainly attractive, supporting evidence is rather limited, and the observed results could equally be due to the activities of novel bacterial assemblages. "Aerobic denitrification" has been a thorny issue for over 100 years, but was brought to popular attention with the isolation of *Thiosphaera pantotropha* from a denitrifying wastewater treatment plant (Robertson and

Kuenen, 1991). Cultures of *T. pantotropha* are able to simultaneously utilize oxygen and nitrate as electron acceptors at levels of dissolved oxygen approaching air saturation. Little is known of the environmental significance of aerobic denitrification outside of highly specialised niches, although Bengtsson and Annadotter (1989) reported complete reduction of nitrate to nitrogen gas in aerobic groundwater.

The situation is further complicated by reports that ammonium oxidising *Nitrosomonas* species may be capable of full or partial denitrification under anoxic conditions (Bock *et al.*, 1986; Poth, 1986; Stuven *et al.*, 1992), so the distinction made between groups of organisms able to carry out either nitrification or denitrification may not be as clear cut as once thought.

1.8. The role of sediments in N_2O cycling

The role of sediments in near-shore N_2O cycling is not yet fully understood, and may be dependent on a number of factors including water column nitrate concentration, organic carbon content, tidal resuspension and bioturbation. In a survey of the Tamar Estuary, southwest England, Law *et al.* (1992) proposed that the most important source of N_2O to the water column was sediment release. The mean measured sediment flux of 16.8 μmol N_2O m^{-2} d^{-1} largely accounted for the estimated total estuarine production rate. The flux measurements did not appear seasonally dependent, whereas water column nitrification was thought to be a secondary seasonal source. The authors hypothesised that tidal resuspension, and bioturbation, enhanced N_2O production in the sediments by increasing the diffusional flux of pore water gases and nutrients. In contrast, Barnes and Owens (1999) found water column nitrification at the turbidity maximum to be the main source of N_2O in the Humber estuary (UK), although sediment fluxes in the range 4-605

μmol N_2O m^{-2} d^{-1} were measured. Sediment denitrification played an important role in nitrogen cycling, removing an estimated 25% of the inorganic nitrogen loading annually, and appeared related to organic carbon content. Again, bioturbation was thought to stimulate denitrification by actively promoting a flux of nitrate-rich water to the sites of denitrification, and by increasing the sediment surface area.

While these studies support the view that the carbon-rich sediments of macro tidal estuaries are a net source of N_2O, this may not be the case for all coastal sediments. Naqvi and Noronha (1991) observed appreciable horizontal gradients in the concentration of dissolved N_2O near the continental margin off the west coast of India. The gradients were consistent with the marginal sediments being a net sink for water column N_2O. These conflicting observations serve to illustrate our incomplete understanding of the role of sediments in marine N_2O cycling, and there is scope for a great deal more work on this topic.

1.9. Thesis objectives

The primary objective of this work is to determine the relative importance of nitrification and denitrification in nitrous oxide production in the pelagic coastal zone. An understanding of how these processes contribute to coastal N_2O emissions is necessary to predict the effects of anthropogenic nitrogen inputs to the coastal margin on the global N_2O budget. From the introductory remarks it may be concluded that these processes will be partitioned, perhaps both spatially and temporally, by changes in dissolved oxygen concentration. Nonetheless, the relative contribution of nitrification and denitrification to net observed levels of dissolved N_2O has so far proved difficult to

resolve, not least because production by these pathways, and consumption in the denitrification pathway, may operate concurrently.

In order to address this primary objective, a number of aims should be met. These are:

1. To develop a method for independently measuring N_2O production from ammonium oxidation and nitrate reduction, and also for measuring N_2O consumption.

2. To investigate the main environmental factors controlling N_2O production (substrate availability, temperature, dissolved oxygen) in a coastal region.

3. To deduce the cause of apparent enhanced N_2O production at low oxygen levels. Is this due to an increased yield of N_2O from nitrification at low oxygen concentrations as indicated by the findings of Goreau (1980), or is it the case that denitrification makes a progressively greater contribution to the total N_2O production as oxygen decreases? To address this question, the conversion efficiency of ammonium to nitrous oxide will be assessed over a range of oxygen concentrations.

4. To investigate the effect of dissolved oxygen on N_2O production and consumption rates in denitrification. Field data suggest that there is a shift from net production to net consumption coinciding with a reduction of a few $\mu mol\ L^{-1}$ in oxygen, but as yet there are few actual rate measurement data from marine environments.

Chapter 2 of this thesis describes the novel stable isotope tracer technique developed for directly measuring production and consumption rates of N_2O, and also its ambient concentration in seawater. Chapter 3 details additional methods used to make measurements in this study. The stable isotope method was first applied to making measurements in the Scotian Shelf and Labrador Sea region during a short cruise in 2001. The results of this cruise are presented in Chapter 4. Chapter 5 describes a study undertaken in a local coastal embayment spanning a total of 18 months. Measurements were made of N_2O production and consumption rates, nitrification rates, and a number of environmental variables in an effort to determine the important sources and sinks for N_2O. Chapter 6 documents a series of laboratory incubation experiments using locally obtained coastal seawater, where the oxygen concentration was manipulated to investigate the effect on production and consumption rates by the denitrifying community. Finally, Chapter 7 offers conclusions and suggestions for future work.

Chapter 2

A stable isotope method for measuring N_2O production and consumption rates in seawater

2.1. Introduction

The record of nitrous oxide measurements in the ocean dates back to the early 1960's, probably beginning with the work of Craig and Gordon (1963) in the southern Pacific. In succeeding years, a number of different approaches have been developed and applied to improve our understanding of N_2O in the ocean. Nevertheless, the basic analytical procedure used for the majority of marine N_2O measurements has remained little changed since the earliest work and comprises three stages. First, extraction of N_2O along with other dissolved gases from seawater either by purge-and-trap preconcentration or equilibration methods, second, separation of the extracted gases by chromatography, and third, measurement with a detector calibrated using standards of known concentration. Quite a diverse array of measuring techniques have been used in N_2O studies due either to the adoption of new detectors as they have become commercially available, or by adapting existing detectors to address specific questions. For example, early pioneers of ocean-going N_2O measurements were limited in their choice of suitable detectors to the universal but relatively insensitive thermal conductivity detector (TCD). Consequently, relatively large seawater samples (>1L) were required to provide sufficient material to provide measurable chromatographic peaks, necessitating lengthy purge times. In contrast, the modern electron-capture detector (ECD) developed from the prototypes invented by James Lovelock in the 1960's is highly sensitive to N_2O. Following their commercial introduction in the mid 1970's, ECD's became commonly employed for both

measurements of atmospheric N_2O, and oceanic N_2O in conjunction with seawater equilibration techniques. Many modifications of the seawater equilibration/ECD method have arisen, ranging from small-sample-volume automated systems for rapid repeated analyses (Butler and Elkins, 1991) to large-sample configurations for high-precision measurements (Upstill-Goddard *et al.*, 1996).

While there are a great number of surface water and depth profile measurements of N_2O from a wide range of ocean regions, simple bulk concentration measurements obtained using ECD's or other non-mass selective detectors reveal little information about its origin. The microbial pathway, or pathways, contributing to the net observed levels of N_2O in seawater can only be inferred from such measurements by comparison with other seawater properties. Hence, the frequently observed negative correlation in open ocean depth profiles between N_2O and oxygen concentrations, together with a positive correlation with nitrate concentrations, is regarded as evidence for a production mechanism based on the oxidation of organic carbon and subsequent remineralisation of organic nitrogen, i.e. nitrification. Unfortunately the situation is not always clear cut, particularly in low oxygen regions where denitrification may also contribute to net levels of N_2O. The last decade has seen a great deal of work devoted to measuring the natural abundance of ^{15}N and ^{18}O isotopes in oceanic N_2O in the hope that this information may better constrain the ocean source and provide clues about the production mechanisms involved (e.g. Yoshinari *et al.*, 1997; Dore *et al.*, 1998; Naqvi *et al.*, 1998; Ostrom *et al.*, 2000). However the results have often proved difficult to interpret, sometimes raising more questions than have been answered. More recently, it has also become possible to determine the intramolecular nitrogen isotope distribution in environmental N_2O

(Brenninkmeijer and Röckmann, 1999) and it is hoped that this new technique may eventually be a valuable tool in resolving the global N_2O budget.

The alternate use of nitrogen labelling as a tracer of marine N_2O production or loss pathways has so far received relatively little attention. It seems certain that N_2O production rates in most open ocean regions are very low, and achieving the desired sensitivity to detect changes in isotopically-labelled N_2O will therefore require lengthy incubations and hence relatively large water samples. Yoshida *et al.*, (1989) measured N_2O production rates in the North Pacific arising from ammonium oxidation. 5L water samples were enriched to 1 μmol $^{15}NH_4^+$ L^{-1} and incubated for 48 hours after which mercuric chloride was added to halt microbial activity. N_2O was later stripped and analysed for ^{15}N enrichment. The results were surprising in that the observed rates of N_2O production were extremely low, of the order 10^{-14} mol L^{-1} h^{-1}. It is also possible that increasing the ambient level of ammonium in oligotrophic microbial systems that are potentially nitrogen limited could result in unrealistically high rate measurements. Yoshida *et al.* acknowledged this, using the term *potential* rates for their measurements, as distinct from *in situ* rates. True tracer studies of N_2O production rates that use below-ambient additions of nitrogen will certainly demand extreme analytical sensitivity.

Determining the relative contributions of nitrification and denitrification to N_2O production poses a particularly challenging problem in shallow water regions where the situation may be further complicated by inputs of allochthonous N_2O from anthropogenic point sources, sediment outgassing (Law *et al.*, 1992), and rapid dispersal of water column N_2O by advection and diffusion across the sea/air interface. In contrast to oligotrophic ocean environments, the ocean margins in general, and estuaries in

particular, seem to present more amenable environments in which to directly measure production rates of nitrous oxide. Substrates such as NH_4^+ and NO_3^- are usually abundant, hence microbial processes are less inclined to be nitrogen limited. Recently, some progress has been made in determining the relative importance of nitrification and denitrification to estuarine N_2O production through the use of nitrification inhibitors such as acetylene in sea or river water incubations, and measuring N_2O accumulation by conventional non mass selective detectors (Bonin *et al.*, 2001; de Bie *et al.*, 2002). Both nitrification and denitrification are, however, sensitive to the same compounds to some extent (Bonin *et al.*, 2001). For example, acetylene also inhibits the activity of the nitrous oxide reductase enzyme within the denitrification pathway, forming the basis of the "acetylene block" assay of denitrification. In this technique, the increase of N_2O concentration with time in samples incubated with acetylene is used to estimate the rate of nitrate reduction. Great caution is therefore required in the application and interpretation of inhibitor techniques. Furthermore, simultaneous production and consumption of N_2O by denitrification in low-oxygen environments can probably not be resolved in this manner. A trial isotope tracer method for determining the relative importance of nitrification and denitrification in estuarine water was tested in the Humber estuary by Barnes and Owens (1999). 1L water samples were spiked with 100 μmol $^{15}NH_4^+$ or $^{15}NO_3^-$ and, after incubation, dissolved N_2O was stripped from the samples and analysed for ^{15}N enrichment.

All the isotopic studies mentioned so far have employed dual inlet isotope ratio mass spectrometers (e.g. Thermo-Finnigan MAT 252). While such instruments have very high mass resolution, they are extremely expensive to purchase and operate. In addition, they

cannot be considered portable, hence samples obtained at sea must be stored and possibly transported for long distances, raising concerns about N_2O stability. Furthermore, the high resolution offered by these spectrometers is not strictly essential in situations where relatively high concentrations of labelled tracers are added, and where the target analyte has a mass to charge ratio (*m/z*) of at least one or more difference from the naturally occurring species. In these situations, the relatively low-cost and portable quadrupole mass spectrometer, although having low mass resolution, offers a great deal of potential in unravelling N_2O production mechanisms. Such instruments have been routinely employed in sea-going GC-MS studies of marine halocarbons for about ten years (Moore *et al.*, 1996; Moore and Groszko, 1999). Stable isotope tracer methods employing purge-and-trap gas chromatography/quadrupole mass spectrometry have already been employed for a number of years to separate biological and chemical degradation rates of halocarbons, including methyl bromide and methyl chloride, in seawater (King and Saltzman, 1997; Tokarczyk and Saltzman, 2001; Tokarczyk *et al.*, 2003). These studies have employed short-term incubations of seawater samples enriched with an isotopically-labelled substrate, coupled to purge-and-trap gas chromatography/mass spectrometry analysis. The use of an isotopically labelled structural analogue of the target compound as an internal standard has been adopted to achieve the level of analytical precision necessary for kinetic studies. A similar approach is adopted here to directly measure marine production and consumption rates of N_2O using ^{15}N-labelled substrates.

2.2. Outline of method

This method measures potential rates of N_2O production arising from nitrification or denitrification and also N_2O consumption rates by incubating small volume (100mL)

water samples with the appropriate ^{15}N-labelled substrate ($^{15}NH_4^+$, $^{15}NO_3^-$ and $^{15}N_2O$ respectively). The incubation vessels are 100-mL glass syringes, which enable subsamples to be drawn without the introduction of a headspace. Incubation times are kept as short as possible consistent with levels of microbial activity. The concentration of $^{15}N_2O$ in each incubation syringe is monitored by making a time-series of measurements using purge-and-trap gas-chromatography/mass-spectrometry. The instrumental configuration utilised in this study is adapted from that of Moore *et al.*, (1996). Dissolved gases are stripped from ~10mL samples using a stream of UHP helium purge gas, then water vapour and the bulk of CO_2 are removed. N_2O and other less-volatile gases are trapped under liquid nitrogen. Following desorption, N_2O is separated on a fused-quartz chromatographic column (J&W Scientific) and analysed with a quadrupole mass spectrometer. A precisely metered volume of fully-labelled internal standard gas ($^{15}N_2{}^{18}O$) is injected along with each sample and used to correct for variations in detector sensitivity and stripping efficiency. Typically, about 40 measurements are made over a period of 8-12 hours, demanding rapid sample turnabout time, and sustained high precision. Production and consumption rates are calculated from best-fit linear regressions of the changes in $^{15}N_2O$ concentrations over time. The production rates obtained by this method are perhaps best described as maximum potential rates. This is because $^{15}NH_4^+$ and $^{15}NO_3^-$ are enriched by factors of 5-100, and the possibility of enhanced microbial activity within the incubation vessels as a result of super-ambient substrate concentrations must be acknowledged. However it should also be noted that the substrate saturation concentration for ammonium oxidation is thought to be very low, perhaps only about 0.1 μmol NH_4^+ L^{-1} (Hashimoto *et al.*, 1983).

2.3. Sample Collection and incubation

Seawater is collected in standard 10L Niskin or GoFlo sampling bottles. Immediately after collection, subsamples are transferred to chemically clean, 100-mL capacity borosilicate glass syringes (Popper & Sons) in which the samples are incubated. The major advantage of large glass syringes as incubation vessels is that subsamples can be periodically removed without the introduction of a headspace, or air contamination. To facilitate transfer from the sampling bottle, the syringes are fitted with a 50-mm Luer-Lok stainless steel needle with a ferrule fitted close to the tip. This provides a clean watertight seal against the outlet spigot of the Niskin bottle, enabling a seawater sample to be drawn into the syringe without contamination or exposure to air. The syringes are filled and emptied twice before final sample collection. Samples to be incubated with $^{15}NH_4^+$ are collected in syringes wrapped in a black polythene film to prevent potential photoinhibition of ammonium oxidising bacteria (Guerrero and Jones, 1996b).

Duplicate samples are then spiked with ^{15}N-labelled substrates. To measure N_2O production from nitrification or denitrification, ^{15}N-labelled NH_4Cl or KNO_3 solutions are added to give a final concentration of 100 μmol L^{-1}. In the samples studied, this has resulted in concentrations of the order 10-100 times ambient, therefore most of the N_2O produced is $^{15}N_2{}^{16}O$. In the case of degradation rate measurements, $^{15}N_2O$ gas is added to give an initial concentration of ~1nmol L^{-1}, or around 10% ambient. Duplicate control samples are also collected and poisoned with 0.2 mL of saturated mercuric chloride solution. After spiking, the syringes are capped and transferred to a temperature regulated water bath maintained at ± 1°C of the *in situ* temperature.

An underlying assumption inherent in incubation experiments is that the *in vitro* biochemical reaction rates under examination do not appreciably differ from the equivalent *in situ* rates. However, an important consequence of confining a natural population of aquatic microorganisms within a glass container for physiological rate measurements is the so-called "bottle effect" (Karl and Dore, 2001). The population structure and metabolic rates of micro organisms within a contained sample may change unpredictably over hours to days resulting in non-representative production or consumption rates of the compounds of interest. Two basic principles are adopted here to minimise the influence of bottle effects upon N_2O production and degradation rate measurements. First, the duration of incubations is kept to a minimum consistent with the reaction rates and detection limits of the method. In practice, this has resulted in incubation times of around 8-12 hours for typical estuarine production or consumption rates of N_2O, although incubations have sometimes been continued for up to 24 hours to improve detection limits and precision where rates are low. Second, four or five measurements are made from each subsample between the time of spiking with substrate (t_0) and the end of the incubation. Drastic changes occurring in the confined bacterial community, such as rapid population increase or mortality should be revealed by causing the production or consumption rate of $^{15}N_2O$ to deviate from linearity. In such a situation, rates are calculated from the initial linear change in $^{15}N_2O$ concentration from t_0 to the onset of non-linearity.

2.4. Analytical procedure

A schematic diagram of the purge and trap GC/MS system is shown in figure 2.1. V1-V4 are Valco two-position chromatography valves. V1 is an eight port liquid-

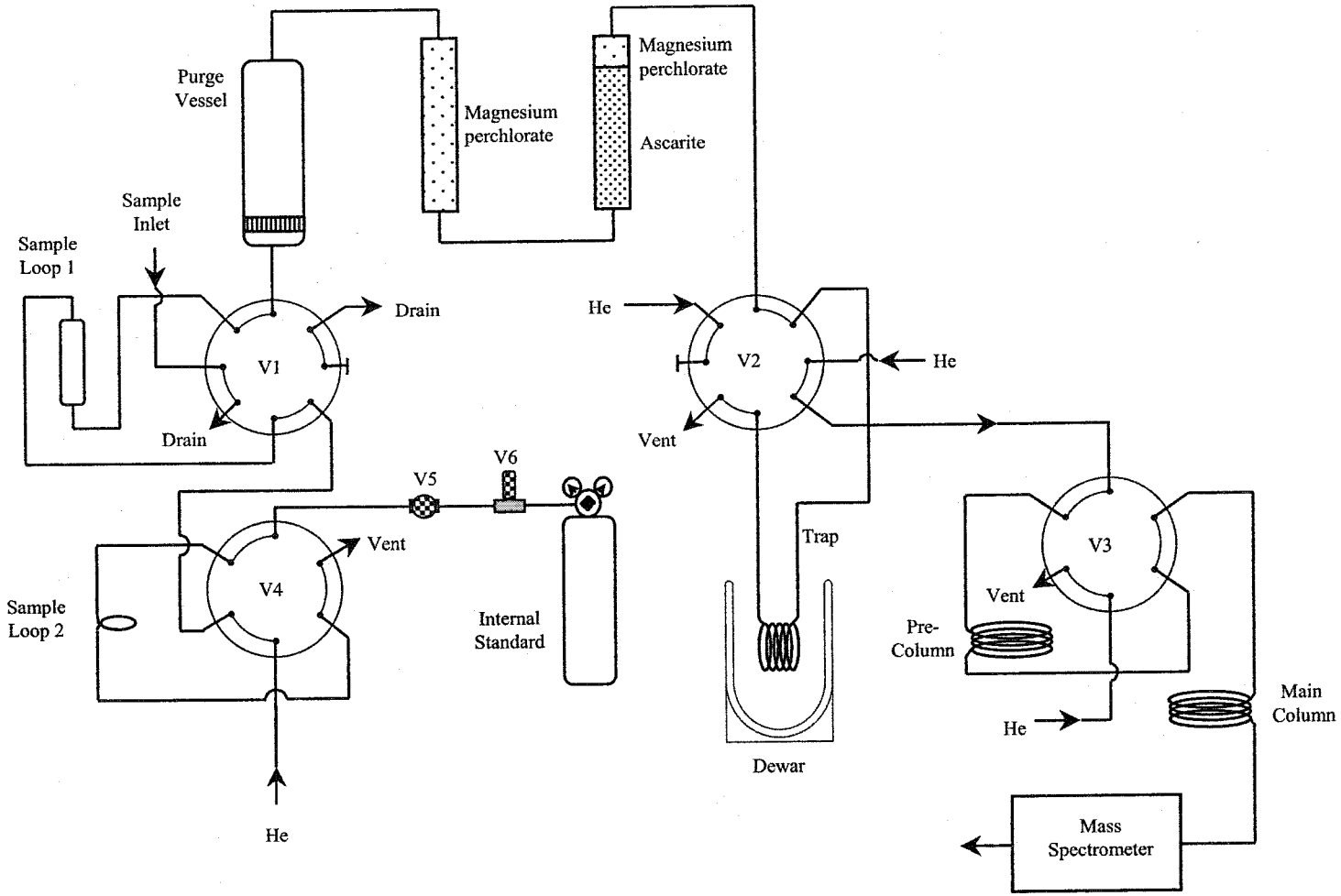

Figure 2.1. A schematic diagram of the analytical apparatus

chromatography valve with 1.5 mm i.d. ports, manufactured from corrosion resistant Hastelloy™ nickel-chromium-molybdenum alloy. V2, V3 and V4 are 0.75 mm port diameter stainless steel valves. V1, V2 and V3 are computer controlled by means of motorised actuators and are shown in the "purge" configuration. V4 is used to inject a calibrated volume of the internal standard gas into each sample, and is operated manually. V5 is a shut-off valve and V6 is a needle valve. Sample loop 1 is a gravimetrically calibrated loop, nominally 10 mL volume, formed from a glass pipette and Hastelloy 2 mm i.d. tubing. The purge vessel is borosilicate glass tube of 1-cm i.d. × 15-cm length with an internal fine glass frit.

The analytical procedure is as follows. Sample loop 1 is filled with seawater directly from a 100 mL syringe fitted with a Millipore Swinney in-line filter. V1 is then switched to the "purge" position as shown and a 20 mL min^{-1} flow of UHP helium purge gas (99.999 % purity) displaces the sample from the loop to the glass purge vessel, subsequently forming a stream of fine bubbles through a frit and initiating the stripping procedure. At this point, a stainless steel sample loop of ~50μL volume previously filled with internal standard gas is manually switched into the purge gas stream using V4. The stripped gases from the sample flow first through a magnesium perchlorate trap to remove water vapour, and then an Ascarite trap removing approximately 99.99% of purged CO_2. A small amount of $Mg(ClO_4)_2$ is also packed in this trap to remove additional water vapour liberated by the reaction of CO_2 with Ascarite. The scrubbed gases are then directed by V2 through the cryogenic trap, a coil formed from a 30 cm length of 0.5 mm i.d. stainless steel tube immersed in a small dewar of liquid nitrogen. After 5 minutes of purging, V1 and V2 are switched, and the GC progam started. The

flow of helium purge gas through the purge vessel and chemical traps is now reversed, forcing the spent seawater to drain, and the cryogenic trap is switched into the carrier gas line. At this point, the liquid nitrogen dewar is removed, and the cryogenic trap heated to ~60 °C by a low-voltage electric current through the stainless steel tubing. The desorbed gases are swept by the carrier gas (UHP helium, 5mL min^{-1}) to the GC. When the purge vessel has emptied, V1 and V2 are returned to the "purge" position in readiness for the next sample.

The chromatographic column is a 'GS-Gas Pro' 60m × 0.32mm i.d. PLOT column (J&W Scientific) installed in two sections in a Thermo-Finnegan GC 8000 oven. A 15m pre-column and a 45m main-column are plumbed in a "front-cut" configuration. Desorbed gases enter the pre-column and chromatographic separation ensues. Immediately after N_2O has entered the main column, high boiling point compounds remaining in the pre column are backflushed to vent by a second helium supply of 5 mL min^{-1}. This technique eliminates the need for temperature ramping between samples, and helps prevent contaminants reaching the source and analyser components. Oven temperature is isothermal at 30 °C. Eluting gases are analysed with a Thermo-Finnegan MD800 quadrupole mass spectrometer employing electron ionisation (EI). Ions are scanned in selected ion recording (SIR) mode, allowing a number of ions to be monitored in a repetitive, cyclic manner. Under the described conditions, the purging efficiency of N_2O is 100%, while the trapping efficiency is 94%, determined by comparing analyses of cold-trapped injections of a standard gas with analyses of replicate volumes of the same gas injected directly into the carrier gas flow. Seawater samples can be analysed at the rate of 4-5 h^{-1}.

With GC oven temperatures equal to, or greater than, ambient laboratory temperature, N_2O and CO_2 peaks are partially resolved, with retention times of 3.79 minutes and 3.87 minutes at 30 °C. In the atmosphere, CO_2 is about 1000 times more abundant than N_2O, therefore the potential for interference with the parent ions of N_2O (*m/z* 44, 45 and 46) is a cause for concern, as changes in the efficiency of CO_2 removal over time could lead to spurious results. While sub-ambient column temperatures could be used to achieve chromatographic separation, there will be a concomitant increase in retention time, a significant disadvantage where many samples must be analysed in a limited time in addition to the increased expense and hardware requirements. The alternative approach adopted here is to measure peaks corresponding to the major ion fragments, as about 30% of N_2O molecules dissociate in the ion source to give NO^+ ions. The ions monitored are therefore *m/z* 30 for bulk N_2O, 31 for $^{15}N_2O$ and 33 for the internal standard. In addition, the internal standard parent ion peak (m/z 48) is also routinely monitored to determine the fragmentation ratio R_1 where $R_1 = NO^+/N_2O^+$. The value for R_1 is typically 0.32 at the standard electron energy of 70 eV, varying by no more than ±0.002 over a course of measurements. In principle, variations in the analyte fragment peak size due to changes in R_1 will be compensated for by a similar effect on the internal standard fragment. No interference with the NO^+ peaks from CO_2 has been seen. Although CO_2 generates a CO^+ ion fragment of about 10% parent ion abundance, the *m/z* 31 signal produced by $^{13}C^{18}O$ does not exceed the background noise level. Figure 2.2 shows typical chromatograms generated by the NO^+ fragment ions and N_2O^+ parent ions in a seawater sample. The parent ion traces at *m/z* 44, 45 and 46 reveal a small peak with a retention time of 3.863 minutes produced by the residual CO_2 retained in the cryotrap.

2.5. The internal standard method

Kinetic studies that employ a number of repeated mass spectrometric analyses demand a high level of overall analytical precision sustainable for the duration of the measurements. The detection limit of a production or degradation rate will be governed by the overall analytical error arising from errors ascribable to sample handling, plus errors associated with measurement of the analyte. In the case of sample handling, variations may occur in purging and trapping/desorption efficiencies, while the actual analysis may be affected by changing conditions in the mass spectrometer ion source leading to fluctuations in sensitivity (detector response per unit mass of analyte). Perhaps more important, there is a danger that a systematic trend in either of these factors may be falsely interpreted as an actual change in analyte concentration over time. Fortunately, these errors can be minimised by using an internal standard. The ideal internal standard is a structural analogue of the analyte with the same physical and chemical properties and therefore chromatographic retention time, but having no natural occurrence. A metered volume of internal standard gas, the same for each sample, is injected along with the sample at the purging stage of the analysis. Factors affecting the analyte in the stripping, trapping and analytical stage will affect the internal standard in the same way, therefore the analyte peak areas can be corrected by normalising to the initial internal standard peak. Fully labelled nitrous oxide, $^{15}N_2{}^{18}O$ was chosen as an ideal internal standard for this study as its natural occurrence is negligible, however this compound is not readily available commercially, therefore a small quantity was synthesised in the laboratory.

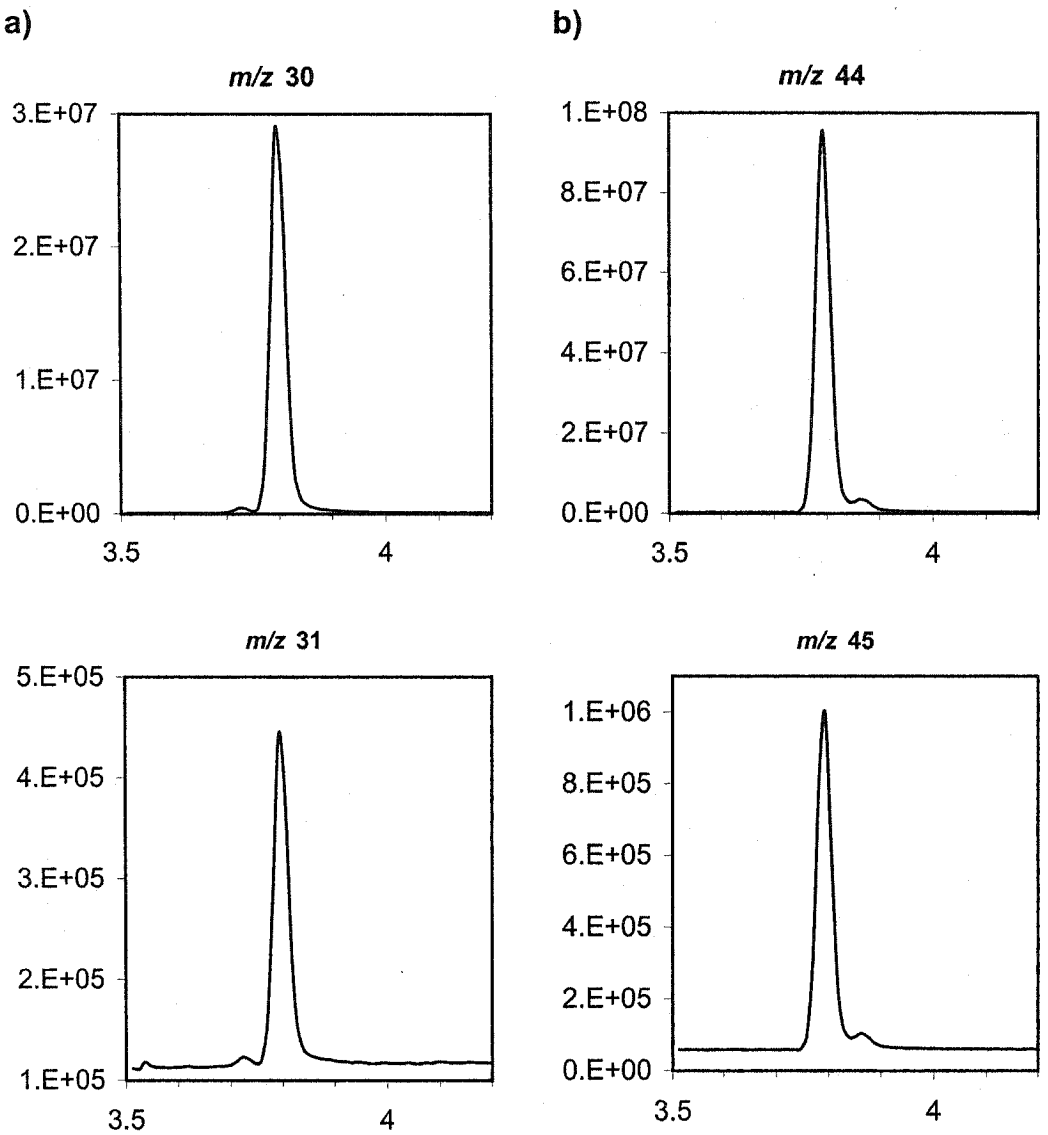

Figure 2.2. Chromatograms from a typical seawater sample showing; a) NO^+ fragment ions (*m/z* 30 and 31) and b), parent N_2O^+ ions (*m/z* 44 and 45). The x axes show retention time in minutes, the y axes show relative peak height. The top chromatograms represent bulk N_2O while the bottom chromatograms represent ^{15}N-labelled species. The small amount of residual CO_2 shows as a small peak at a retention time of 3.863 minutes in the parent ion traces.

2.6. Synthesis of the internal standard

The internal standard gas was synthesised using the well-known thermal decomposition of ammonium nitrate (NH_4NO_3). At temperatures above its melting point (170 °C) ammonium nitrate decomposes according to the reaction

$$NH_4NO_3 \rightarrow N_2O + 2H_2O$$

The arrangement of nitrogen and oxygen atoms in the linear N_2O molecule is predictable: the nitrogen and oxygen atoms occupying the central and end positions respectively originate from the nitrate ion, while the end nitrogen atom originates from the ammonium ion (Friedman and Bigeleisen, 1950). This synthesis therefore allows nitrous oxide with any permutation of labelled atoms to be produced, according to the arrangement of labelling in the ammonium nitrate reactant. Multiply-labelled ammonium nitrate ($^{15}NH_4{}^{15}N^{18}O_3$) was prepared from a solution of ^{15}N-labelled ammonium chloride (98% ^{15}N, Cambridge Isotopes) and multiply-labelled sodium nitrate (99% ^{15}N, 95% ^{18}O, Isotec Inc.) in a minimal volume of deionised water. The amounts used were 12.2 mg NH_4Cl and 24.1 mg $NaNO_3$ to give a target N_2O volume of 0.5 mL, assuming 10 % decomposition based on previous trial experiments with non-labelled ammonium nitrate. The solution was injected into a borosilicate glass breakseal vial, which was then evacuated and heated gently until a white residuum remained. Care was taken not to completely desiccate the residuum, as experiments by Friedman and Bigeleisen (1950) showed that a trace of water vapour is required to catalyse the initial decomposition of ammonium nitrate. After flame sealing, the evacuated vial was placed in a GC oven and heated for 4 days at 230 °C. Trials with non-labelled ammonium chloride showed a decomposition rate of around 2-3 % per day at this temperature. It is inadvisable to

exceed 250 °C as above this temperature, appreciable amounts of N_2 and higher oxides of nitrogen are produced, and the reaction carries an increased risk of explosion (Spindel, 1962). After about 3 days of heating a faint reddish-brown colour was seen in the vial, disappearing on cooling. This colouration was probably due to trace amounts of nitrogen dioxide (NO_2).

Purification and transfer of the fully labelled N_2O was achieved using a vacuum line and cold traps (Figure 2.3). The gaseous contents of the breakseal vial were drawn first through Trap A, a stainless steel tube held at approximately -20 °C in a freezing mixture of ice and sodium chloride to remove water vapour and NO_2/N_2O_4. N_2O was retained in Trap B, a loop of 2 mm i.d. stainless steel tubing packed with glass beads and immersed in liquid nitrogen. More volatile gases were allowed to vent through the pump. Upon desorption, the contents of Trap B were directed to an evacuated stainless steel cylinder in a stream of UHP nitrogen. After final pressurisation of the cylinder to about 300 psi, the isotopic composition of the N_2O fraction was determined by making three replicate injections of the internal standard through the purge and trap system and analysing the N_2O using the mass spectrometer by monitoring the N_2O^+ ions at *m/z* 44, 45 46 and 48. Assuming an equal detector response per unit mass, the measured composition was 89% $^{15}N_2{}^{18}O$ (*m/z* 48), 9% $^{15}N_2{}^{16}O$ and $^{14}N_2{}^{18}O$ (*m/z* 46), 1% $^{15}N{=}^{14}N{=}^{16}O$ and $^{14}N{=}^{15}N{=}^{16}O$ (*m/z* 45), and 1% $^{14}N_2{}^{16}O$ (*m/z* 44). The contribution of ^{17}O was ignored, as its natural abundance is only 0.037%. Consequently the internal standard does contribute to the principal analyte peak at either *m/z* 31 or 46, according to whether the fragment or parent ions are analysed. In sample measurements, the analyte peak area was corrected by

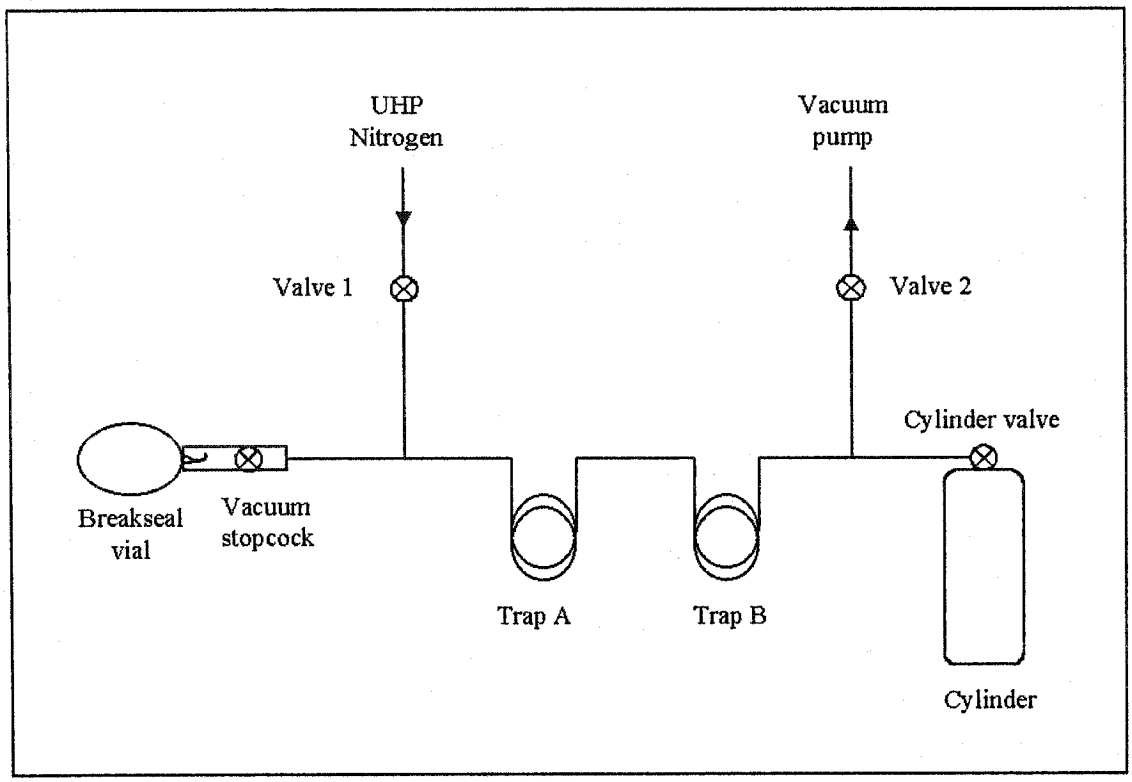

Figure 2.3. Vacuum transfer line used for preparation of the internal standard

subtracting the product of the *m/z* 33 peak area and the *m/z* 31: *m/z* 33 ratio, determined from the internal standard at the start of each set of analyses.

2.7. Calibration

In the early stages of this work, $^{15}N_2O$ and bulk N_2O measurements were calibrated using air as a standard. This practice is quite reasonable because, first, nitrous oxide has a long atmospheric lifetime (~120 years) and its distribution in the troposphere is relatively uniform with very little interhemispheric or seasonal variability (Khalil *et al.*, 2002). Second, the tropospheric mixing ratio of N_2O is continuously monitored at a high level of accuracy at several locations worldwide because of its role as a greenhouse gas. Also, the absolute accuracy of ambient seawater N_2O concentrations in these studies are of secondary importance, as the focus here is on measuring relative changes in N_2O concentration within incubation samples. Nonetheless, there are some limitations to the use of atmospheric N_2O as a standard. For example, relatively large injections of air, up to several mL, are required for the calibration plot to include the range of N_2O concentrations found in seawater, and this introduces practical difficulties and raises concerns including the increased possibility of introducing contaminants into the analytical system. In addition, with air as a standard it is necessary to assume that the detector response for *m/z* 31 is the same as for 30. This is because ion fragment monitoring will only 'see' the nitrogen atom that is adjacent to the oxygen atom within the linear N_2O molecule, notwithstanding rearrangement in the ion source. While the isotopic ratio of tropospheric N_2O has been measured, the intra-molecular distribution of ^{15}N is not yet known with certainty, therefore it is not possible to construct an accurate calibration plot for ^{15}NO. While the assumption of equal detector response for *m/z* 30

and 31 is probably sound for most of the time, more confidence can be obtained where the standard and analyte are identical compounds. Consequently it was decided to prepare a gravimetric $^{15}N_2O/N_2$ standard gas mixture.

A nominal 100-mL volume of 99% pure $^{15}N_2O$ in a breakseal ampoule was obtained from Icon Isotopes, New Jersey, USA. The ampoule was fitted with a vacuum stopcock as in Figure 2.3, and its contents transferred to an evacuated 5.9 L Aculife-coated aluminium cylinder (Scott Specialty Gases) using a purpose-built vacuum line. The cylinder was then pressurised to about 900 psi with UHP nitrogen. Careful weighing of the ampoule/stopcock assembly (precision ± 1mg) and the aluminium cylinder (precision ± 0.1g) before and after the procedure enabled the amounts of N_2O and N_2 transferred to the cylinder to be determined. The resulting N_2O:N_2 mixing ratio was found to be 264.2 ±1.3 ppmv. The actual $^{15}N_2O$:N_2 mixing ratio will be slightly less because of the presence of ^{14}N in the supplied $^{15}N_2O$ sample. To determine the extent of isotopic dilution by ^{14}N, the purge vessel was substituted by a glass injection port fitted with a septum, and the isotopic composition of the $^{15}N_2O$ standard was assessed by consecutively analysing five replicate 4 µL injections using the mass spectrometer. Assuming an equal detector response per unit mass for each N_2O isotope, and ignoring the contribution of ^{17}O and ^{18}O, the measured composition of the N_2O was 94.77 ± 0.07 % $^{15}N_2{}^{16}O$ (mass 46), 4.91 ± 0.05 % $^{15}N{=}^{14}N{=}^{16}O$ or $^{14}N{=}^{15}N{=}^{16}O$ (mass 45), and 0.33 ± 0.02 % $^{14}N_2{}^{16}O$ (mass 44). The corrected mixing ratio for $^{15}N_2O$ is therefore 250 ppmv compared to a value of 263 ppmv for total labelled N_2O. The former value of 250 ppmv has been used to construct the calibration plots used in these studies of N_2O concentration versus detector response for the *m/z* 31 ion fragment. This figure is probably two or three

percent too low, as a fraction of the additional ~ 5% of total ^{15}N labelled N_2O of *m/z* 45 will have the atomic configuration $^{14}N=^{15}N=^{16}O$ and therefore also generate an NO^+ fragment of *m/z* 31. However it is not possible to determine the isotopomeric composition of this fraction, and it is also inappropriate to presume a figure, as the commercial procedure employed to synthesise the $^{15}N_2O$ sample may bias the intramolecular positioning of a single ^{15}N atom beyond the statistics of chance.

During the course of each set of analyses, a calibration curve is plotted by introducing metered volumes of the standard, corrected to the syringe temperature and atmospheric pressure, into the purge and trap system through an injection port with a gas-tight syringe and measuring peaks at *m/z* 46 and 31. The detector response is invariably linear over the range 0 - 20 μL (0 - ~200 pmol $^{15}N_2O$). For convenience, background $^{14}N_2O$ concentrations are estimated from the same plot. While this assumes equal detector response per unit mass for parent ions 44 and 46, and the fragment ions 30 and 31, calibration plots constructed from injections of laboratory air return very similar slopes, giving some confidence in this assumption. Background marine N_2O is inevitably a mix of different isotopes, therefore its concentration will be underestimated by measuring only *m/z* 44 or 30. However, making the approximation that the natural abundance of ^{15}N, ^{17}O and ^{18}O is the same in N_2O as in air, the underestimation will be less than 1%. The standard gas also serves as the source of $^{15}N_2O$ used in degradation measurements: 10 μL dissolved in a 100 mL syringe of seawater gives a $^{15}N_2O$ concentration of about 1 nmol L^{-1}.

2.8. Precision and accuracy

The overall precision of the analytical procedure with respect to both N_2O parent and fragment ions was assessed by repeated analysis of a seawater sample at atmospheric equilibrium. A 1L volume equilibration flask was filled with seawater with a salinity of 30.69 collected from a local embayment. The flask was then immersed in a slush of ice and distilled water, and the temperature monitored using an Omega microprocessor thermometer and copper-constantan thermocouple. When the temperature of the seawater sample had stabilised at 0 °C, cooled, moist laboratory air was pumped through a fine glass frit immersed in the seawater at a rate of about 50 mL min^{-1} for three hours. Subsamples were then drawn from the flask and analysed for N_2O using the internal standard method described, monitoring masses 44, 45, 46, 30, and 31 in addition to the masses corresponding to the internal standard. Ten such samples were analysed over a 3-hour period during which time the temperature in the flask remained at 0 °C, and the atmospheric pressure remained between 995 and 997 mbar. The analytical precisions in relative standard deviation $(100 \cdot \sigma/\bar{x})$ for each mass to charge ratio were as follows; *m/z* 44: ± 0.7%, *m/z* 45: ± 2.2%, *m/z* 46: ± 1.2%, *m/z* 30: ± 0.9% and *m/z* 31: ± 1.0%

For an assessment of analytical accuracy, the expected total equilibrium N_2O concentration in the seawater sample was calculated from the solubility equation of N_2O in moist air (Weiss and Price, 1980) assuming a 2003 atmospheric N_2O mixing ratio of 319 ppbv. This latter value was extrapolated from an average northern hemisphere atmospheric mixing ratio of 314.5 ppbv in 1996 and assumes a continued rate of increase of 0.6 ppbv yr^{-1} (Khalil *et al.*, 2002). To estimate the equilibrium N_2O concentration for *m/z* 44 only, a small correction was made for the natural abundance of ^{15}N and ^{18}O in

tropospheric N_2O. Although the isotopic composition of atmospheric N_2O is not known with certainty, the values obtained by Yoshida and Toyoda, (2000) were used as a reference to give an estimated bulk $^{14}N_2{}^{16}O$ concentration in the seawater sample of 15.11 nmol L^{-1}. The measured concentration for *m/z* 44 was in good agreement at 15.18 ± 0.10 nmol L^{-1}, accurate within the margin of analytical error.

2.9. Example measurements from the field

Figure 2.4 shows plots of $^{15}N_2O$ concentration versus time for samples collected at 60 m depth in the Bedford Basin, Halifax Harbour, on 21st August, 2002. The *in situ* temperature was 2.75 °C, salinity was 31.16 and dissolved oxygen concentration was 93 μmols L^{-1}. The N_2O production rates obtained from ammonium oxidation were in good agreement at 92 ± 3 pmol L^{-1} d^{-1} and 88 ± 6 pmol L^{-1} d^{-1}. The regression slopes for the denitrification, degradation and control data showed no significant difference from zero ($p > 0.05$).

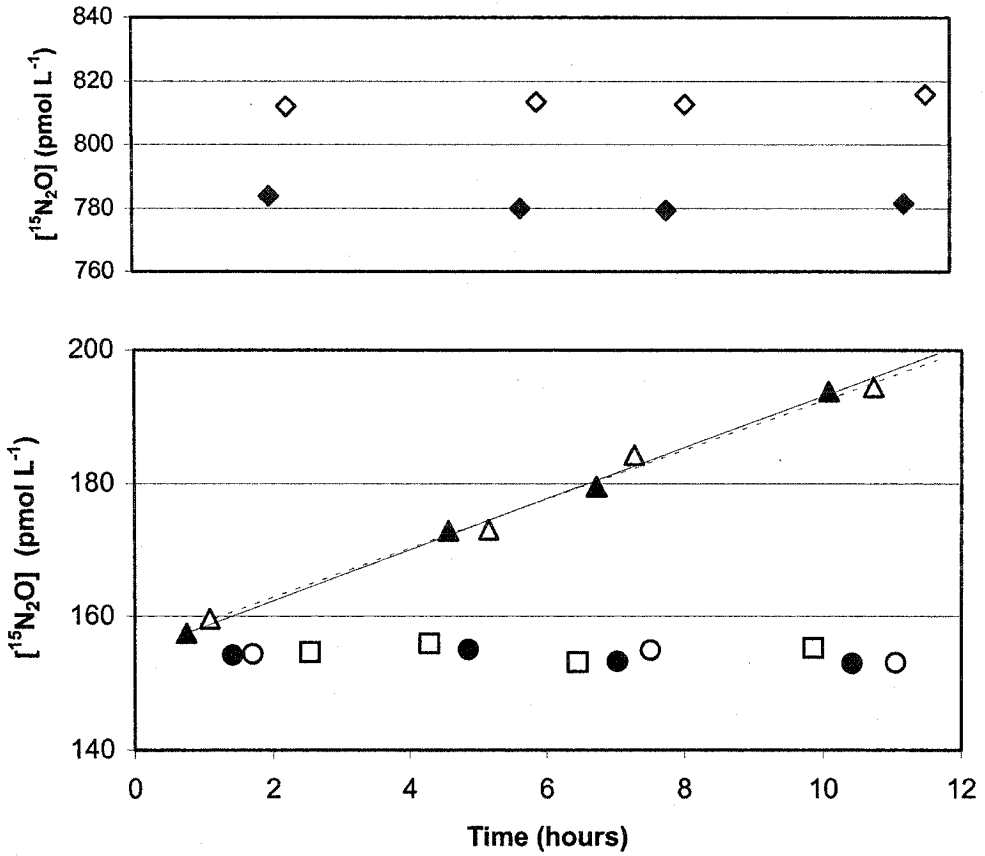

Figure 2.4. $^{15}N_2O$ measurements made on 21st August 2002. The symbols (▲△) represent duplicate samples incubated with $^{15}NH_4^+$, (●○) represent samples incubated with $^{15}NO_3^-$, (◆◇) represent samples enriched with $^{15}N_2O$, and (□) are measurements from a poisoned seawater sample. The best-fit linear regressions for ▲ (solid line) and △ (dashed line) are shown. Statistical data for the slope of the regression m (pmols $^{15}N_2O$ h^{-1}) and the standard deviation of the slope (σ) in the format (m, σ) are; ▲(3.83, 0.13); △(3.69, 0.25); ● (-0.18, 0.13); ○(-0.11, 0.17); ◆(-0.3, 0.29); ◇(0.35, 0.16); □(-0.02, 0.17). The vertical height of the symbols approximates the errors in individual measurements. The duplicate syringes used to measure degradation rates show differing levels of $^{15}N_2O$ due to slight differences in the volumes of gas injected to each syringe.

Chapter 3

Additional methods

In addition to the primary measurements of N_2O production and consumption rates, a number of ancillary measurements were made. These included ammonium oxidation rates, oxygen, ammonium and nitrate concentrations.

3.1. A review of established methods for measuring nitrification rates

3.1.1. Comparative measurements of substrate and products

Perhaps the most obvious method of determining a nitrification rate is to isolate a water sample and measure the changes in concentration with time of the substrate, ammonium, or the product, nitrate. With the exception of the primary and secondary nitrite maxima near the base of the euphotic zone (Capone, 2000), the concentration of nitrite generally remains low as it is oxidised rapidly to nitrate. A pertinent consideration when adopting this approach is that ammonium and nitrate are extremely labile. Both compounds are assimilated as sources of nitrogen by phytoplankton, therefore such incubations should be performed in the dark. Also, at low oxygen concentrations, other microbial nitrogen transformations such as dissimilatory nitrate reduction may influence the results. Furthermore, dark incubations may release the population of nitrifying bacteria within the sample from photoinhibition, resulting in an overestimate of *in situ* rates. Nevertheless, in spite of its limitations, this method has the merit of relative simplicity and has been used with some confidence in regions of very high nitrifying activity where rates of nitrogen uptake by phytoplankton are relatively low (Pakulski *et al.*, 1995; de Wilde and de Bie, 2000).

3.1.2. Specific inhibitors

A number of compounds have been discovered that specifically inhibit either ammonium oxidation or nitrite oxidation. Commonly used examples of ammonium oxidation inhibitors are N-Serve (nitrapyrin 2-chloro-6-(trichloromethyl) pyridine)), allylthiourea, methyl fluoride and acetylene (Bianchi *et al.*, 1999; Bonin *et al.*, 2002; de Bie *et al.*, 2002), while sodium chlorate is a well-known inhibitor of nitrite oxidation (Hynes and Knowles, 1983; Bianchi *et al.*, 1999). It is therefore possible to determine total nitrifying activity (ammonium oxidation plus nitrite oxidation) by using three sets of subsamples. One is treated with an ammonium oxidation inhibitor, one is treated with a nitrite oxidation inhibitor, while the third set acts as a control series. The subsamples are incubated in the dark at in situ temperatures. A time series of nitrite measurements are made for each set of subsamples, and the change in nitrite with time, corrected by the control series, is presumed equal to the rate of ammonium oxidation or nitrite oxidation depending on the inhibitor used.

One possible cause for concern is that blocking ammonium oxidation may affect nitrite oxidation rates by reducing the supply of substrate. However, the half-saturation constant (K_s) for nitrite oxidation in natural nitrifying communities has been estimated at 0.07 μmol L^{-1} (Olson, 1981a), similar to that for ammonium oxidation. Nitrite oxidation should therefore be first order, other than in the euphotic zone. Also, dark incubations may release the nitrifying community from light inhibition, and lengthy incubations may be required to produce detectable changes in nitrite concentration such that conditions inside the bottle may become unrepresentative of the natural environment. Nonetheless, this approach is relatively simple to implement and requires no specialised equipment

apart from the equipment required to perform colorimetric nitrite analyses. Consequently, this approach to nitrification rate measurement has been widely adopted, even in oligotrophic and mesotrophic regions (Bianchi *et al.*, 1999).

3.1.3. N-Serve sensitive ^{14}C-bicarbonate incorporation

This method was designed to provide a highly sensitive assay of ammonium oxidation. Chemoautotrophic nitrifying bacteria convert CO_2 into organic carbon using energy derived from the oxidation of nitrogen compounds. Ammonium oxidation rates can be estimated by the difference in dark incorporation of $H^{14}CO_3$ between water samples with or without the addition of the ammonium oxidation inhibitor, N-Serve (Billen, 1976; Somville, 1978; Owens, 1986). The results are often reported in $\mu g\ C\ L^{-1}\ h^{-1}$ for direct comparison, but for estimating actual nitrification rates, an empirically derived conversion factor (mol N oxidised: mol C fixed) must be used. Unfortunately, it seems that this ratio can vary widely between species of nitrifying bacteria and with respect to their growth phases. Reported conversion factors obtained from rivers, estuaries and seas range from 5.9 - 14.3 (Somville, 1978, 1984; Owens, 1986; Berounsky and Nixon, 1990; Feliatra and Bianchi, 1993).

3.1.4. ^{15}N-tracer technique

Nitrifying activity can be measured directly by the transfer of a ^{15}N tracer from the substrate pool (ammonium) to the product pool (nitrite or nitrate). Water samples are incubated with the addition of a ^{15}N-labelled precursor such as $^{15}NH_4Cl$ under *in situ* conditions. After incubation, the particulate matter is removed by filtration. ^{15}N-labelled nitrite is then extracted from the filtrate using an azo dye complexation method (Wada and Hattori, 1972; Olson, 1981; Ward *et al.*, 1982) in which the N=N component of the

dye consists of one N atom from the reagent and one N atom from the ambient nitrite. The dye is then extracted from the sample and transferred to a glass fibre filter which is combusted using the micro-Dumas method (Barsdate and Dugdale, 1965) converting the organic dye to N_2 gas. The ^{15}N:^{14}N ratio of the resulting nitrogen is then determined by isotope ratio mass spectrometry. ^{15}N-labelled nitrate can be analysed using the same technique by first reducing the nitrate to nitrite in a copper-cadmium column.

The ^{15}N-tracer method is advantageous in that, unlike inhibitor methods, there is little perturbation to nutrient cycling within the incubated samples. Also, the analytical method is highly sensitive so that relatively short incubations are required, minimising bottle effects. On the other hand, the procedure is complicated and requires the use of expensive, highly specialised equipment.

3.2. Measurement of nitrification rates in this study

In the Bedford Basin study, which is further described in Chapter Five, ammonium oxidation rates were measured using chlorate inhibition of nitrite oxidation (the "chlorate block" method). This method is attractive because it is simple to implement and requires little specialised equipment beyond a spectrophotometer. More important, nitrite measurements are rapid to perform and can be run concurrently with N_2O measurements by a single operator. It has therefore been possible to obtain N_2O production rates and nitrification rates for the same seawater samples over similar incubation periods.

For each depth sample, eight subsamples were collected in 300 mL black biological-oxygen-demand bottles following the method used for Winkler sample collection (described below). For four of the bottles, 1 mL of sodium chlorate solution was added prior to stoppering to give a final ClO_3^- concentration of 10 mmol L^{-1}. The remaining

four bottles were left untreated as control samples. The bottles were then stored in an insulated box containing ice and transported to the laboratory within one hour of sample collection. All samples were then incubated in the dark at *in situ* temperature. At intervals of about 4 hours, one control sample and one sample containing chlorate were analysed for nitrite using the manual colorimetric method of Hansen and Koroleff, (1999). 50 mL of sample was transferred from the incubation bottle to a 125 mL flask and 1mL each of the reagents, sulphanilamide and N-(1-naphthyl)-ethylenediamine dihydrochloride (NED) were added, allowing at least 15 minutes but no more than 1 hour for the colour to develop. Sample absorbance at 540 nm was measured in a 10-cm pathlength cell with a precision of 1%. Ammonium oxidation rates were obtained from a linear regression of the blank-corrected increase in nitrite concentration over time. A five point calibration curve was constructed using prepared NO_2^- standards in the range 0.1 - 2 μM. The working standards were prepared each day from a 1 mM stock solution made up from dried, analytical grade sodium nitrite, stored for a maximum of 1 month at ~4 °C. In practice, no significant change in nitrite concentration over time was seen in sets of control subsamples, suggesting that ammonium oxidation and nitrite oxidation rates in the Bedford Basin were closely matched. This is not an uncommon finding in that part of the water column between the base of the euphotic zone and the primary nitrite maximum (Ward *et al.*, 1984; Dore and Karl, 1996; Bianchi *et al.*, 1999).

Accuracy in nitrite determination may be affected by impurity or partial decomposition of the nitrite standard, however the errors introduced by either of these factors will be systematic and should not affect the overall precision of the method.

3.3 Dissolved oxygen determination

3.3.1. The standard Winkler method

Dissolved oxygen concentration was routinely determined by a modified Winkler method. Seawater samples for oxygen analysis were collected from the Go-Flo sampling bottle following sample collection for N_2O and nutrient analysis. In this way, the possibility of contaminating the latter samples by the use of rubber tubing on the sample bottle outlet was minimised. The sample collection procedure is as follows: A ~30 cm length of silicon tubing is attached to the outlet valve of the Niskin bottle and the valve opened. After all air bubbles have been flushed, a small amount of sample water is used to rinse a BOD bottle, while the surgical tubing is pinched to control the flow. With the tube fully inserted, a steady flow of water is allowed to fill the bottle then overflow by two volumes. In the last few seconds of this procedure, the tube is fully withdrawn. One mL each of saturated solutions of manganese chloride and alkaline iodide are then immediately injected into the seawater sample using plastic tuberculin syringes. Care is taken to just immerse the syringe tips in the surface of the sample to avoid entraining air bubbles in the flow of reagent. Following the addition of reagents, the stopper is rinsed with sample, dropped into position, and the bottle inverted several times to mix the reagents. Filled bottles are stored in the dark until analysis to avoid photochemical effects.

3.3.2. Spectrophotometric Determination of Dissolved Oxygen at Low Concentrations

High-precision measurements of dissolved oxygen in seawater are usually made by a modification of the classic Winkler method. However at low oxygen concentrations

(<20μM), contamination from the surrounding air during the conventional sampling procedure, described above, becomes a concern. Consequently, the standard Winkler method is thought to overestimate dissolved oxygen concentrations within hypoxic environments (Tiedje, 1988).

The following spectrophotometric method for oxygen determination is adapted from Broenkow and Cline (1969) and Duval *et al.* (1974). It is specifically designed to enable high-precision, low-sample-volume analysis of low-oxygen water, and minimise the problems associated with air contamination.

a) Simplified reactions

As in the classic Winkler method, a basic, divalent manganese solution is oxidised by molecular oxygen.

1. $$4Mn^{2+} + 8OH^- \rightarrow 4Mn(OH)_2$$

$$4Mn(OH)_2 + O_2 + 2H_2O \rightarrow 4Mn(OH)_3$$

Upon acidification in the presence of excess iodide, an amount of the triiodide ion, chemically equivalent to the original dissolved oxygen is formed.

2. $$4Mn(OH)_3 + 4I^- + 12H^+ \rightarrow 4Mn^{2+} + 2I_2 + 12H_2O$$

$$2I_2 + 2I^- \rightarrow 2I_3^-$$

One mole of dioxygen therefore gives rise to two moles of the tri-iodide ion.

b) Procedure

Water samples are collected in 30 ml glass Luer-Lok syringes (Popper & Sons Inc.). A length of tubing from the sampling bottle or incubation vessel terminates in a 3-way Luer-Lok valve to which the glass syringe is connected. This arrangement facilitates sample collection and flushing without introducing air into the syringe. First, a volume

of water is allowed to flush through the tubing and valve to drive out residual air. The glass syringe with the plunger in the fully-depressed position is then attached to the valve and a water sample is drawn into the syringe then ejected. All air bubbles originating from air spaces in the syringe are expelled at this stage. The syringe is flushed again with a second sample, before over-filling by a few ml with the final sample. After the syringe is unscrewed from the Luer-Lok fitting, the plunger is then carefully depressed to the calibrated 30 ml mark and reagents introduced to the syringe tip using 1 ml tuberculin syringes (Becton, Dickinson & Co.) and 21 gauge needles. 0.1 ml each of manganous chloride solution and alkaline iodide solution are injected in turn. The syringe tip is sealed with a gloved finger and the syringe shaken between each addition. The syringe is then capped and stored in the dark with the capped end upright until analysis, allowing the precipitate to settle. Immediately prior to analysis, the cap is removed and 0.1 ml of 10 N sulphuric acid injected into the syringe barrel, and the syringe shaken once more until the precipitate is dissolved. The resulting tri-iodide concentration is measured spectrophotometrically in a 1 cm pathlength cell by the absorbtion of UV light from a deuterium lamp at 352 nm.

c) Calibration

All standard and blank determinations are carried out using the same syringe and reagent volumes. Volume changes due to the addition of reagents will therefore be the same throughout and not corrected for independently. The iodate ion is used for the primary standard as in the conventional Winkler method. In the presence of an acidified iodide solution, one mole of iodate results in the formation of 3 moles of tri-iodide.

3. $$IO_3^- + 5I^- + 6H^+ \rightarrow 3I_2 + 3H_2O$$

$$3I_2 + 3I^- \rightarrow 3I_3^-$$

One mole of iodate therefore produces an amount of tri-iodide equivalent to that produced in reactions 1 and 2 by 1.5 moles of dioxygen.

A primary standard solution is made by dissolving 0.214 g of oven-dried (~110°C) analytical grade KIO_3 in 1L of de-ionised water to give an iodate concentration of 1 mol L^{-1}. Working standards in the range 1 – 20 umol IO_3^- L^{-1} are prepared from this solution as required. A working standard solution is drawn into the 30 mL glass syringe which is first rinsed with the solution. 0.1 mL each of sulphuric acid, alkaline iodide and manganous chloride reagents are then injected in that sequence, and the syringe shaken well after each addition. The absorbance is measured immediately to avoid photochemical effects. A calibration plot is linear over the range 0 - 20 μmol IO_3^- L^{-1}. A small absorbance results from the optical properties of the reagents and traces of free iodine in the alkaline iodide solution, therefore a reagent blank is measured in a similar manner as the standards, substituting deionised water for the standard solution.

It is also necessary to quantify the amount of oxygen contained in the reagents. For this purpose, around 1L of seawater was purged overnight with a flow of about 20 mL min^{-1} UHP nitrogen to remove as much dissolved oxygen as practically possible. A 30 mL sampling syringe was flushed and filled with this water, then 0.1 mL volumes of reagents added following the same method as for oxygen sampling, and the absorbance measured. This procedure was repeated using 0.2 mL volumes of reagents and then repeated again with 0.3 mL volumes of reagents. A regression of absorbance against reagent volume was then used to derive the amount of oxygen added with the reagents.

3.4. Determination of ammonium

Samples for ammonium determination were collected in 125 mL high density polyethylene sample bottles, previously cleaned with chromic acid and rinsed with deionised water. Analysis was performed either within about 2 hours of sample collection, or the samples were frozen for up to 2 weeks prior to analysis. Ammonium concentrations were measured following a method described by Parsons *et al.*, (1984), adapted from Solorzano (1969). Water samples were treated with phenol in the presence of sodium nitroprusside and an alkaline oxidising solution comprising sodium citrate, sodium hydroxide and hypochlorite. A commercial bleaching agent containing 5.25% NaOCl was used as a hypochlorite source. Ammonium reacts with hypochlorite in an alkaline solution (pH 8–11.5) to give monochloramine (NH_2Cl) which further reacts with phenol to give indophenol blue. Nitroprusside ions ($[Fe(CN)_5NO]^{2-}$) catalyse the reaction, which is further speeded by a reaction temperature of ~ 40 °C. The reaction mechanism is reportedly not fully understood, however the sum of NH_4^+ and NH_3 is measured. After 30 minutes at 40 °C had been allowed for the blue colour to develop, the samples were allowed to cool for a further 30 minutes and the absorbance at 640 nm was measured in a 10 cm pathlength cell. A major concern in ammonium analysis is atmospheric contamination derived from sources such as cleaning agents and ammoniacal solutions. All glassware was therefore rinsed in acid prior to use, and flasks containing samples and standards were sealed with parafilm for the duration of the reaction period. Analytical precision was typically ± 5% for 3 replicates.

Calibration

A 1 mM primary ammonium sulphate standard was prepared by dissolving 132.1 mg of dried analytical grade ammonium sulphate in 1 L deionised water. This analysis is subject to a salt effect causing the blue colouration produced by a given amount of ammonium to be less in seawater than in freshwater (Hansen and Koroleff, 1999). Working standard solutions were therefore prepared using low-nutrient-seawater (LNSW) this being either surface water from the Sargasso Sea region, or surface water obtained from the Bedford Basin during summer and filtered through a 0.45 micron pore-size filter. The ammonium content of the LNSW was assessed prior to standard preparation by comparing the absorbance of a triplicate set of reagent blanks made with the LNSW with a triplicate set of blanks prepared using freshly produced deionised water from an analytical grade water purification system (Millipore).

3.5. Determination of nitrate

Samples for nitrate determination were collected, as for ammonium, in acid cleaned 125 mL high density polyethylene sample bottles. Duplicate samples were normally collected and stored frozen for up to about 1 month before analysis. Nitrate was determined manually by the reduction of nitrate to nitrite in a ~30 cm long × 8 mm i.d. reduction column packed with copper-coated cadmium granules (Wood *et al.*, 1967). A 50 mL seawater sample was made up to 100mL volume with an ammonium chloride buffer solution. This sample solution was then passed through the reduction column at a flow rate of 10 mL min^{-1}. The first 40 mL of eluant was discarded, and the next 50 mL collected and analysed for nitrite as previously described, measuring absorbance in a 1 cm cell at a wavelength of 540 nm. Prior to each series of analyses, the column was

activated by passing about 200 mL of ammonium chloride buffer containing 100 μmols L^{-1} nitrate, then rinsed with a further ~100 mL of buffer solution. The efficiency of the reductor (*E*) was periodically checked by analysing triplicate prepared standards of 10 μmol L^{-1} nitrate and 10 μmol L^{-1} nitrite where;

$$E = 100 \cdot \frac{[\text{nitrate}]}{[\text{nitrite}]}$$

The column was reactivated or renewed if E declined to around 90%. A calibration curve was established by analysing a series of nitrate standards in the range 0-30 μmol L^{-1} made by diluting a 1 mmol L^{-1} stock solution of dried analytical grade potassium nitrate with deionised water.

3.6. CTD measurements

Weekly depth profiles of conductivity, temperature and pressure were made at the Compass Buoy Station, Bedford Basin using a Seabird SBE 25-03 CTD (Li and Dickey, 2001). In addition, photosynthetically-active radiation (PAR) was measured using a LiCor LI 193SA spherical quantum sensor.

3.7. Statistical analysis

Statistical analysis of the data was performed with Microsoft Excel 5.0. Nitrous oxide production/degradation rates and nitrification rates were determined from non-weighted linear regression of measured concentrations versus time, fitted by the sum of least squares. The estimated uncertainty of a rate is the standard deviation of the slope *m* (called the "standard error of slope" in Excel) generated by the LINEST function.

Where reported, the significance of a slope at the 95% confidence level is given by the p-value generated by Excel in the regression analysis add-in. The regression slope coeffient *m* is not significantly different from a zero slope coefficient where $p > 0.05$.

The equations used by Excel to generate these statistics are shown in Appendix I.

Propagation of errors

The errors of individual measurements are propagated by the simple method described by Miller and Miller (1993).

Linear combinations

The standard deviation of the sum or difference of independent measurements *a* and *b* is calculated from the sum of the variances (squares of standard deviations) of the individual measurements.

$$\sigma_y = \sqrt{(\sigma_a)^2 + (\sigma_b)^2}$$

Multiplicative expressions

In an expression of the form *Rate a* / *Rate b*, where the rates *a* and *b* are independently measured, there is a relationship between the squares of the relative standard deviations (coefficients of variance)

$$\frac{\sigma_y}{y} = \sqrt{\left(\frac{\sigma_a}{a}\right)^2 + \left(\frac{\sigma_b}{b}\right)^2}$$

Chapter 4

Nitrous oxide production rates and concentration profiles in the Labrador Sea and Scotian Shelf surface waters

4.1. Introduction

The Labrador Sea is one of only three regions in the world where deep winter convective mixing occurs, the other two being the Greenland Sea and the Weddell Sea. It is therefore an important component of the global thermohaline circulation, popularly known as the "Great Ocean Conveyer" (Broecker, 1991). As a consequence, a great deal of effort is being directed towards quantifying the magnitude of anthropogenic carbon dioxide sequestration in the Labrador Sea, resulting from its dissolution in cold surface water and subsequent transport to the deep (e.g. Tait *et al.*, 2000).

In contrast, very little is known about marine nitrous oxide in this region. Available N_2O data are very sparse, being mainly confined to some continuous underway measurements of surface N_2O obtained during the Transient Tracers in the Ocean /North Atlantic Study 1981-83 (Weiss *et al.*, 1992). The measurements obtained by that study indicated that surface water nitrous oxide concentrations in this part of the North Atlantic sub-polar gyre were generally close to atmospheric equilibrium. Perhaps as a result of these findings, and perhaps also in part due to the relatively inhospitable nature of the region outside the brief summer, little further interest in this sub polar region has been shown by N_2O investigators. Nevertheless, the Labrador Sea, while largely ice-covered during the winter, is capable of supporting high rates of primary production, up to 80 g C m^{-2} $month^{-1}$, during the spring bloom that takes place in May and June (Longhurst, 1998). Although the productive season is short lived, there is clearly some potential for

nitrogen cycling to occur in the near-surface ocean, with accompanying N_2O production from nitrification.

The Arctic is also thought to be extremely vulnerable to projected climate change and likely to respond rapidly and more severely than any other area on Earth, with consequent effects on sea ice cover and water column stability (Everett and Fitzharris, 1998). The role of the Arctic sub-polar region in the global N_2O budget is currently uncertain, and it is as yet unclear whether the Labrador Sea is a net source or sink for atmospheric N_2O. It is therefore important to establish a baseline of information on N_2O behaviour in this region so that future changes can be assessed.

4.1.1. Study area

The Labrador Sea covers an area of about 10^6 km^2, being somewhat arbitrarily defined as the sea bounded to the north by the 66° N line of latitude that joins Greenland and Baffin Island, and to the south by a line from the southern tip of Greenland to Cape St. Charles on the coast of Labrador. The Labrador Sea forms the western part of the North Atlantic Sub polar Gyre and is bounded by three major currents forming a strong cyclonic circulation gyre. These are the West Greenland Current to the east, the Labrador Sea Current to the west, and the Gulf Stream with its extension, the North Atlantic Current, to the south. These currents encompass a wide range of sea surface temperature. Figure 4.1 shows a monthly composite sea surface temperature for June 2001 obtained from the Oceans Pathfinder Advanced Very High Resolution Radiometers (AVHRRs) on board the National Oceanic and Atmospheric Administration (NOAA) polar-orbiting satellites. The image clearly shows the cold West Greenland Current and Labrador Current fringing

the central Labrador Sea, with the Labrador Current extending south towards the much warmer Gulf Stream.

In winter the average mixed layer depth for this province extends to >500 m, shoaling to 20 m in the summer months (Longhurst, 1998). The photic depth ranges from around 20 to 60 m, although this is highly dependent on ice cover.

The measurements described in this chapter were made on board the Canadian Coast Guard Vessel *Hudson* during the Labrador Sea cruise of spring 2001. This cruise was conducting operations in support of ongoing scientific programmes, including the Climate Variability and Predictability project, and the Labrador Sea biological programme in support of the Department of Fisheries and Oceans greenhouse gas research. Figure 4.2 shows the location of the sampling stations. The cruise track can be divided into three geographically distinct regions. Station 34 was situated above the Scotian Shelf break, Station 44 was in the Gulf of St. Lawrence while the remainder of the stations fell along a transect of the southern Labrador Sea.

4.2. Methods

At the time of this cruise, the analytical method described in Chapter 2 was in an early testing stage. As a result, the measurements made on this cruise concentrated on the production of nitrous oxide from ammonium oxidation in the upper 100m of the water column. Seawater was normally collected from shallow (< 120m) CTD casts at stations occupied each morning for primarily biological measurements. Table 4.1 shows the station locations and sampling details. For each station, three depths were chosen for the incubation experiments, usually 20, 60, and 100m or near-equivalent depths depending on the samples available. Station 98 was an exception, and samples were taken from 35,

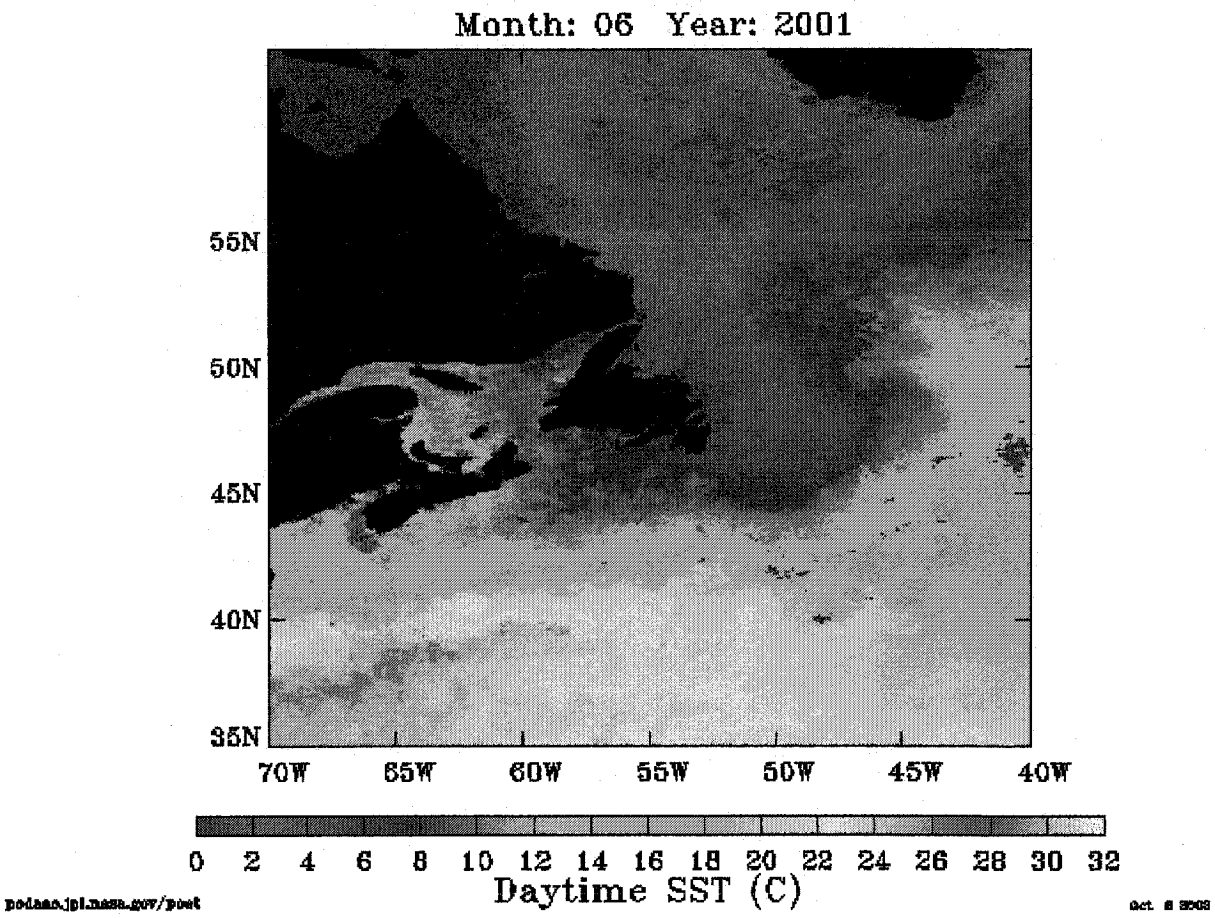

Figure 4.1.
Composite daytime sea surface temperature plot of the study area for June 2001. This multi channel sea surface temperature image was obtained from the website http://podaac.jpl.nasa.gov/sst, maintained by the NASA Physical Oceanography Distributed Active Archive Center (PO.DAAC), at the Jet Propulsion Laboratory, Pasadena, CA. 2003. Data for the image were provided by the Naval Oceanographic Office.

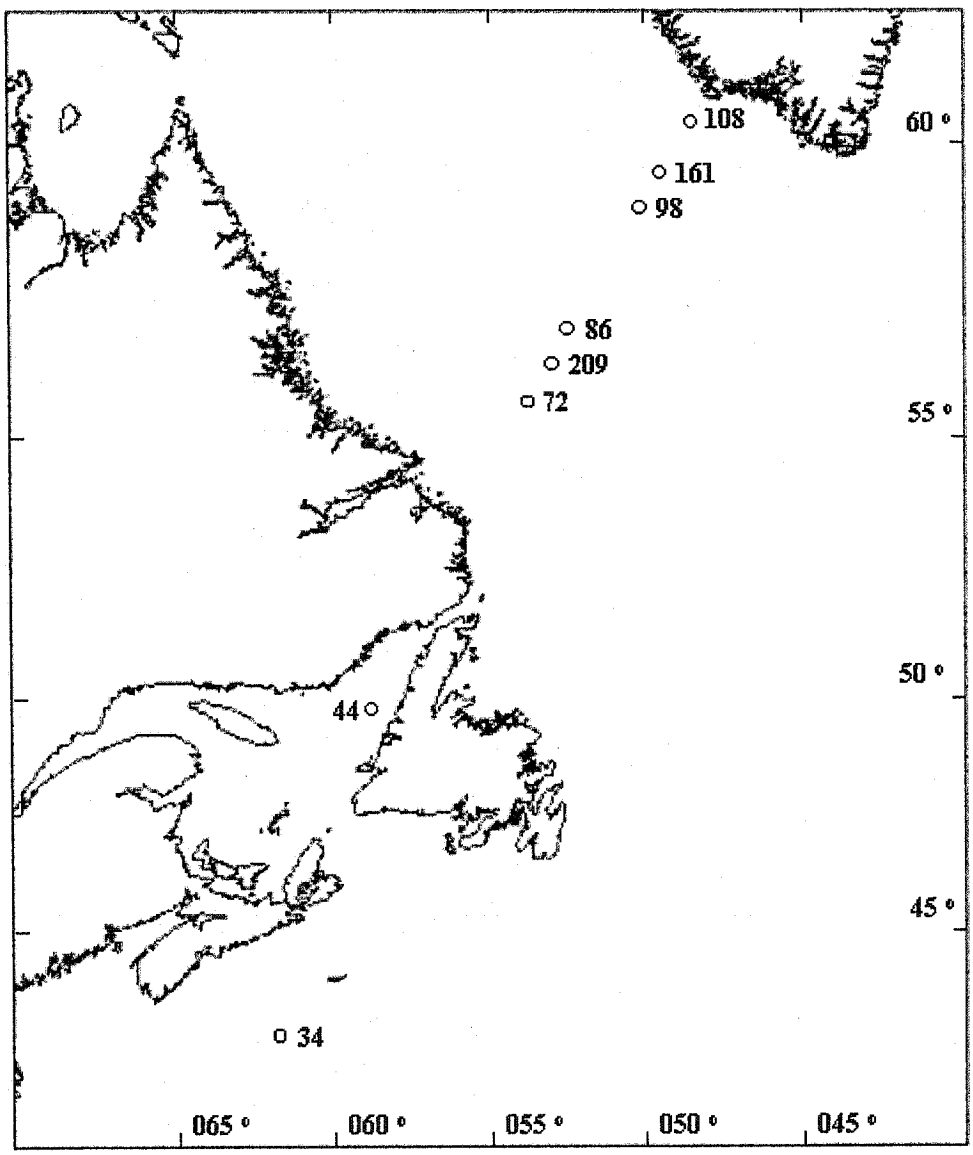

Figure 4.2. Sampling stations on the Hudson 2001 cruise

Date	Station	Latitude	Longitude	N_2O measurements
June 1	34	42.528	-61.400	Production rates from 20, 60 and 100m
June 3	44	49.843	-58.453	Production rates from 20, 50 and 80m Additional concentration measurements
June 5	72	55.615	-53.634	Production rates from 20, 60 and 100m Additional concentration measurements
June 6	86	56.696	-52.490	Concentration profile
June 7	98	58.640	-50.417	Production rates from 35, 240 and 680m Additional concentration measurements
June 8	108	60.567	-48.263	Concentration profile
June 9	161	59.065	-49.956	Production rates from 20, 60 and 100m Additional concentration measurements
June 10	209	56.114	-53.116	Concentration profile

Table 4.1. Details of station locations and the measurements obtained from the Labrador sea cruise

240 and 680m to compare shallow with deep waters. For each depth, two 100 mL samples were incubated with 100 μmol L^{-1} $^{15}NH_4^+$. Control samples consisting of surface seawater poisoned with mercuric chloride were also periodically analysed to assess analytical drift. Additional samples were obtained from intermediate depths for N_2O concentration measurements, to provide further detail to depth profiles. N_2O production rates were found to be very low, and incubation times exceeding 24 hours were required to show changes in $^{15}N_2O$ concentrations. As a result, sets of incubation measurements were initiated on alternate days. On intervening days, samples were obtained in the morning to provide a depth profile of N_2O concentration, and analysed as instrument time became available.

4.3. Results and discussion

4.3.1. Temperature and salinity

Temperature and salinity profiles are shown in Figure 4.3. Stations 34 and 44 have highly contrasting TS characteristics, which render them distinct from stations on the Labrador Sea transect. Station 34, located above the Scotian Shelf break, shows considerable variability with depth in both temperature and salinity. The most striking feature is a core of relatively warm (14 °C) saline (> 35) water at 50 m depth. This has resulted in a reversed thermocline below the colder, fresher mixed layer. This core is most likely of Gulf Stream origin, given the proximity of this station to the "North Wall" of the Gulf Stream. In contrast, Station 44 has a shallow thermocline below which lies extremely cold (~ 0 °C) water. This station is approximately at the junction of the Gulf of St. Lawrence and the Strait of Belle Isle over the 200m depth contour and the water properties here are greatly influenced mainly by the very cold, low salinity (30-34),

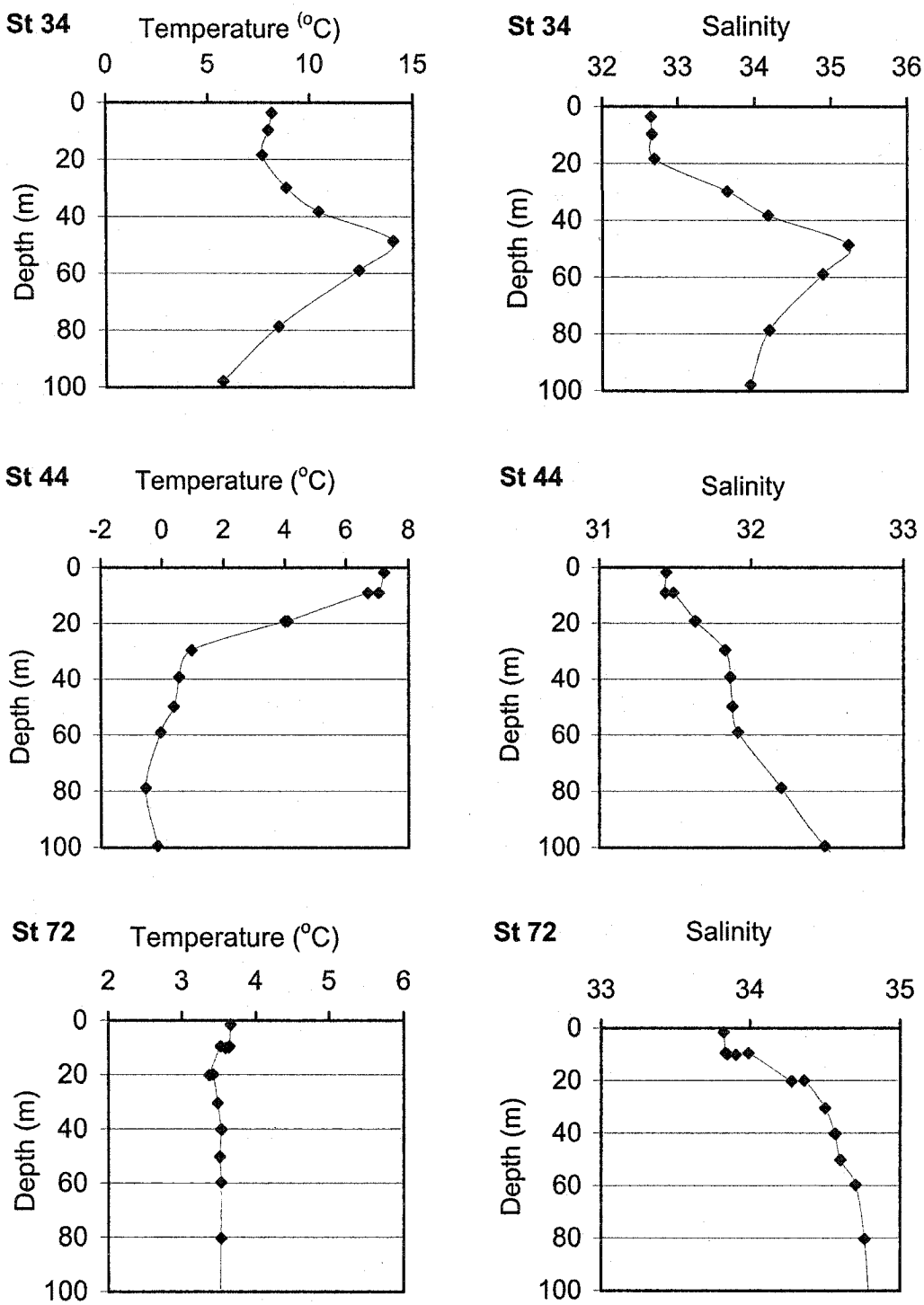

Figure 4.3. Temperature and salinity profiles for the Labrador Sea stations 34, 44, and 72

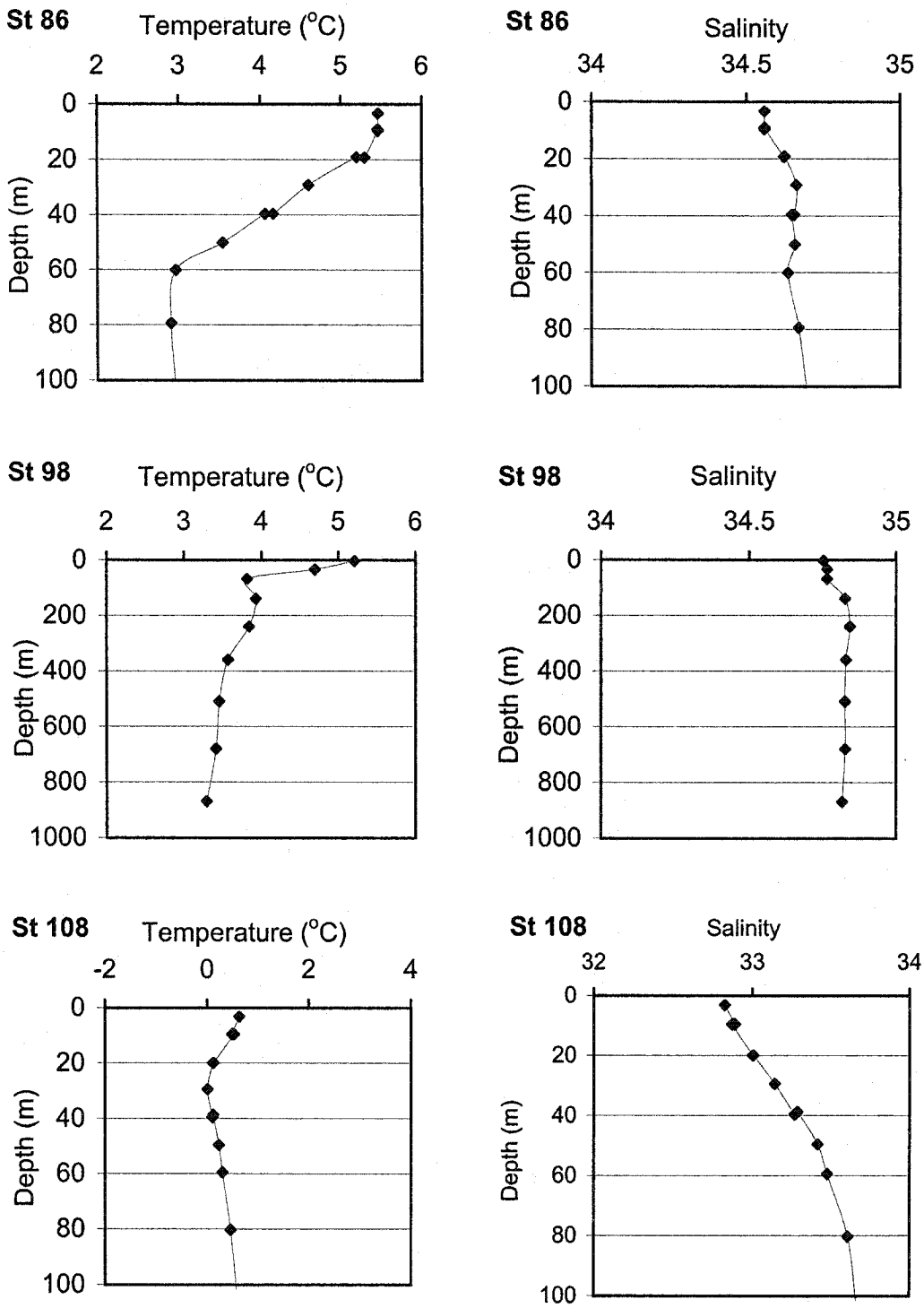

Figure 4.3 (Continued). Temperature and salinity profiles for the Labrador Sea stations 86, 98 and 108

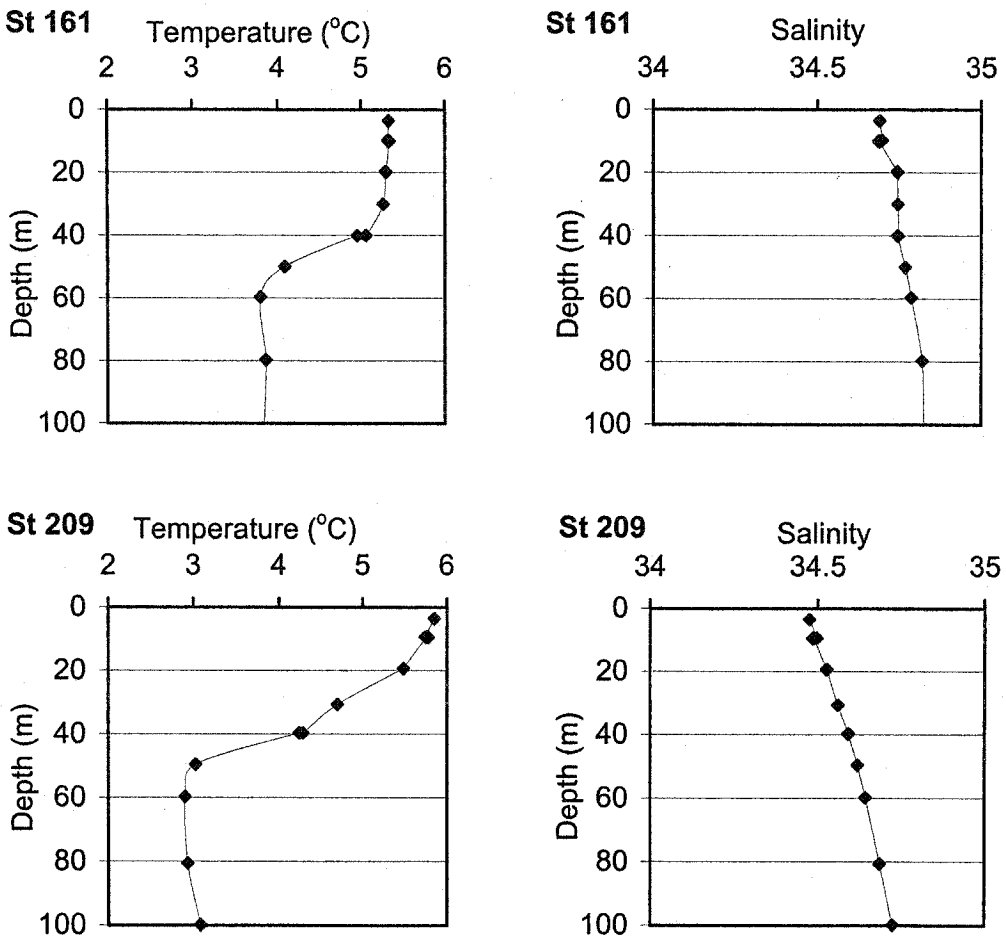

Figure 4.3 (Continued). Temperature and salinity profiles for the Labrador Sea stations 161 and 209

Labrador Current entering the Gulf of St. Lawrence through the Strait of Belle Isle. Stations 72, 86, 98, 161 and 209 are located within the central Labrador Sea and have similar water characteristics including a sub-thermocline water temperature around 3-4°C, and near uniform salinity of around 34.5. While the majority of this group of stations have surface-water temperatures around 5-6°C, station 72 shows a shallow surface layer of colder, less saline water, possibly as a result of melting sea-ice. Finally, station 108, although lying on the Labrador Sea transect, is located over the Greenland shelf. Here, the upper 100 m of the water column is very cold (0-0.6°C), and rather less salty than the central Labrador Sea area, probably due to the influence of the West Greenland Current.

4.3.2 Ammonium

Figure 4.4 shows ammonium profiles for stations 44 to 209. Data are not available for station 34. All stations showed low levels of ammonium, usually well below 1 μmol L^{-1}, in the surface mixed layer, consistent with utilisation by phytoplankton in the euphotic zone. Stations 44, 86, 161 and 209 showed subsurface ammonium maxima at about 50-60 m depth, while the profile for station 98 also suggested a subsurface maximum at 70 m. The depth resolution for this latter station was, however, much lower than the others, with only four measurements in the surface 200-m, so it is possible that the true maximum value lay at a shallower depth, in line with contiguous stations. The appearance of subsurface ammonium maxima at these stations suggests that this may be a characteristic feature of the central Labrador Sea in summer. A similar subsurface ammonium maximum is a recurrent phenomenon at Station Papa in the Pacific Ocean (Saino *et al.*, 1983). The Station Papa feature has been reproduced by the coupled

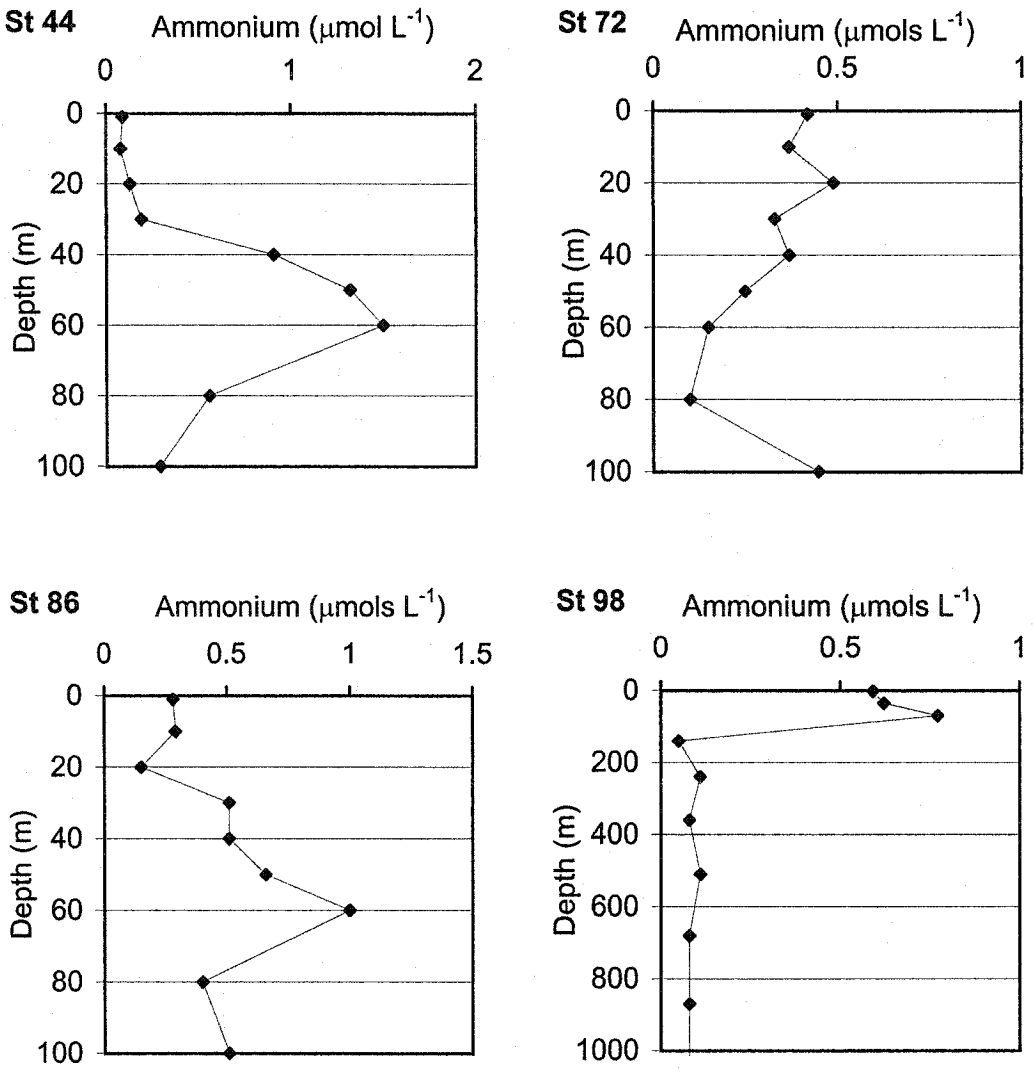

Figure 4.4. Depth profiles of ammonium concentration for stations 44, 72, 86 and 98

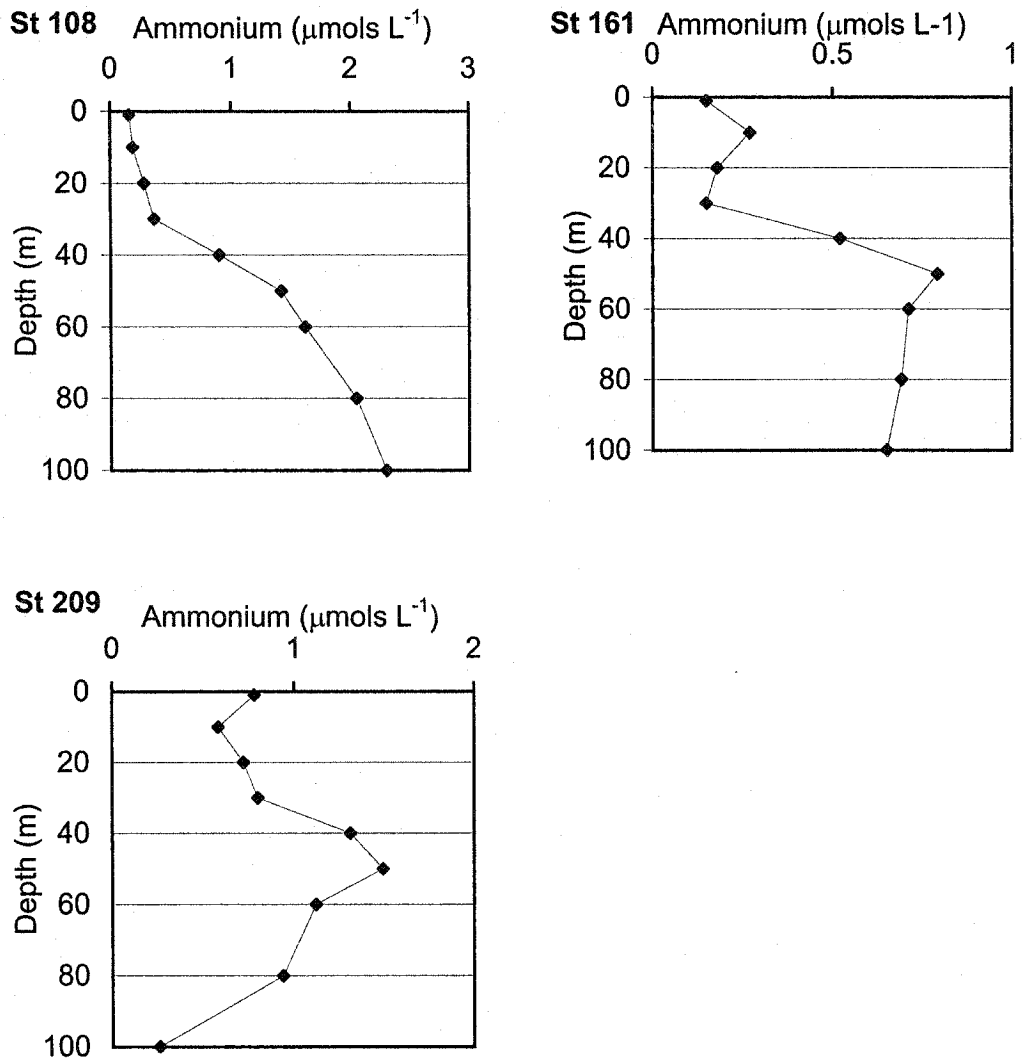

Figure 4.4. Depth profiles of ammonium concentration for stations 108, 161 and 209

ecological-physical model of Kawamiya *et al.* (1995), and appears to be sustained by two major subsurface ammonium sources: zooplankton excretion and the degradation of dissolved organic nitrogen. More information will be needed to establish whether these processes are also responsible for the observed ammonium maxima in the central Labrador Sea.

The ammonium profiles for stations 72 and 108 were rather different from the others. At station 72, ammonium did not exceed 0.5 μmol L^{-1} in the upper 100 m and showed a minimum at 80 m. For station 108 situated on the Greenland shelf, ammonium measurements showed a classic nutrient profile with low concentrations above the thermocline, and a steep gradient below the thermocline rising to 2.3 μmol L^{-1} at 100 m, the highest recorded concentration in this data set. This latter feature suggests that ammonium utilisation below the thermocline was low compared to its rate of supply.

4.3.3 Ambient nitrous oxide

Figure 4.5 shows depth profiles of ambient nitrous oxide concentrations. Also plotted as reference are the atmospheric equilibrium concentrations of N_2O (C_a) at *in situ* temperature and salinity calculated using the solubility coefficient F (mol L^{-1} atm^{-1}) of Weiss and Price (1980) in moist air at a total pressure of one atmosphere, and assuming an atmospheric N_2O mixing ratio of 318 ppbv. Concentrations of nitrous oxide in surface waters are also reported here as percentage saturation (%sat):

$$\%\text{sat} = 100\ C_w/C_a$$

Where C_w is the measured bulk seawater concentration of N_2O near the interface (mol m^{-3}). Dissolved nitrous oxide was supersaturated in surface waters at all stations with a

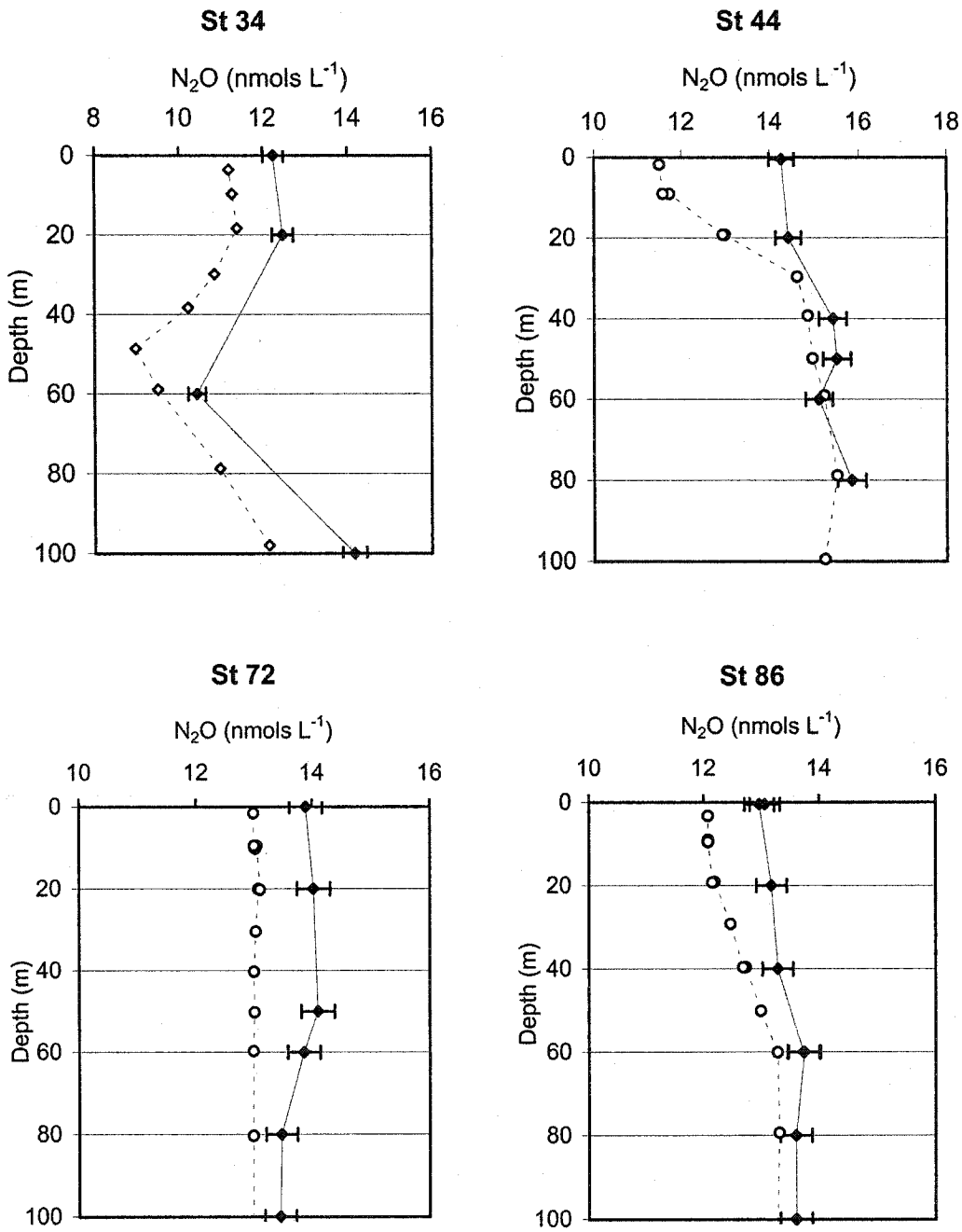

Figure 4.5. Depth profiles of nitrous oxide concentration for stations 34, 44, 72 and 86. Solid lines represent measured concentrations while dashed lines represent the concentration at atmospheric equilibrium

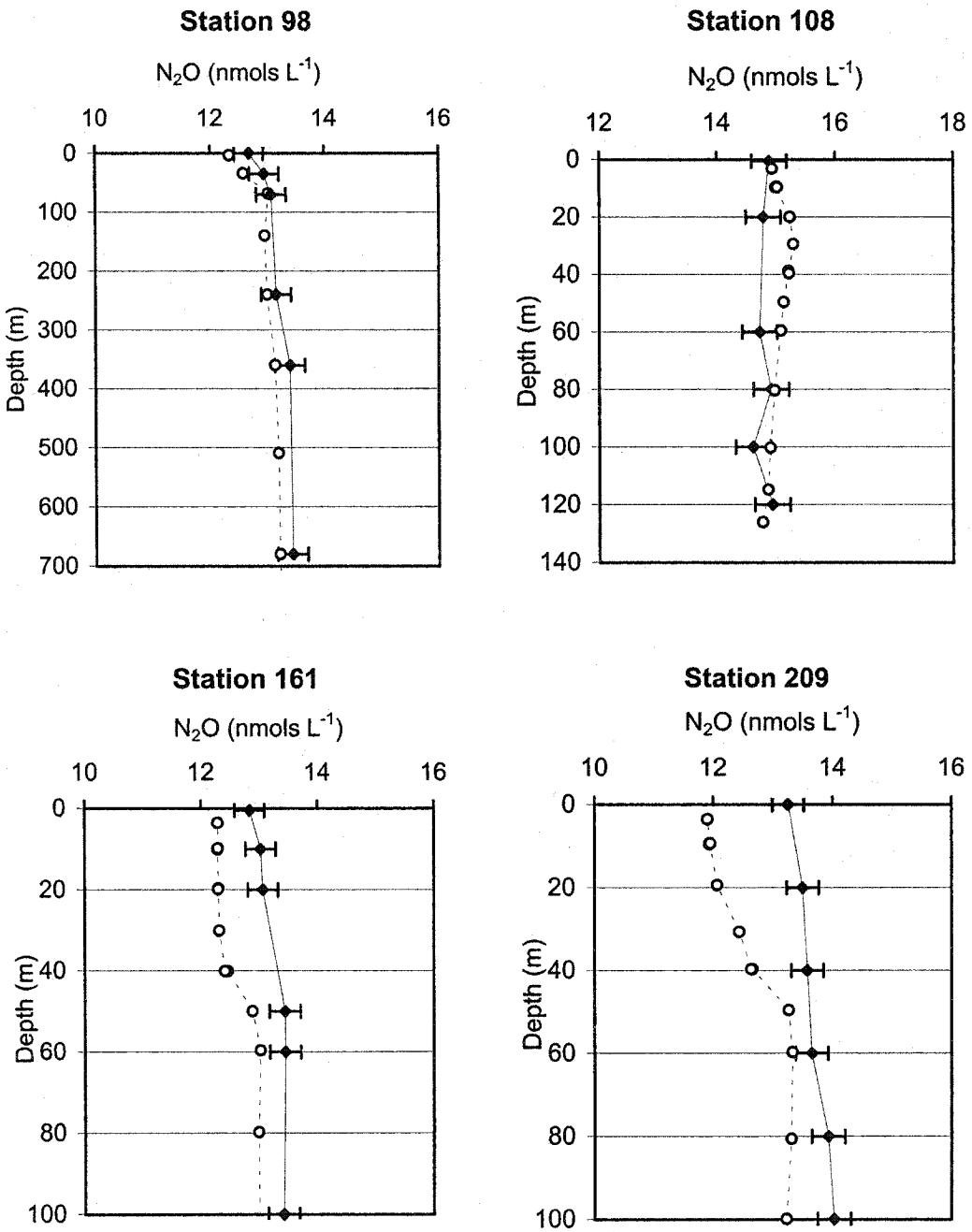

Figure 4.5 (Continued). Depth profiles of nitrous oxide concentration for stations 98, 108, 161 and 209. Solid lines represent measured concentrations while dashed lines represent the concentration at atmospheric equilibrium

mean value of 108 %, whereas the mean saturation for the Labrador Sea transect (Stations 72-209) was slightly lower at 105%. These values are very similar to those from a range of marginal seas and oceanic regions, shown for comparison in Table 4.2, and are consistent with observations that, apart from estuarine and upwelling regions, most ocean surface water is close to atmospheric equilibrium with a mean N_2O saturation of around 103 - 104% (Weiss, 1978, Butler *et al.*, 1989). With respect to the depth profiles, Station 34 was supersaturated throughout the range of depths measured, but with the greatest value at 100 m. For the other stations, the degree of supersaturation was greatest in the top 40-60 m, while the deeper waters were close to atmospheric equilibrium. This pattern of N_2O distribution has more than one feasible explanation. The first is that a biological production mechanism, presumably nitrification, is generating N_2O in the surface ocean. This possibility will be examined further using the production rate measurements. An alternative explanation is that the observed supersaturation is at least partially due to the seasonal surface warming of a cold uniform water column at atmospheric equilibrium. This could result in a transient supersaturation, disappearing as re-equilibration with the atmosphere takes place. In an attempt to quantify this temperature effect, monthly average sea surface temperatures were obtained for an area at approximately the midpoint of the Labrador Sea transect for the period March - September 2001. A relatively small area of 2° × 2° (56°N-58°N, 051°W-053°W) was chosen to exclude temperature anomalies caused by the Labrador and West Greenland currents. The data were collected by NOAA Pathfinder AVHRRs, quoted accurate to ± 0.3-0.5 °C. Figure 4.6a shows the spatially averaged sea surface temperature for this area, while Figure 4.6b shows the corresponding N_2O solubility

Region	Mean N_2O saturation %	Reference
Central North Sea	104	Law *et al.*, 1992
Black Sea shelf waters	111	Amouroux *et al.*, 2002
Baltic Sea	103	Bange *et al.*, 1996a
Aegean Sea	105	Bange *et al.*, 1996b
Drake Passage	100	Rees *et al.*, 1997
West Pacific and East Indian oceans	102	Butler *et al.*, 1989
Atlantic and Indian oceans	104	Weiss, 1978
Labrador Sea	105	This study

Table 4.2. Comparison of mean N_2O surface water saturation values for a range of marginal sea and ocean regions

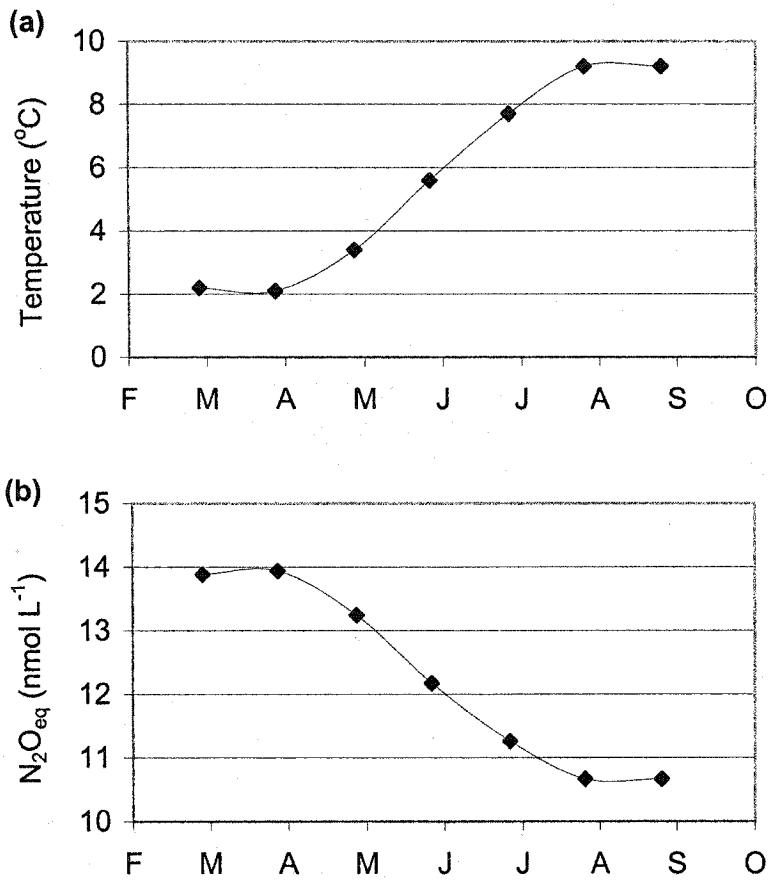

Figure 4.6. (a) Spatially averaged sea surface temperature in a 2° x 2° area of the central Labrador Sea derived from NOAA Pathfinder satellite data. (b) Corresponding N_2O solubility at atmospheric equilibrium (N_2O_{eq}) for a constant salinity of 34.5.

coefficient F at atmospheric equilibrium, assuming a constant salinity of 34.5. From the beginning of April to the beginning of August 2001, there was a linear increase in sea surface temperature of 1.8 °C per month resulting in a decrease in N_2O solubility of 0.82 nmol L^{-1} $month^{-1}$, or about 0.03 nmol L^{-1} d^{-1}. Assuming that the surface mixed layer remained isothermal to 20 m depth, and that the diffusive flux of N_2O across the thermocline was insignificant compared to exchange across the air/sea interface, then seasonal heating of the water column over this period could alone potentially sustain a mean sea to air N_2O flux of about 0.54 μmol m^{-2} d^{-1}.

4.3.4 N_2O production rates

Table 4.3 shows N_2O production rates from the five stations where water samples were obtained for incubation experiments. Only three samples showed N_2O production rates where the slope coefficient *m*, of the regression of $^{15}N_2O$ concentration against time, differed significantly from zero ($P<0.05$). These were the 100 m depth at Station 34 (27 ± 2 pmol L^{-1} d^{-1}), the 60 m depth at Station 72 (22 ± 3 pmol L^{-1} d^{-1}), and the 35 m depth at Station 98 (17 ± 1 pmol L^{-1} d^{-1}). Spatially, these results appear rather disparate and difficult to reconcile. However, a closer inspection does reveal some consistency. On no occasion was there significant N_2O production at 20 m depth, although this is not entirely unexpected. The temperature and salinity data show that in most cases, the upper mixed layer extended to around 20 m depth. As the photic depth for this cruise track is generally in the range 30 - 50 m in early summer, it is likely that photoinhibition will limit ammonium oxidation in the upper mixed layer. Ward (1985) found that ammonium oxidation rates were negatively correlated with light intensity at stations off the Washington coast. In addition, ammonium concentrations are generally very low in the

Station no.	Sample depth (m)	production rate (pmol L^{-1} d^{-1})	Error (± pmol L^{-1} d^{-1})	Significance P value
34 Scotian Shelf	20	-3.5	1.4	NS
	60	2.9	2.1	NS
	100	26.9	2.1	p<0.001
44 Gulf of St. Lawrence	20	1.9	1.6	NS
	50	-3.9	3.7	NS
	80	0.7	5.2	NS
72 Labrador Sea	20	7.6	7.4	NS
	60	21.6	3.4	p<0.001
	100	6.9	6.1	NS
98 Labrador Sea	35	17.2	0.7	p<0.001
	240	1.4	0.6	NS
	680	-1.9	0.9	NS
161 Labrador Sea	20	-1.3	1.2	NS
	60	-0.1	2.0	NS
	100	-1.0	2.1	NS

Table 4.3. N_2O production rates from ammonium oxidation. NS – not significant at p=0.05.

mixed layer due to uptake by phytoplankton with the result that nitrifying bacteria may be substrate limited.

Turning to the stations where nitrous oxide production was detected, Station 34 was surprising in that it showed the highest rate of production (27 pmol L^{-1} d^{-1}) measured on the cruise at 100 m, yet no significant production at 60 m. The temperature and salinity profiles for this station are however highly heterogeneous, with a peak in temperature and salinity centred at about 50 m. This is probably due to a core of high salinity Gulf Stream water, and, while there are no ammonium measurements for this station, one could speculate that water at 60m is relatively nitrogen-poor because of its origin in an oligotrophic region. As a result, ammonium oxidation is proceeding at a very low rate at 60m due to lack of available substrate, in contrast to 100 m where the water is colder and perhaps higher in nutrients. The depth profile of ambient N_2O shows the highest level of supersaturation at 100 m rather than in near surface water, which agrees with measurable production being found only at this depth.

The data from Stations 72 and 98 are in general agreement, with production rates of 22 and 17 pmol L^{-1} d^{-1} at depths of 60 and 35 m respectively. No significant production was detected at 100 m for Station 72, or at greater depths at Station 98. Stations 44 and 161 showed no significant N_2O production at any depth. In the case of Station 44, low temperature may have contributed to low levels of biological activity as sub-thermocline temperatures were only slightly above 0°C. The effect of low temperatures (<5°C) on marine nitrification is not well understood. Temperature has been proposed as an important environmental variable in explaining seasonal variations in estuarine rates of nitrification (Berounsky and Nixon, 1993). It has also been suggested that, in the long

term, nitrifying bacteria may acclimate to low temperatures so that other factors such as substrate availability become more important in regulating nitrification rates (Ward, 2000). In comparison to marine nitrification, the effect of temperature on ammonium removal by nitrifying bacteria in drinking water treatment is relatively well known. Bouillot *et al.* (1992) conducted measurements on the rate of ammonium removal in nitrification filters used to treat water from the Seine and Marne rivers (France) at temperatures ranging between 1 and 15 °C. Andersson *et al.* (2001) studied seasonal fluctuations in ammonium removal rates at a water treatment plant in Laval (Canada), where temperatures below 2 °C prevail for more than 4 months from late fall to early spring. Both studies found very similar relationships between temperature and nitrifying activity, as indicated by the rate of ammonium removal in sand filters, that are best described by the equation:

$$V_{T1} = V_{T2}\ e(k\,(T1\text{-}T2))$$

Where V_{T1} and V_{T2} are the ammonium removal rates at temperatures $T1$ and $T2$ respectively, and k is the temperature coefficient with a value of 0.122. If this relationship can be applied to marine nitrification rates, then the rate of nitrification at 0°C would be about 54% lower than that at 5°C

For Station 161, the reason for the lack of production is not obvious as this station was close to Station 98 where N_2O production was found, and appears to have very similar temperature and salinity properties.

4.4. Flux estimate

The flux F of N_2O across the air/sea interface was estimated for each sampling station using the simple equation:

$$F = k_w(C_w\text{-}C_a)$$

Where k_w is the gas transfer velocity (m s^{-1}) which is dependent on the degree of interfacial disturbance and the Schmidt number *Sc* of the gas in question, where *Sc* is the ratio of the kinematic viscosity of seawater and the diffusion coefficient. *Sc* was calculated according to the least squares third-order polynomial fit of *Sc* versus temperature for seawater given by Wanninkhof (1992).

The transfer velocity has been parameterised as a function of windspeed *U*, and two such parameterisations derived from wind tunnel experiments, tracer release experiments, and ocean ^{14}C gas transfer data are commonly used to estimate oceanic gas fluxes (Liss and Merlivat, 1986; Wanninkhof, 1992). However, a comparison of modelled N_2O surface distributions conducted by Suntharalingam and Sarmiento (1995) and Suntharalingam (1997) has shown that output generated by the formulae of Wanninkhof (1992) are more consistent with observed data. The relationship of Wanninkhof (1992) between gas transfer and a short-term steady windspeed is therefore adopted here and is represented by;

$$k_w \text{ (cm h}^{-1}) = 0.31u^2(Sc/660)^{-0.5}$$

where *u* is the windspeed at 10 m above the sea surface, *Sc* is the Schmidt number of N_2O in seawater at *in situ* temperature, and 660 is the Schmidt number of CO_2 in seawater at 20 °C. Windspeeds (knots) for each station were obtained from *Hudson's* logbook. These were estimated from observations of sea state according to the Beaufort Wind Scale, therefore the uncertainty in these estimates is probably quite high, perhaps around ± 5 knots (~2.5 m s^{-1}), and they are assumed to represent actual windspeeds at 10 m height. Table 4.2 shows windspeed data, surface seawater saturation, Schmidt

numbers, and calculated N_2O fluxes for the stations sampled. The mean sea to air flux for the Labrador Sea stations was 1.9 ± 1.3 μmol N_2O m^{-2} d^{-1}. Extrapolating this figure to the entire Labrador Sea (approximate area of 10^6 km^2) gives a flux of 1.9 ± 1.3 × 10^6 mol N_2O d^{-1}, or about 50 × 10^6 g N d^{-1}.

If it is assumed that no biological N_2O production occurs either in the surface 20 m, due to photoinhibition, or below 100 m due to substrate limitation, the average N_2O production rate required to sustain a steady state sea to air flux of 1.9 ± 1.3 μmol N_2O m^{-2} d^{-1} at steady state would be about 24 pmol N_2O L^{-1} d^{-1}. This is a minimum value, as there will be some downward flux of N_2O to deep water due to vertical eddy diffusion. As the data show only three depths where N_2O production was of this order, it may be concluded that *in situ* measured production rates were insufficient to sustain the estimated sea-to-air flux. However the apparent N_2O production due to seasonal mixed layer warming has already been estimated to be around 0.5 μmol N_2O m^{-2} d^{-1}, so the revised flux of biologically produced N_2O across the thermocline required to balance the loss to the atmosphere at steady state would therefore be about 1.4 μmol m^{-2} d^{-1}, or 17 pmol L^{-1} d^{-1}. Furthermore, the Labrador Sea flux estimate has a statistical uncertainty of about ± 70%, plus errors associated with windspeed estimates and inherent in the Wanninkhof transfer velocity parameterisation. Given that the total uncertainty in this estimate could be up to ± 100 %, it is conceivable that the reduction in N_2O solubility caused by seasonal warming could entirely support the estimated sea-to-air flux.

Station	Surface N_2O (nmol L^{-1})	Saturation (%)	Windspeed (m s^{-1})	Schmidt no.	Flux (μmol m^{-2} d^{-1})
34	12.26	109	8.8	1353	4.2
44	14.27	124	0.0	1434	0.0
72	13.90	107	6.2	1809	1.5
86	12.97	107	8.8	1607	3.3
98	12.68	103	12.9	1634	2.7
108	14.88	100	1.0	2208	0.0
161	12.83	104	10.3	1621	2.8
209	13.25	111	3.6	1567	0.8

Table 4.4. Surface water N_2O data, windspeeds, Schmidt numbers and flux estimates for all stations

Although no significant N_2O production was detected in the majority of incubated samples, this is not preclusive of nitrification as an important source of N_2O in the Labrador Sea. More likely, the production rates were mostly too low to give measurable results over 24 hour incubations. At the time of the Labrador Sea cruise, the method for determining production rates was still being refined. Preliminary measurements using water samples from eutrophic coastal waters had shown that it was certainly feasible to measure changes in $^{15}N_2O$ over time. However, the enhanced microbial activity encountered in nutrient rich coastal water perhaps raised expectations of what could be measured in the open surface ocean. Following the Labrador Sea cruise, the analytical set-up was amended by increasing the seawater sample volume from 4.5 mL to 9.5 mL in order to improve the signal-to-noise ratio of the *m/z* 31 peak. Even so, a return to this region to obtain further production rate measurements would require other modifications to the analytical method, e.g. larger samples and longer incubation times.

The dependence of seasonal warming and primary production on the annual pattern of insolation suggests that the estimated sea/air N_2O flux for this sub-polar region is highly seasonal. Figure 4.3 shows, assuming that 2001 was a typical year, that surface heating of the water column is limited to only four months. Also, the temporal patterns of primary and secondary production, which are the most important, if not the only sources of ammonium to offshore waters, are unimodal in these high latitudes, with relatively short growth seasons (Longhurst, 1998). Cooling of the sea surface in autumn and winter will likely reverse the sign of the N_2O flux by raising solubility. Given that this region is noted for deep-water formation, this raises the possibility that deep winter mixing of

water at atmospheric equilibrium, may result in long-term sequestration of anthropogenic N_2O to the deep ocean.

Chapter 5

Nitrous oxide production and consumption in a eutrophic coastal embayment

5.1. Introduction

5.1.1. Study site

The Bedford Basin is a small coastal embayment, with a surface area of about 17 km^2, forming the inner part of the Halifax Harbour network on the eastern shore of Nova Scotia, Canada (Figure 5.1). The Basin has a maximum depth of 70m and is connected to the outer harbour by a 400m wide, 20m deep channel (Halifax Narrows) which effectively forms a sill. The Sackville River enters the head of the Bedford Basin and is the primary component of a total freshwater input varying between 10^4 and 10^7 m^3 d^{-1}. The Bedford Basin can therefore be described as a small fjord-type estuary.

Halifax Harbour is surrounded by Halifax Regional Municipality, the largest conurbation on the Atlantic coast of Canada comprising the former cities of Halifax and Dartmouth, and the town of Bedford, and serves as a convenient natural disposal conduit for sewage. The Bedford Basin currently receives an average of over 20 million litres per day of secondary effluent from the Mill Cove wastewater treatment plant located near the mouth of the Sackville River, and additional amounts of untreated sewage are discharged into the outer harbour. Average 2002 concentrations of nitrate and phosphate in Bedford Basin seawater were 18% and 41% higher than those recorded for 1967 (Li *et al.*, 2003), and growth in effluent discharge levels over recent decades is a likely contributing factor to this increase in nutrient loading.

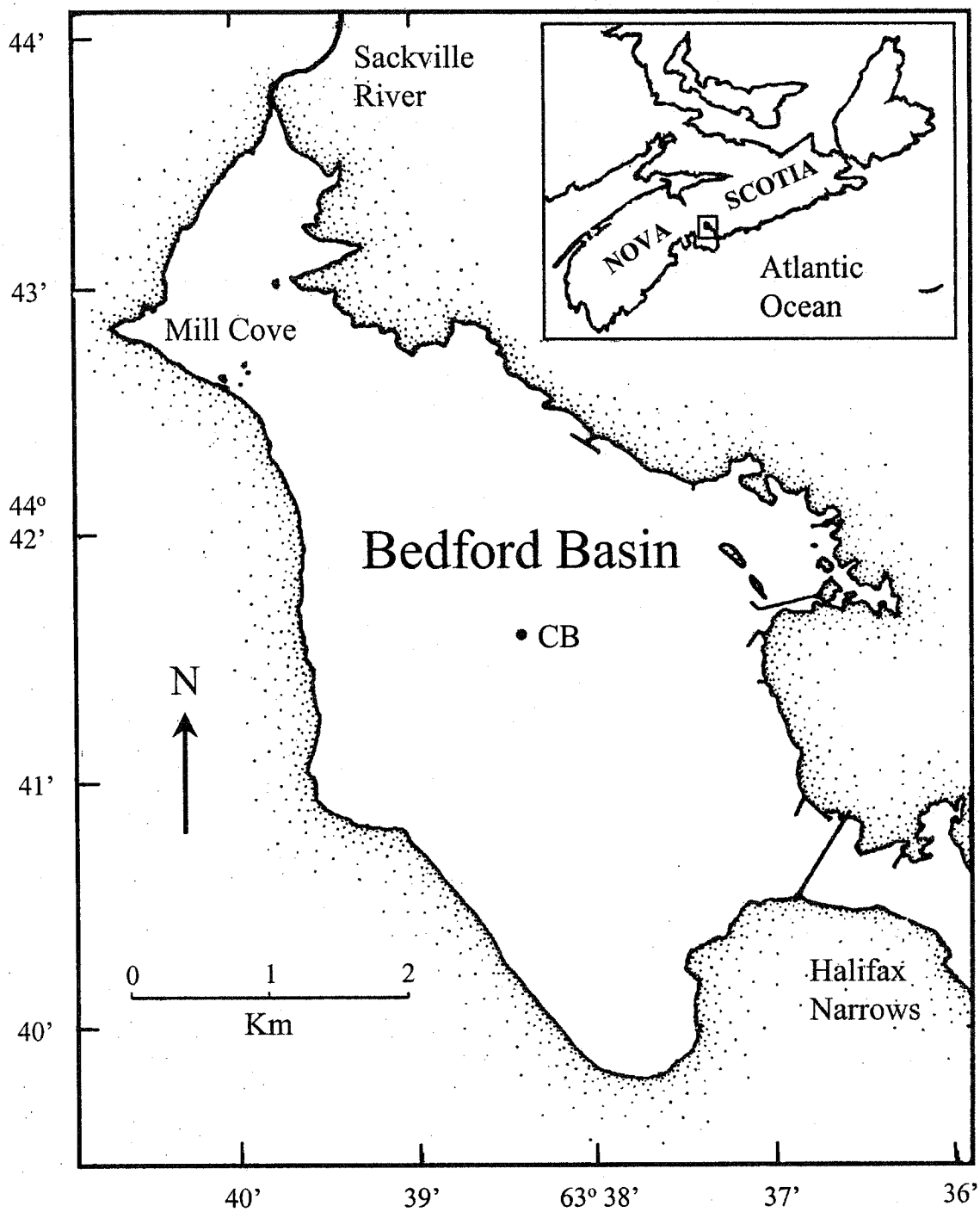

Figure 5.1. Map of the Bedford Basin, Nova Scotia. CB indicates the position of the ompass Buoy Station.

During summer months, the water column is typically well stratified. The upper layer consists of warmer, fresher water usually with an estuarine circulation. The deep water mass isolated by the sill generally remains cold (< 3°C) throughout the year and may infrequently become anoxic (Platt and Conover, 1975). Water replacement events occur irregularly but most notably during the late summer and fall (Platt *et al.*, 1972). These events are often associated with periods of northeast winds causing a build up in coastal sea level due to Ekman transport (Platt *et al.*, 1972; Sandstrom, 1980; Petrie *et al.*, 1987; Mitchell, 1990). The euphotic depth is shallow, averaging 15 m, due to high turbidity (Platt *et al.*, 1970). Tides in this region are semi-diurnal with a maximum amplitude of about 2m.

5.1.2. Objectives

The Bedford Basin is an interesting coastal study site with respect to N_2O cycling, because the deep-water mass, isolated by stratification and topography, affords an opportunity to study N_2O production over a range of oxygen levels, while temperature and salinity remain relatively constant. Thus, the task of a researcher investigating the environmental factors that affect these processes is somewhat simplified, as the major variables are reduced to dissolved oxygen and substrate supply.

The objectives of this study were: (1), to determine the relative importance of ammonium oxidation (nitrification) and nitrate reduction (denitrification) to sub-surface water column N_2O production, and (2), to assess the yield of N_2O from ammonium oxidation over a range of oxygen concentrations. Physical and chemical water properties were also examined to determine the major controls on N_2O production

4.1.3. Sampling

All samples were collected at the Compass Buoy station (44° 41'30"N, 63° 38'30"W) between 18th July 2001 and 27th November 2002. The Compass Buoy is above the deepest point of the Basin, and is the site of the Bedford Basin Plankton Monitoring Program undertaken by the Bedford Institute of Oceanography (Li *et al.*, 2003; Li *et al.*, 1998). This study was co-ordinated with the weekly collection of conductivity and temperature data by the Bedford Institute group.

Water samples were collected from a coastguard patrol boat using a chemically clean, non-sterile 10 L Go-Flo sampling bottle. This was attached to a weighted stainless steel cable and lowered to the required depth, routinely 60m, using a powered winch. Depth measurement was by means of a meter wheel, therefore the indicated depth was true as long as the cable was perpendicular to the sea surface. Occasionally, very strong winds caused the vessel to drift while sampling. This resulted in the cable noticeably deviating from the perpendicular, with the effect that the actual sampled depth was certainly shallower than the indicated depth. This situation does introduce some uncertainty to the depth measurements, however such occasions were fortunately relatively rare.

Only the 60 m depth was regularly sampled owing to the large number of analyses involved. In addition to routine 60m sampling, additional samples were obtained from 40 and 50 m depths on September 24th, October 2nd and October 8th, 2002.

5.2. Results

5.2.1. Temperature, salinity and dissolved oxygen

Figure 5.2 shows temporal records of temperature and salinity and dissolved oxygen at 60 m, while Figure 5.3 is a temperature *vs* salinity plot for the study period. Three

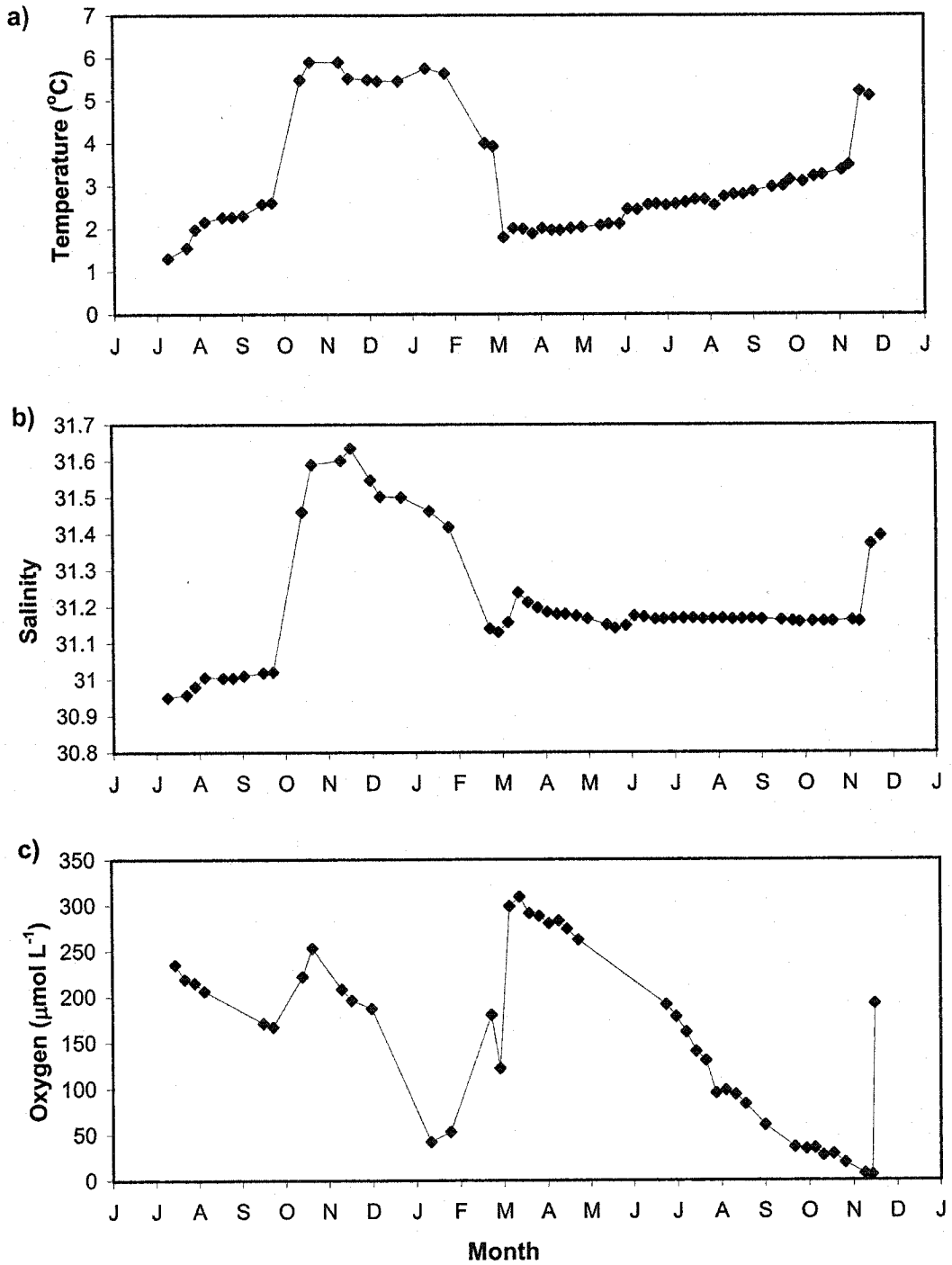

Figure 5.2. Measurements of a) temperature, b) salinity, and c) dissolved oxygen at 60 m depth for the period June 2001 to December 2002.

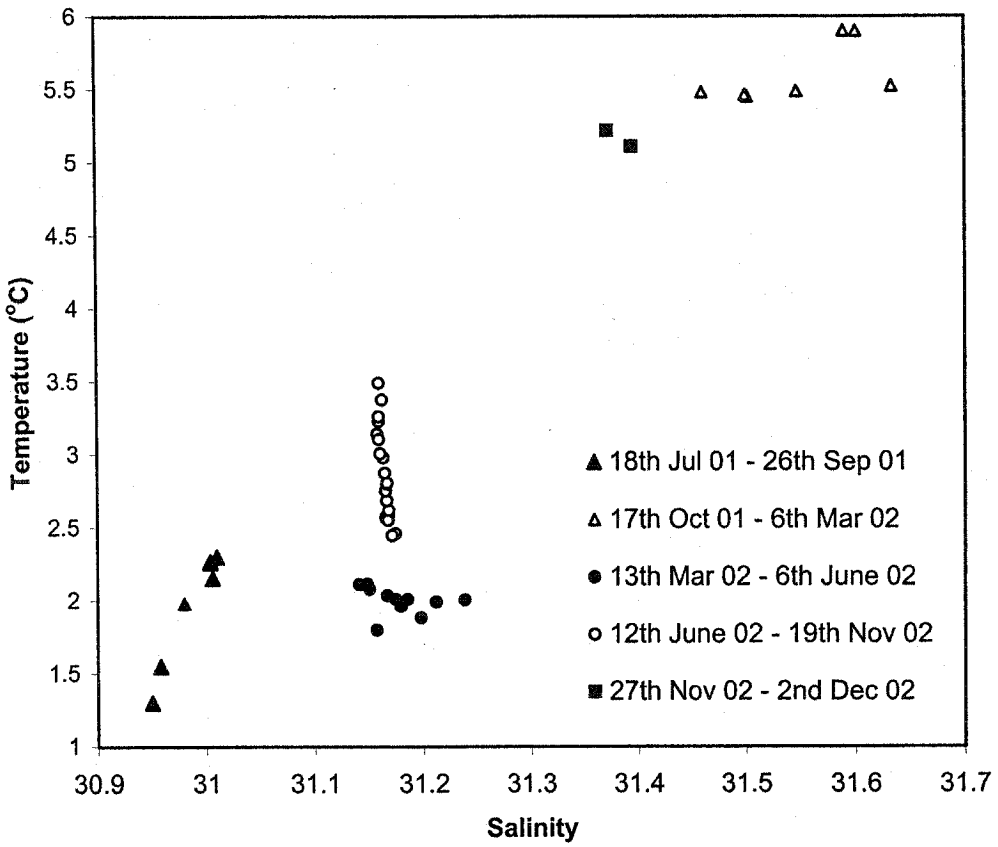

Figure 5.3. Temperature/salinity plot for the study period.

obvious mixing events, resulting in sudden increases in dissolved oxygen concentration, punctuated the study period.

From the start of the study up to 26th September 2001 there was a small increase in salinity with an associated rise in temperature of around 1°C. The most likely cause was downward diffusive mixing of warmer, saltier water during this period, however, oxygen was consumed faster than the rate of supply, and decreased from 235 to 167 μmol L^{-1}. The first major mixing event, taking place between 26th September and 17th October 2001, occurred after periods of high winds and affected only the lower water column, suggesting that this was an incursion of dense water originating from the outer harbour (Figure 5.4a). This resulted in a 3.6 °C temperature increase, a salinity increase of about 0.6, and an increase in oxygen to 253 μmol L^{-1}. For the following 3 months, the temperature remained above 5.5 °C, however, temperature fluctuation and an erratic downward trend in salinity indicated some instability in the deep water. Nevertheless, oxygen declined to 42 μmol L^{-1}, the lowest recorded level in 2001, while the upper water column remained well stratified.

From the end of January to mid-March, 2002, there was an extended episode of deep winter mixing, when the water column attained almost uniform temperature and salinity, and consequently became relatively well ventilated (Figure 5.4b). The temperature at 60 m fell to about 2 °C, accompanied by a 0.2 decrease in salinity, while oxygen rose from <50 to >300 μmol L^{-1}. This was probably in response to a reduction in water column stability, caused by seasonal cooling of the surface water, and incursions of seawater from the outer harbour driven by wind forcing.

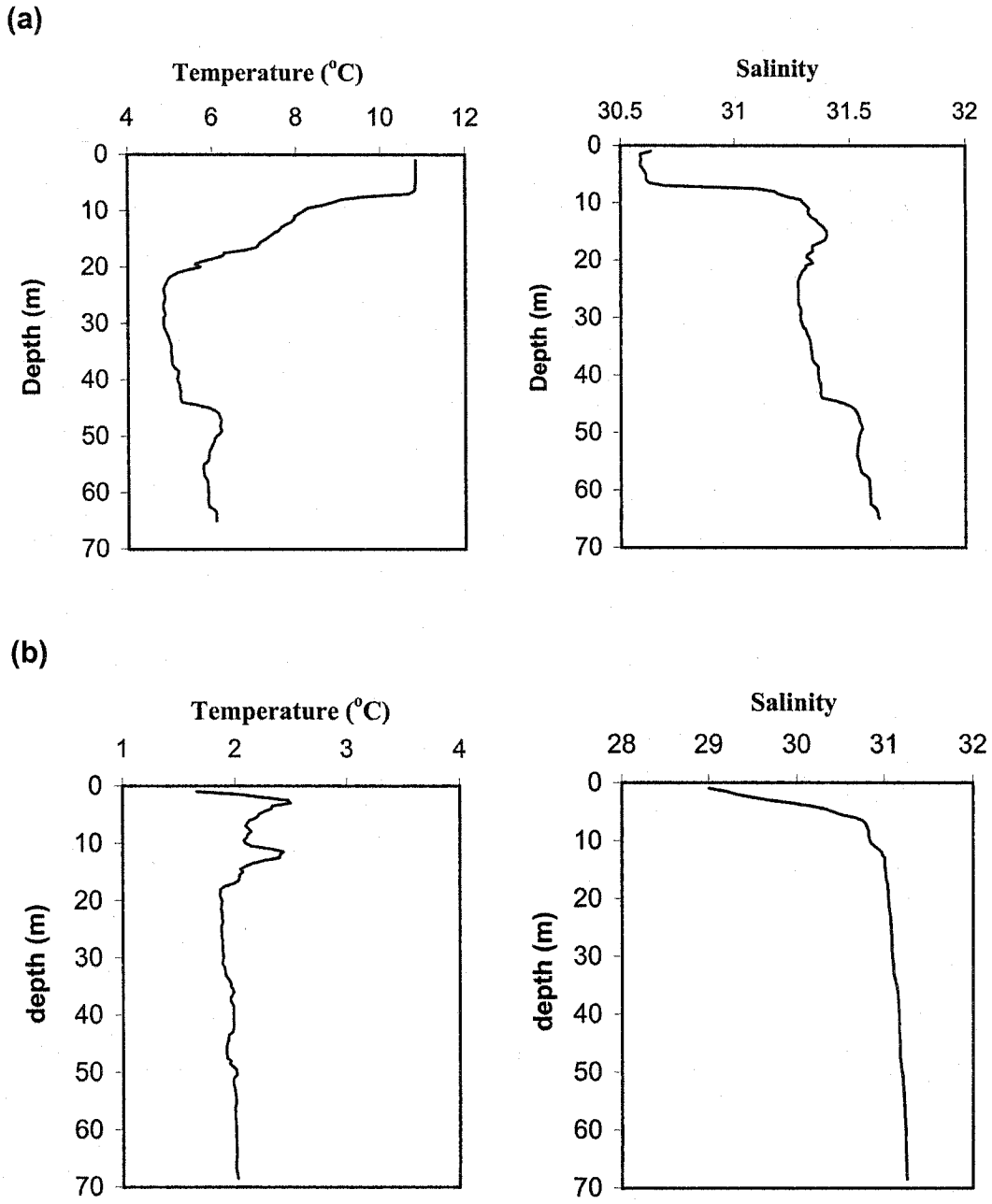

Figure 5.4. (a) Temperature and salinity profiles for 24th October 2001. The incursion of water below 45 m is clearly shown by a change in water properties. (b) Temperature and salinity profiles for 20th March 2002, showing relative uniform properties below 15 m as a result of deep mixing.

The beginning of April marked the onset of seasonal stratification, and the start of a long period of relative stability, where oxygen showed an approximately linear decrease from 300 μmol L^{-1} to near anoxia by late November, consistent with biological oxygen removal comprising bacterial heterotrophic oxidation of sinking particulate organic matter and possibly phytoplankton respiration. The lowest oxygen level observed in this study was 5 μmol O_2 L^{-1}, measured using the Winkler method on 25th November. However it should be noted that the sampling on this occasion was hampered by high wind and rain, conditions not conducive to obtaining good measurements on a small, open deck boat. A syringe sample, measured according to the method for low oxygen waters of Broenkow and Cline (1969), returned a value of 2.5 μmol O_2 L^{-1}, and this is assumed to be the correct concentration.

The net rate of oxygen utilisation from April to November 2002, estimated from a linear regression of the oxygen data, is about 1.3 μmol O_2 L^{-1} d^{-1}, falling within a range of mean respiration rates (0.5 – 10.1 μmol O_2 L^{-1} d^{-1}) reported in coastal and shelf studies (Williams, 1984; Smith *et al.*, 1986; Iriarte *et al.*, 1991; Pomeroy *et al.*, 1994; Pomeroy *et al.*, 1995). However, the true rate of oxygen utilisation was probably rather higher, due to an invasive flux of oxygen to the deep water driven by the increasing oxygen concentration gradient from the surface to 60 m during the latter half part of 2002.

Figure 5.3 reveals that this apparently stable period can be further subdivided into the time prior to 6th June where a decline in salinity indicates an influx of water, and the period 6th June to 19th September where salinity is constant, suggesting that the deep water remained relatively unperturbed during this time. A ~1°C temperature rise during

this latter period can be attributed to seasonal heating of the Basin. The study was terminated after a mixing event which took place after 25th November 2002, causing the third substantial increase in oxygen, from near anoxia, to 192 μmol L^{-1}.

5.2.2. Nitrate +nitrite and ammonium

Figure 5.5a shows the time-series measurements of total nitrate + nitrite. The concentration ranged between about 5 and 20 μmol L^{-1} d^{-1}, with the lowest concentration coinciding with the period of deep mixing in March 2001. The record of total nitrate + nitrite concentration closely mirrors that of dissolved oxygen, and there is indeed a strong negative linear correlation between these two quantities (Figure 5.5b). This suggests that the process of nitrate supply to the deep-water mass is mainly through the oxidative decomposition of organic matter and subsequent nitrification of liberated ammonium.

In contrast, the record of ammonium displays no obvious pattern when compared with the recorded water parameters (Figure 5.5c). The main features are a large peak in August/September 2001 and a smaller peak in September/October 2002. Although the timing of these peaks is similar, it is not known whether they are recurring seasonal features, or whether their origin is natural or anthropogenic.

5.2.3. N_2O production from ammonium oxidation

$^{15}N_2O$ production rates measured in samples incubated with $^{15}NH_4^+$ were generally in the range 0-200 pmol L^{-1} d^{-1}, however exceptionally high rates of up to 1.7 nmol L^{-1} d^{-1} (about 8% d^{-1}) were recorded in September 2001 (Figure 5.6a). The rate uncertainty (relative standard deviation) ranged from ± 4-10 %. Measurements from duplicate

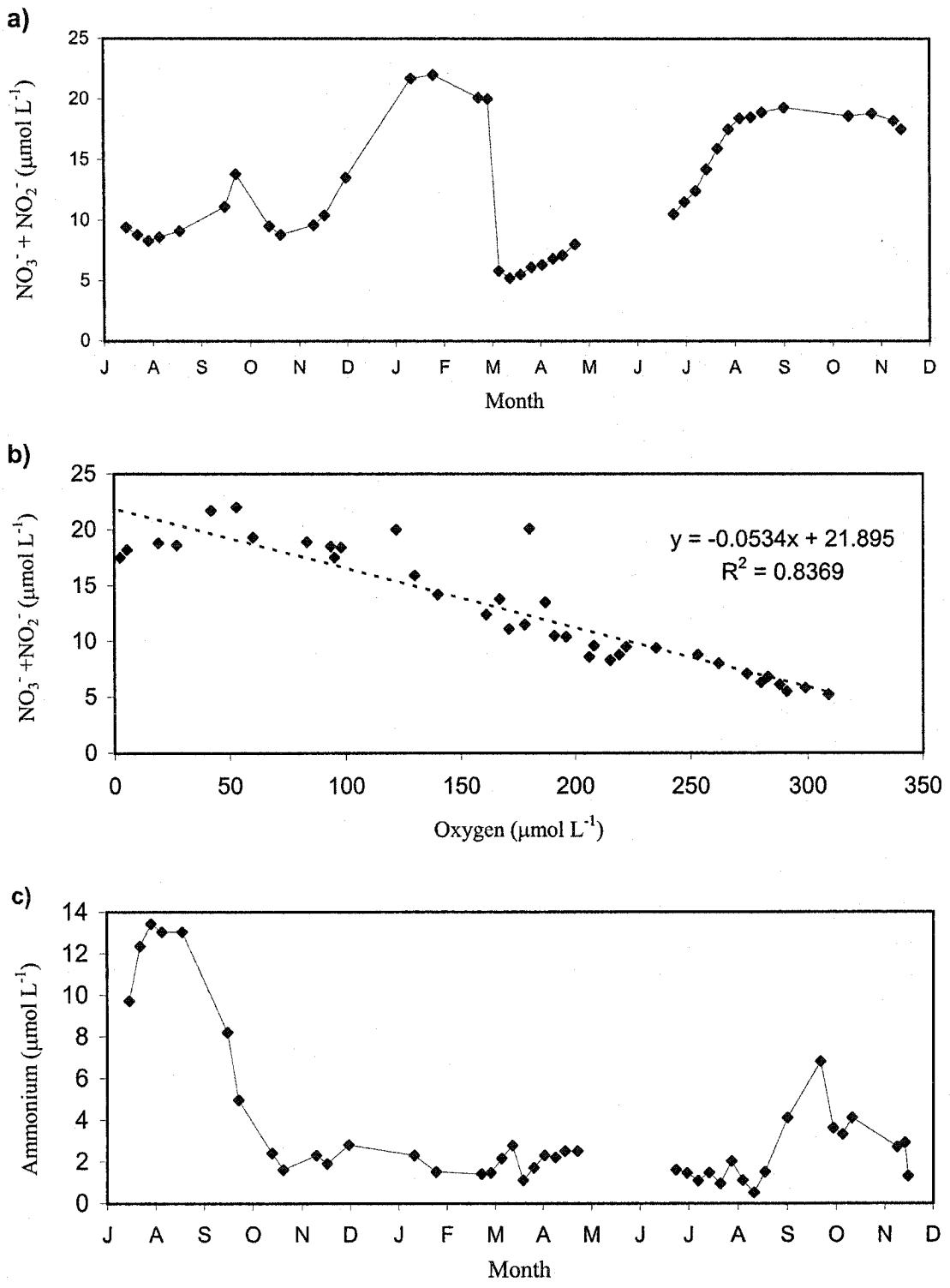

Figure 5.5. Measurements of (a) total nitrate+nitrite, (b) nitrite+nitrate versus oxygen, and (c) ammonium at 60 m depth.

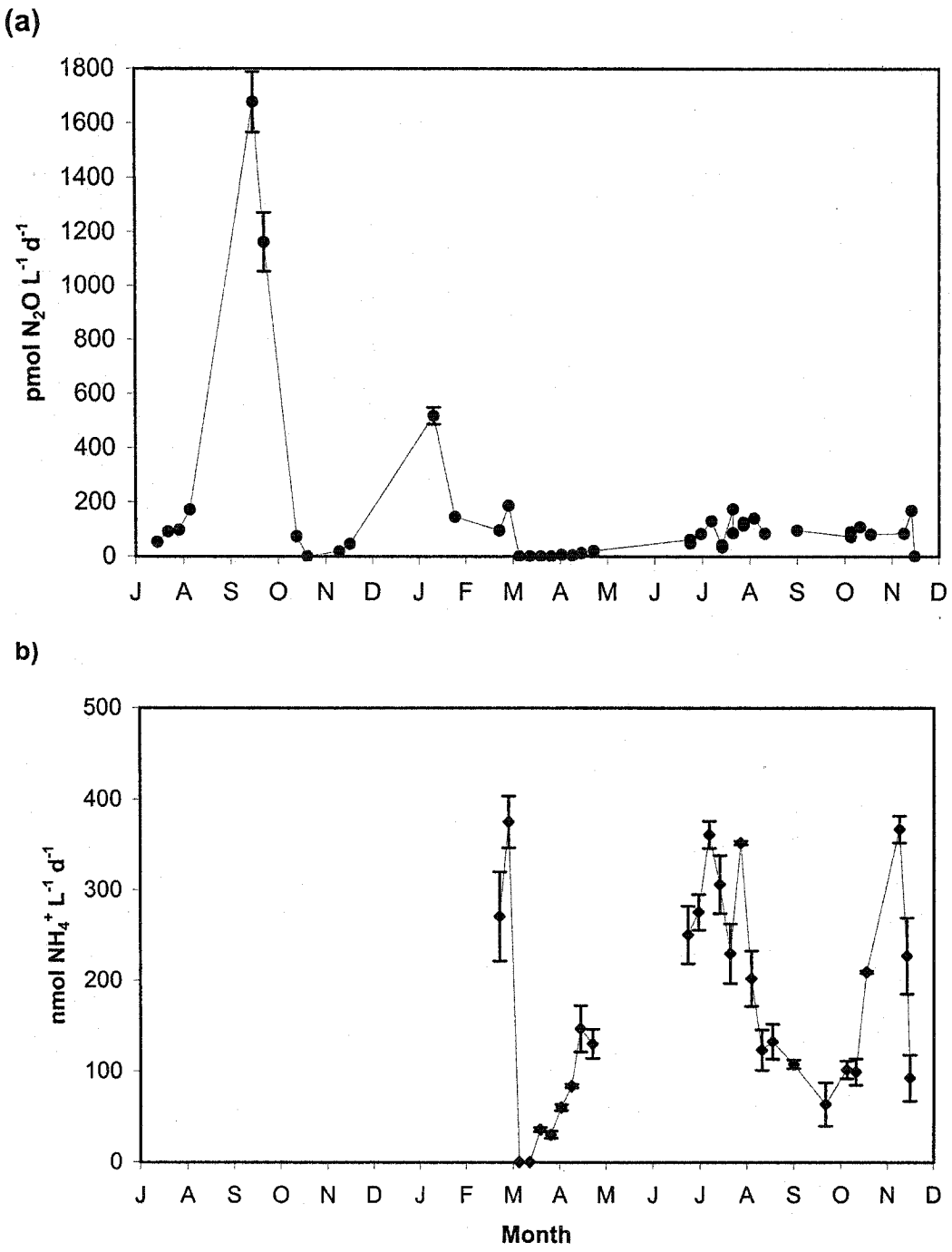

Figure 5.6. (a) $^{15}N_2O$ production rates at 60 m from samples incubated with ^{15}N-labelled ammonium. Error bars are shown only for the three highest measurements for clarity, and ranged from about 4-10%. (b) Ammonium oxidation rates for the same samples determined by the chlorate inhibition method. Error bars indicate the standard deviation of regressions of nitrite concentration versus time.

samples were normally identical within the margin of error but occasionally deviated by no more than ~10% from the mean.

There was no correlation between $^{15}N_2O$ production rates and ammonium concentrations, but it is noteworthy that the highest recorded production rates occurred shortly after the highest recorded level of ammonium and coincided with a steep net decline in ambient ammonium. On three occasions, coinciding with the mixing events, $^{15}N_2O$ production declined below the limits of detection (< ~ 5 pmol N_2O L^{-1} d^{-1}). The loss of production during the period of deep mixing in March 2002 was sustained for four consecutive weeks and was followed by a further four weeks of very low production rates (~5-20 pmol N_2O L^{-1} d^{-1}). This period of very low N_2O production was also associated with the highest levels of dissolved oxygen seen over the study period.

5.2.4. Ammonium oxidation rates

Ammonium oxidation rates were measured from 28th February to 27th November 2002 and ranged between 0 and about 400 nmol NH_4^+ oxidised L^{-1} d^{-1} (Figure 5.6b). There was a high degree of temporal variability, with peaks of over 350 nmol N L^{-1} d^{-1} occurring in early March, July-August and November. As for N_2O production, ammonium oxidation appeared to be inhibited by mixing, and was undetectable for two consecutive weeks coinciding with the onset of deep mixing in winter 2002, although the subsequent recovery was rather more rapid than for N_2O production rates. The final mixing event, occurring just after 25th November 2002, suppressed the rate of N_2O production to below detection limits, but did not completely inhibit the rate of ammonium oxidation (~100 nmol N L^{-1} d^{-1}). No correlation was found between ammonium

concentrations and ammonium oxidation rates (R^2 = 0.09) suggesting that this process was zero order with respect to substrate concentrations in the range 0.1 - 6.8 μmol L^{-1}.

Although ammonium oxidation rates were not measured in 2001, the steep decline in ambient ammonium observed in September of that year, together with very high rates of N_2O production and a sharp spike in nitrate + nitrite, suggests a high rate of nitrification. In contrast, the steep increase in nitrate + nitrite from November 2001 to January 2002, together with a large rise in background N_2O (Figure 7), is also evidence of high nitrification rates, yet the level of ambient ammonium remained relatively constant. This observation supports the conclusion that ammonium oxidation rates were not directly linked to substrate concentration.

5.2.5. N_2O production from nitrate reduction and N_2O consumption

On only two occasions were significant N_2O production rates seen in samples spiked with $^{15}NO_3^-$. These were 16th January and 25th November 2002 with rates of 40 pmol L^{-1} d^{-1} and 20 pmol L^{-1} d^{-1} respectively. Although both instances were associated with oxygen minima, the oxygen concentrations were not comparable (42 and 2.5 μmol L^{-1}). On 25th November, there was also evidence of N_2O consumption, the only instance during this study, with a mean loss rate in duplicate $^{15}N_2O$ spiked samples of 74 pmol L^{-1} d^{-1}. This date was of particular interest as concurrent production from nitrification and denitrification, and consumption, was evident. The reported production rates from ammonium oxidation and nitrate reduction for that date are therefore net values.

5.2.6. Measurements from 40 and 50m depths

Additional measurements of ammonium oxidation rates and N_2O production from labelled ammonium were made on samples collected from 40 m and 50 m depths on 24th

September and 2nd October. There was a well-established pycnocline at ~ 25 m during this period, and temperature and salinity were nearly uniform below this depth. Extremely low levels of ammonium were evident at 40m on both dates. The results are shown in Table 5.1. No significant production of $^{15}N_2O$ was measured in samples collected from 40, 50 and 60m on 8th October 2002 and incubated with ^{15}N-labelled nitrate. The oxygen concentrations in these samples ranged from 96 - 40 μmol L^{-1}.

4.9. Ambient N_2O

The concentration of background N_2O measured at 60 m, together with the atmospheric equilibrium concentration, is shown in Figure 5.7. In early July 2001, at the start of the study, N_2O concentration was close to 100% saturation. This was also the case in spring 2002, following deep mixing of the water column, and is possibly a recurring seasonal feature. The overall pattern of N_2O concentration is the reverse of oxygen, with N_2O accumulating as oxygen declines. During the two month period between November 21st 2001 and January 16th 2002 there is a sharp increase in ambient N_2O of almost 15 nmol L^{-1}, to a peak of 29.7 nmol L^{-1}, or 236% saturation. Although no ammonium oxidation rate data were obtained during this period, it can be concluded that there was a period of high nitrifying activity resulting in a net average N_2O production rate of around 250 pmol L^{-1} d^{-1}, consistent with the observed nitrate+nitrite accumulation.

5.3. Discussion

5.3.1. N_2O production and consumption

The ^{15}N incubation data show that in the Bedford Basin water column, nitrous oxide is derived almost exclusively from nitrification. This finding is in agreement with

Date	Depth (m)	Nitrification rate (nmol N L^{-1} d^{-1})	N_2O production rate (pmol N_2O L^{-1} d^{-1})	O_2 (μM)	NH_4^+ (μM)
24th Sept 02	40	115 ± 16	51 ± 9	110	0.1
	50	101 ± 12	77 ± 6	69	1.9
2nd Oct 02	40	119 ± 17	101 ± 15	96	0.4
	50	86 ± 20	83 ± 4	56	3.0

Table 5.1. Results from 40 and 50 m depth obtained on 24th September and 2nd October 2002

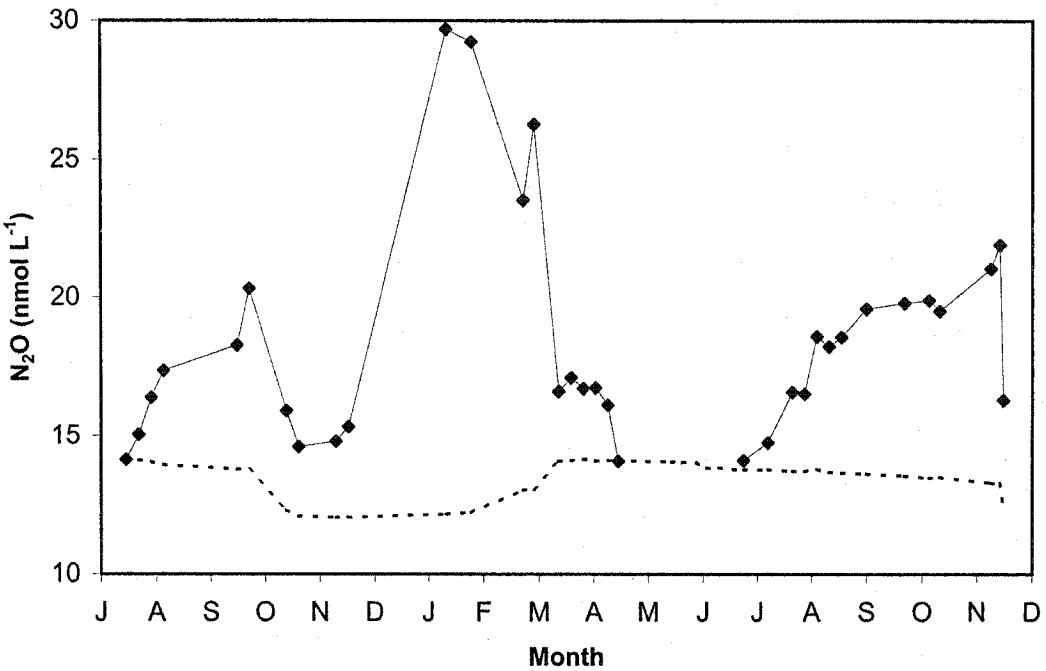

Figure 5.7. The record of ambient N_2O measurements at 60 m (solid line), and the atmospheric equilibrium concentration at 1 atmosphere calculated from temperature and salinity data (dashed line).

observations made in a number of estuarine and coastal locations including the Somali Basin (de Wilde and Helder, 1997), the Humber Estuary (Barnes and Owens, 1999), and the Schelde Estuary (de Bie *et al.*, 2002). The two instances in 2002, of measurable $^{15}N_2O$ production resulting from $^{15}NO_3^-$ reduction, coincided with oxygen minima, consistent with a process that is restricted to low-oxygen zones, however, these minima were not comparable. In the first instance on 16th January, the oxygen concentration was well above the <5 μmol O_2 L^{-1} usually associated with denitrification zones (Codispoti *et al.*, 2001). The circumstances facilitating denitrification at this time may have been unusual, as subsequently in November, oxygen declined to 19 μmol L^{-1} without any commensurate N_2O production in samples spiked with $^{15}NO_3^-$. There has long been speculation that denitrification may take place in anoxic microenvironments within organic particles, releasing N_2O into the relatively well oxygenated surrounding water (Law and Owens, 1990; Ostrom *et al.*, 2000). While such a mechanism offers an attractive explanation for the results seen on 16th January, there are no records of particulate organic matter loading that could support this explanation.

The second instance, in November 2002, of N_2O production from reduction of $^{15}NO_3^-$ is more in line with the conventional view of anaerobic denitrification. The ambient oxygen level of ~2.5 μmol O_2 L^{-1} is in the range of values associated with evidence of denitrification, such as secondary nitrite maxima (Cohen and Gordon, 1978) and isotopic enrichment of N_2O (Yoshinari *et al.*, 1997). In this case, consumption of N_2O in samples incubated with $^{15}N_2O$ outweighs production, indicating that the redox conditions favour the complete reduction of nitrogen oxides to dinitrogen. In both cases of N_2O production

from labelled nitrate, similar samples spiked with labelled ammonia yielded N_2O production rates about 10 times greater.

5.3.2 Ammonium oxidation rates

Previously reported nitrification rates in the Tamar Estuary, Chesapeake Bay and Schelde Estuary lie in the range 3-45 μmol N L^{-1} d^{-1} (Owens, 1986; Horrigan *et al.*, 1990; de Bie *et al.*, 2002). Nitrification rates in the open ocean are generally much lower, typically a few nmol N L^{-1} d^{-1} in the subsurface open ocean (Ward, 1987; Ward and Zafiriou, 1988) rising to a few hundred nmols L^{-1} d^{-1} in areas of high productivity (Lipschultz *et al.*, 1990). During the latter half of this study, ammonium oxidation rates were generally intermediate between pristine ocean and highly eutrophic estuarine environments, but there was nonetheless a high degree of temporal variability. The environmental variables that affect nitrification rates have been reviewed by Ward (2000) and include temperature, light and substrate concentration as potentially important factors. The effects of temperature and light are probably of little consequence during this study. Substantial fluctuations in nitrifying activity occurred while the temperature remained almost constant for long periods. Also, all samples were taken from well below the euphotic zone, therefore the photoinhibition of nitrifying activity (Olson, 1981; Guerrero and Jones, 1996) should be minimal. With respect to substrate, there was no correlation between ambient ammonium concentrations and ammonium oxidation rates in this study ($R^2 = 0.09$), suggesting that substrate limitation was not an important factor in controlling nitrifying activity, even when water column ammonium was near the lower limit of detection. This finding is in agreement with zero-order kinetics for nitrification above about 0.1 μM NH_4^+ reported from the field (e.g. Hashimoto *et al.*, 1983), but

contrasts with half-saturation (K_s) values in the range 0.03-3.3 mmol L^{-1} reported for isolated ammonium-oxidising cultures obtained from the River Elbe (Stehr *et al.*, 1995). One possible explanation for this observation is that most of the nitrifying biomass is particle-attached and therefore living in close association with heterotrophic bacteria. This situation would clearly benefit the ammonium oxidisers, giving them direct access to higher than ambient levels of ammonium and CO_2 released from the decomposition of organic matter. De Bie *et al.* (2002), found that 57-86% of nitrifying bacteria in the Schelde estuary were attached to particles. Such association could permit regeneration of nitrate at the substrate point source, essentially decoupling nitrification from the availability of ammonium in the surrounding water.

A particularly noticeable feature of the data set was that nitrification rates and N_2O production rates were synchronously depressed during deepwater mixing. The sudden associated increase in oxygen concentration is certainly one obvious candidate for causing this effect, however, another potentially important factor for which we have no information is nitrifying bacterial biomass. All other factors being equal, a change in biomass concentration linked to the introduction of a new water mass should have first-order implications for nitrification and hence N_2O production rates. Quantitative information on taxonomic microbial biomass would clearly be helpful in resolving this question.

5.3.3. N_2O yield

If denitrification can be ignored as a source of N_2O in oxygenated water as seems a reasonable approximation in this study, then estimates of N_2O production could be made based upon the level of nitrifying activity. Such estimates would require a knowledge of

the conversion efficiency or yield of N_2O from ammonium, but as yet there are few published N_2O yields from natural populations of marine nitrifying bacteria. Indirect estimates based on observed oceanic ΔN_2O/AOU relationships combined with the Redfield model for nitrogen regeneration typically give N_2O yields of around 0.15% integrated though the water column (Elkins *et al.*, 1978; Kaplan and Wofsy, 1985; de Wilde and Helder, 1997). De Wilde and de Bie (2000) obtained N_2O yields of 0.07-0.42% in the Schelde Estuary based on the ratio of estimated N_2O fluxes to nitrification rates, whereas in the pristine North Pacific Ocean, Yoshida *et al.*, (1989) calculated N_2O yields in the range 0.004-0.027%, 5 to 10 times lower than some previous estimates. A plot of all calculated N_2O yields (mol N_2O per mol NH_4^+) versus oxygen concentration for the latter half of this study 2002 is shown in Figure 5.8. The uncertainties are propagated from estimated errors in nitrification rates and N_2O production rates. In the range 290-27 μmol O_2 L^{-1}, N_2O yields vary by an order of magnitude from around 0.01% to 0.11%. There is an apparent negative non-linear relationship, with an exponential regression giving the best statistical fit ($R^2 = 0.77$). This relationship is in line with other studies proposing maximal N_2O production at low oxygen concentrations (Goreau, 1980; De Wilde and de Bie, 2000; de Bie *et al.*, 2002). Where ambient oxygen levels were below 10 μmols L^{-1}, yields were rather lower than might be expected from this relationship. Correcting the N_2O production rate obtained on 25th November 02 (20 pmol L^{-1} d^{-1}) for reductive removal still leaves the N_2O yield well below those represented by the best-fit curve. The results seems to point to an optimum oxygen concentration, greater than ~5 μmol L^{-1} but less than ~30 μmol L^{-1} where the N_2O production pathway is most efficient.

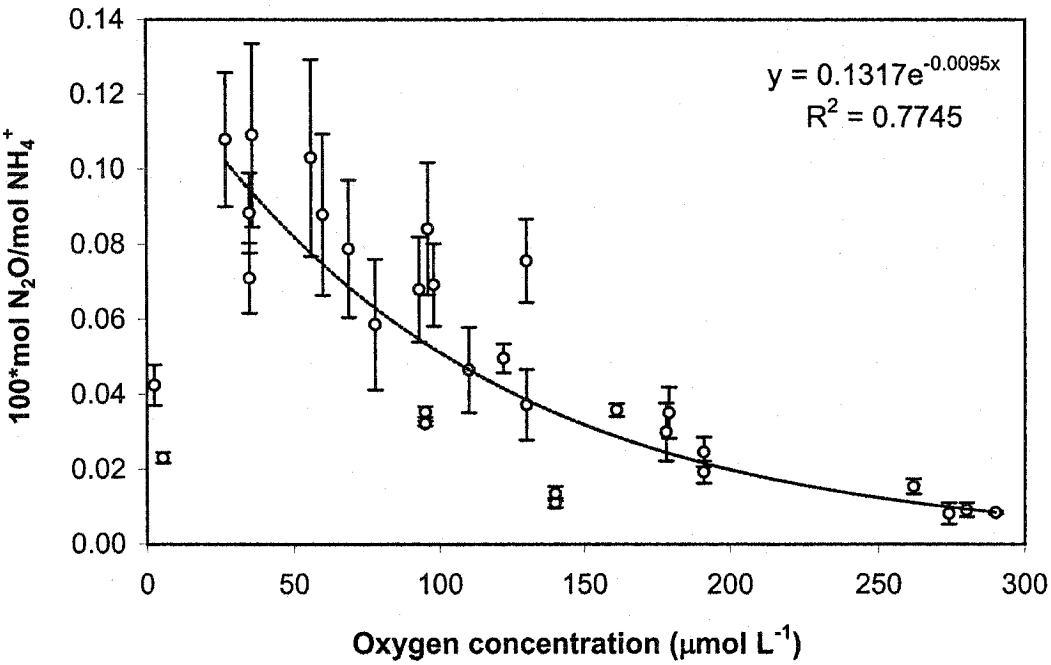

Figure 5.8. Percentage N_2O yields (100*mol N_2O:mol NH_4^+) for data collected between February and December 2002 showing the best-fit curve in the range 27-290 mmol O_2 L^{-1}. Errors are propagated from the standard deviations of N_2 production rates and ammonium oxidation rates.

An alternative possibility that must be considered is that the low apparent N_2O yields at very low oxygen levels are artefacts and result from the different sample collection methods employed for N_2O production and nitrification incubations. In the former case where the incubation syringes are filled directly from the Go-Flo bottle after repeatedly filling and flushing, air contamination is eliminated. In the latter case, where sample collection is similar to the standard Winkler method, there is some potential for air entrainment with the addition of the chlorate reagent, and, in cases where the oxygen concentration is close to zero, invasion of oxygen across the sample surface prior to stoppering. This conclusion is supported by the differing oxygen results obtained by two analytical methods on 25th November, suggesting that the Winkler method was overestimating oxygen concentration by about 2 - 3 μmol L^{-1}. Ammonium oxidation is an oxygen-requiring process, and so rates can be expected to decline sharply, as oxygen becomes limiting, to zero in anoxic water. It is therefore conceivable that the true rates of ammonium oxidation, and hence N_2O production, were sub-optimal in the syringes due to oxygen limitation. On the other hand, nitrifying activity in the BOD bottles may have been relieved of oxygen limitation due to a small amount of air contamination, introduced during the sampling procedure, leading to an overestimate of *in situ* ammonium oxidation rates. Consequently, the N_2O yields, derived from N_2O production rates measured in syringes and ammonium oxidation rates measured in BOD bottles, may have been underestimated at very low oxygen levels. Further measurements are required to address this question.

The N_2O yields obtained from laboratory incubations may be approximately validated by comparing field measurements of nitrate and ambient N_2O. A plot of N_2O

versus NO_3^- for all data is shown in Figure 5.9. A least-squares linear regression gives a slope (nmol/μmol) of 0.54 implying that on average, 0.54×10^{-3} mol of N_2O appears for every mole of ammonium oxidised to nitrate, a yield of 0.05%. This value is in the mid - range of measured yields shown in Figure 5.8. In addition, the N_2O:NO_3^- plot appears decidedly non-linear with the highest apparent N_2O yield at high nitrate/low oxygen values, also strongly supporting the laboratory results.

5.3.4. Ambient N_2O

Turning to the record of N_2O concentration measurements, a plot of ΔN_2O ($[N_2O]_{measured}$ - $[N_2O]_{equilibrium}$) against AOU, shown in Figure 5.10, divides the data into two sets: those obtained prior to 23rd April 02, and those obtained from 3rd July to 25th November. The transition between these two data sets is marked by levels of N_2O near atmospheric equilibrium, and the change in temperature and salinity occurring between June 6th and June 12th suggests an influx of "new" water to the bottom of the Bedford Basin. For both groups of data, the relationship between excess N_2O and AOU is statistically best described by second order polynomial terms. In the case of the first set, the relationship ($\Delta N_2O = 0.0004AOU^2 - 0.059AOU + 4.1$) is remarkably similar to that found by Upstill-Goddard *et al.* (1999) for the upper 500 m of the north western Indian Ocean ($\Delta N_2O = 0.0004AOU^2 - 0.049AOU + 0.83$), although the latter relationship is better constrained by a much greater number of data points. The second data set shows a lower apparent yield of N_2O with increasing AOU ($\Delta N_2O = 0.0001AOU^2 - 0.009AOU - 0.13$).

The yield of N_2O with respect to oxygen consumption (mol N_2O/mol AOU) indicated by these relationships is a net value resulting from production and loss

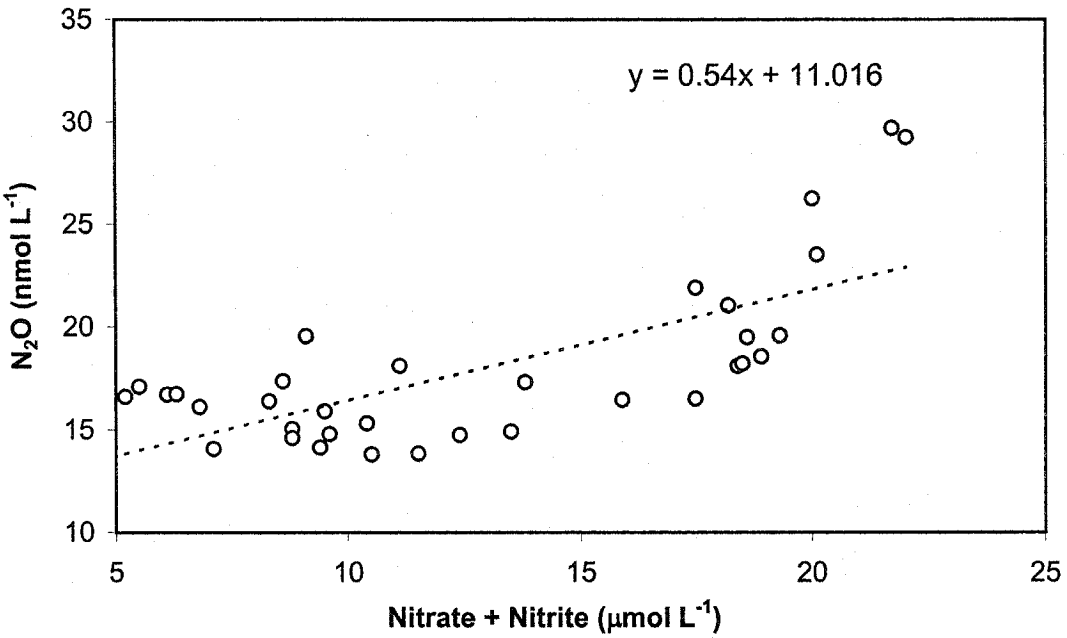

Figure 5.9. A plot of all ambient N_2O data versus all nitrate + nitrite data for the study period. A linear regression line has been fitted to estimate the average N_2O:NO_3^- ratio, although the actual relationship is non-linear.

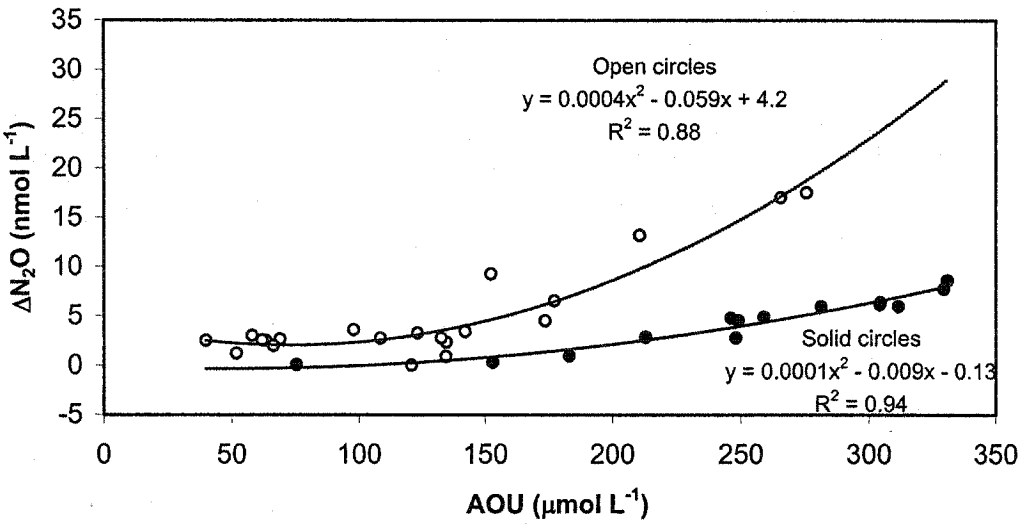

Figure 5.10. Delta N_2O ($N_2O_{measured}$ - $N_2O_{equilibrium}$) versus AOU. The open circles represent data collected prior to May 2002, solid circles represent data collected from July to November 2002.

mechanisms. While there is no reason to suspect changes in the interannual efficiency of N_2O production from nitrification that would explain the disparity between the two curves, there is some evidence to suggest that lower apparent yield of N_2O during the latter half of 2002 was caused by an additional loss process. During the months July-November 2002, there is a reasonably consistent decline in oxygen to very low levels. For nitrate and N_2O, there is a corresponding accumulation for the first half of that period, then the concentrations of these compounds plateau around mid-September coincident with oxygen levels falling below around 40 μmol L^{-1}. This pattern suggests substantial losses of NO_3^- and N_2O from the water column at low oxygen concentrations.

To estimate the magnitude of the apparent N_2O loss, the accumulation of N_2O in the water column for July to November was modelled very simply, neglecting any loss processes and assuming that ammonium oxidation provided the sole source of this gas. Daily oxygen concentrations and ammonium oxidation rates were generated by linear interpolation of the available data. N_2O production was estimated from the relationship between N_2O yield and oxygen concentration proposed in Figure 5.8, with the initial concentration set equal to the first measurement The results (Figure 5.11a) show good agreement between measured and modelled N_2O concentrations for the first half of the time period. Then, a discrepancy develops and grows progressively larger with passing time. The measured N_2O data were then smoothed and interpolated with a 4th order polynomial curve fitted by least-squares regression. Subtracting the best-fit curve of $N_2O_{measured}$ from $N_2O_{modelled}$ gives the apparent N_2O deficit shown in Figure 5.11b.

Although incubations with $^{15}N_2O$ did not reveal significant loss rates until the *in situ* oxygen concentration fell to about 2.5 μmol L^{-1}, it is still possible that N_2O reduction

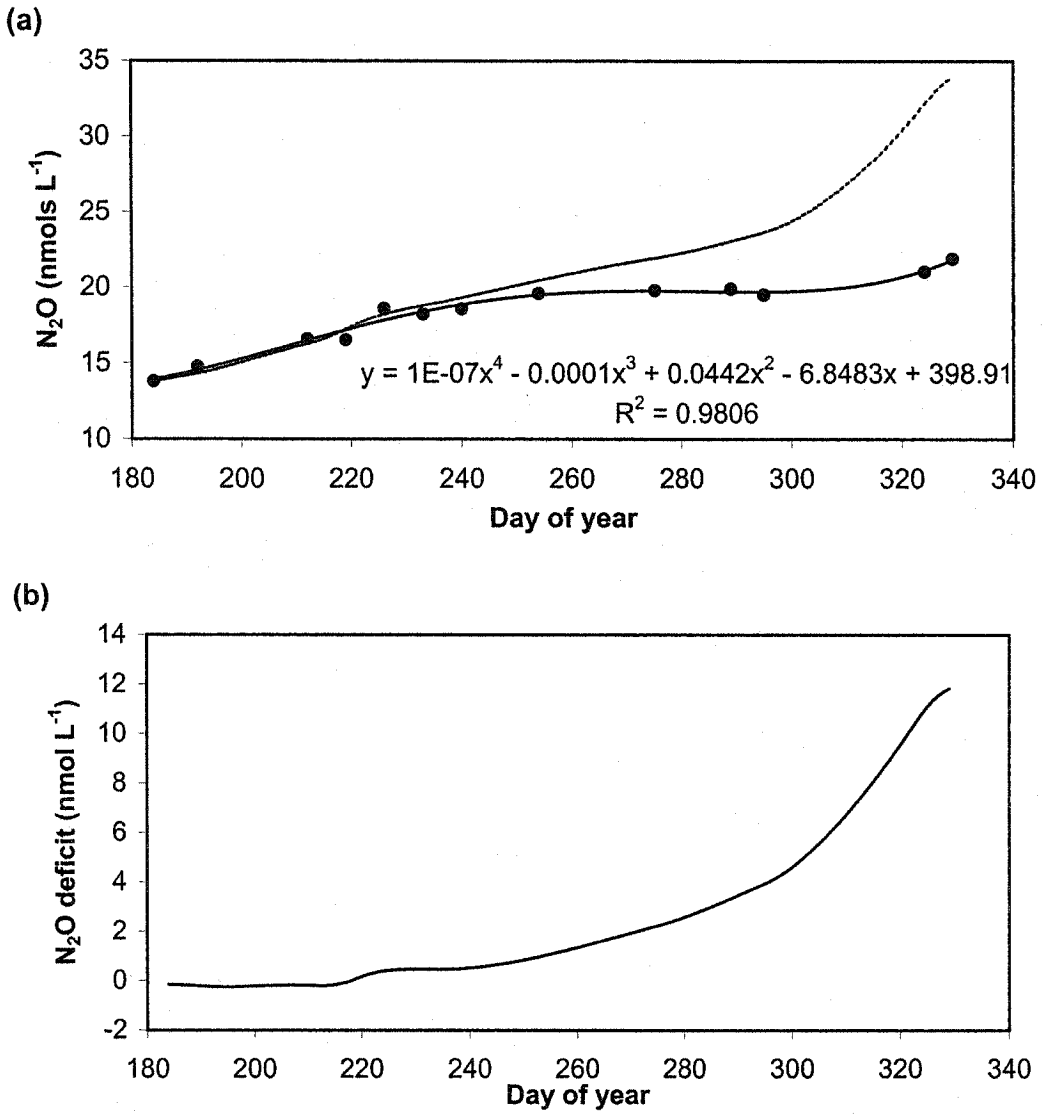

Figure 5.11. (a) Closed circles represent measured N_2O concentrations, smoothed by a fourth order polynomial best-fit curve (solid line). The dashed line shows the expected accumulation of N_2O modelled from measured ammonium oxidation rates and oxygen concentrations. (b) Apparent N_2O deficit derived from (a).

at the sediment/water interface could provide a sink, even though water column oxygen levels were above this threshold. At Compass Buoy Station, the bottom lies 10 m below the sampling depth, and is most likely overlain by a layer of poorly consolidated organic matter, resulting in anoxia at the sediment surface. Moving away from Compass Buoy, the water depth becomes progressively more shallow with increasing distance in all directions until the 60 m isobath is reached at between 500-1000 m. It is therefore suggested that the apparent N_2O deficit, revealed in Figure 5.11b, is predominantly due to diffusive isopycnal and diapycnal flux to anoxic sediments, or to anoxic water overlying the sediments.

5.3.5. The Bedford Basin as a source of atmospheric N_2O

While the Bedford Basin is not typical of the coastal margin, it may well be representative of semi-enclosed coastal basins with a propensity to seasonal subsurface anoxia, e.g. Chesapeake Bay, USA, Saanich Inlet, Canada, and the principles of N_2O production/consumption learned here may also apply to larger water bodies that are subject to oxygen depletion e.g. Sea of Japan. An assessment of the sea to air flux of N_2O from the Bedford Basin was not a primary objective of this study, as the measurements described here were designed rather to unravel the mechanisms underlying the observed net concentrations of this compound. Consequently there are no sea surface measurements of N_2O concentrations to support flux estimates of the type used in Chapter Four. Nonetheless it is possible, with assumptions, to estimate the annual atmospheric source of N_2O from the Bedford Basin. It is assumed here that no production occurs above 30 m (the depth of the major thermocline) owing to photo inhibition of nitrification, and also because relatively high oxygen levels result in very

low yields of N_2O from ammonium oxidation. This assumption is probably not true, but leans the final estimate towards conservatism. It is also assumed that the ammonium oxidation rates and N_2O production rates measured at 60 m are representative of all depths below the 30 m thermocline.

The average N_2O production rate for this eighteen month study period was 150 μmol m^{-3} d^{-1} (Range: 0 – 1700 μmol m^{-3} d^{-1}), and the total volume of water below 30 m in the Bedford Basin is estimated here at approximately 1.32×10^8 m^3, giving a mean production rate of around 2×10^4 mol N_2O d^{-1} or 2×10^8 g N yr^{-1}. This is equivalent to around 1.5×10^9 g N km^{-3} yr^{-1}, a figure which could potentially be applied to other similar eutrophic water bodies.

The fate of this nitrous oxide is not certain, but on the basis of Figure 5.7 it would seem that ventilation of the deep water resulting in N_2O concentrations close to atmosphic equilibrium is an annual feature. Therefore it is likely that episodic deep mixing, occurring at least once a year, transports water that is supersaturated with N_2O to the surface layer. The excess N_2O then either escapes to the atmosphere, or is advected to the shelf sea through tidal and estuarine flushing, where its ultimate fate is again loss to the atmosphere. A caveat, applying to years where the oxygen concentration falls to low levels due to prolonged isolation, as in 2002, is the possibility of *in situ* consumption rates approaching a similar magnitude to production rates.

Chapter 6

A laboratory investigation of the effect of oxygen concentration on N_2O production and consumption by denitrification

6.1. Introduction

The distribution of nitrous oxide in persistent low-oxygen zones suggests that oxygen acts as a control on the balance of NO_2^- and N_2O reduction in denitrification. N_2O undersaturation is frequently observed in anoxic core zones, often contrasting with high levels of supersaturation in peripheral suboxic zones. The biochemical mechanisms leading to this characteristic N_2O distribution are unclear. Laboratory studies have indicated that nitrous oxide reductase is more susceptible to oxygen inhibition than nitrite reductase (Dendooven and Anderson, 1994), so that after nitrite reduction has commenced, a further decrease in oxygen is required to switch on N_2O reduction. It has also been proposed that nitrous oxide reductase is slow to be induced, compared to other enzymes in the denitrification pathway, under conditions of declining oxygen (Firestone and Tiedje, 1979). This hypothetical hysteresis, coined the "spin-up phase" of denitrification, has been invoked to explain the extremely high levels of N_2O sometimes observed in suboxic/anoxic boundaries (Codispoti *et al.*, 2001). However, our present knowledge of the effect of oxygen concentration on denitrifying enzyme synthesis is relatively poor.

The experiments described here attempt to gain a basic empirical understanding of the effect of dissolved oxygen concentration on N_2O production and consumption rates in the denitrification pathway. This knowledge is required as a foundation to explain, and hence help predict, the distribution of N_2O in low oxygen zones. The objectives were (1),

to determine whether there are specific dissolved oxygen thresholds for the onset of N_2O production by denitrification, and consumption, consistent with differing enzyme sensitivity to oxygen inhibition, and (2), to compare the relative N_2O production and consumption rates over a range of oxygen concentrations, and so determine how oxygen levels control N_2O cycling.

In these experiments, no attempt was made to isolate, or identify, any individual species comprising the population of denitrifying bacteria in the seawater samples. The assumption was made that denitrification in coastal regions is performed by a highly diverse and robust assemblage of facultative anaerobes. Furthermore, it was also assumed that the initial population structure of facultative anaerobes in surface water is not of primary importance to the ultimate results obtained. Rather, that the selective environmental conditions imposed upon a water body ultimately govern the functionality of the microbial assemblage, and also the kinetics of transformations between nitrogen oxidation states.

This "black box" approach, while perhaps less than ideal, is adopted here out of necessity due to the current lack of knowledge regarding the significance of denitrifier species composition on ecological function. The application of taxonomy to marine denitrifying microbial communities is still at a very early stage, certainly when compared to work being conducted in the field of soil science (e.g. Cavigelli and Robertson, 2000, 2001). In taxonomic studies of aquatic microbial populations, at least one study has revealed that a large proportion of isolates capable of denitrification were not currently identifiable (Firth and Edwards, 2000). The authors also reminded us that culture experiments favour those groups of bacteria predisposed to grow on agar plates, and that

it is possible that the most important denitrifying organisms are to be found among the great numbers of microbes in the environment that cannot be so cultivated.

6.2. Methods

6.2.1. Sampling location

The sampling location was the Northwest Arm, Halifax Harbour, Nova Scotia (Figure 6.1). Seawater for these experiments was obtained directly from the pipe supplying the Aquatron facility at Dalhousie University. The mouth of this pipe is located at a depth of 15 m on the northeast side of the Arm.

The Northwest Arm is a 5.4 km long inlet with a mean width of around 0.3 km, forming the southwestern boundary of the Halifax peninsular. The average depth of the channel is around 12-15 m with a maximum of 19 m. Tides in the Arm are semi-diurnal with a mean amplitude of 1.5 m. There is no appreciable freshwater input. Exchange with the Harbour is driven by weak tidal mixing and wind driven currents, and the Arm is well-mixed during the winter months (Gregory, 1973).

6.2.2. Primary sample vessel

Figure 6.2 shows a schematic diagram of the primary sample vessel, used to contain water samples for up to about 1 month, and associated apparatus. The vessel was a 220L capacity, high-density polyethylene, cylindrical container. The relatively large volume was desirable to (1), provide a high volume to surface area ratio, thus minimising "bottle effects" caused by the growth of micro-organisms on the interior surface, and (2), to allow several litres of seawater to be drawn off over the course of the experiments, while only reducing the total volume by a few percent. Two existing 7 cm diameter threaded access ports in the top of the container were used for cleaning the interior, filling and

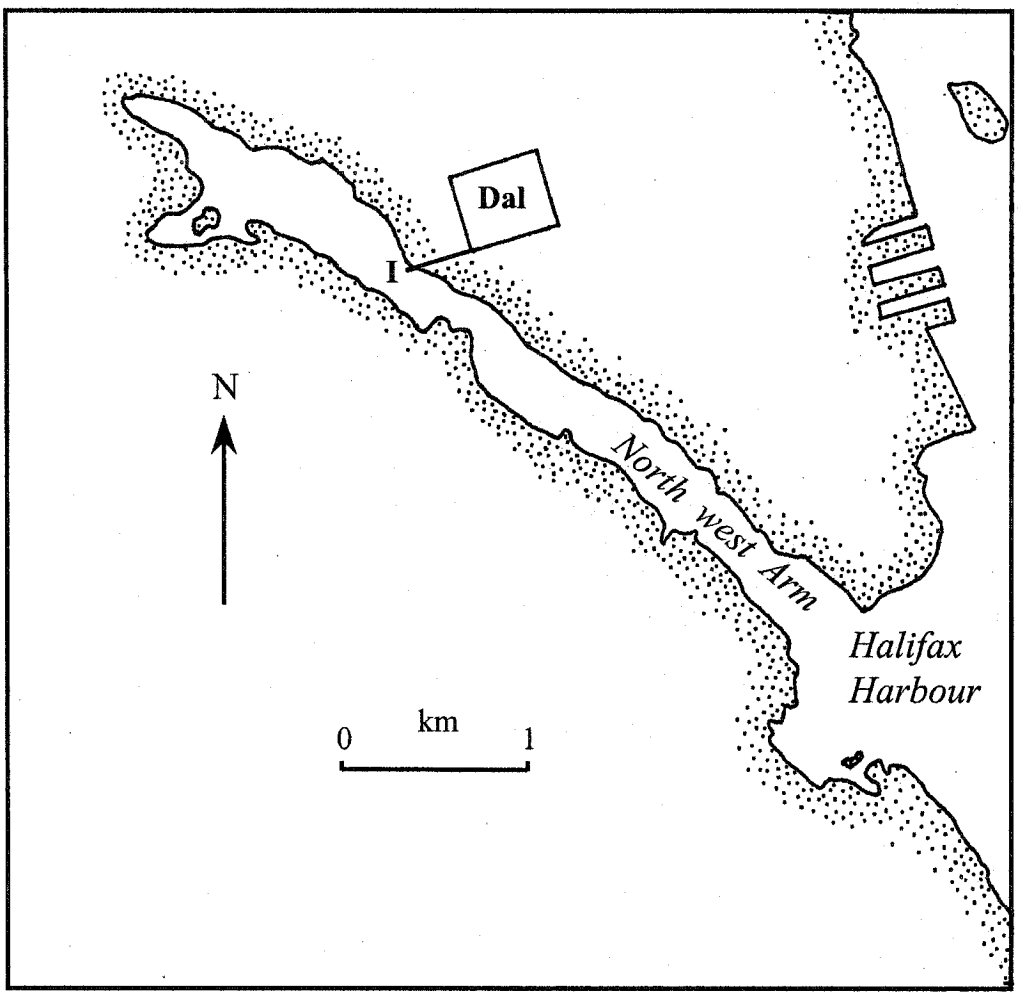

Figure 6.1. A map of the Northwest Arm study site showing the position of the Aquatron seawater intake pipe (I), and Dalhousie University (Dal).

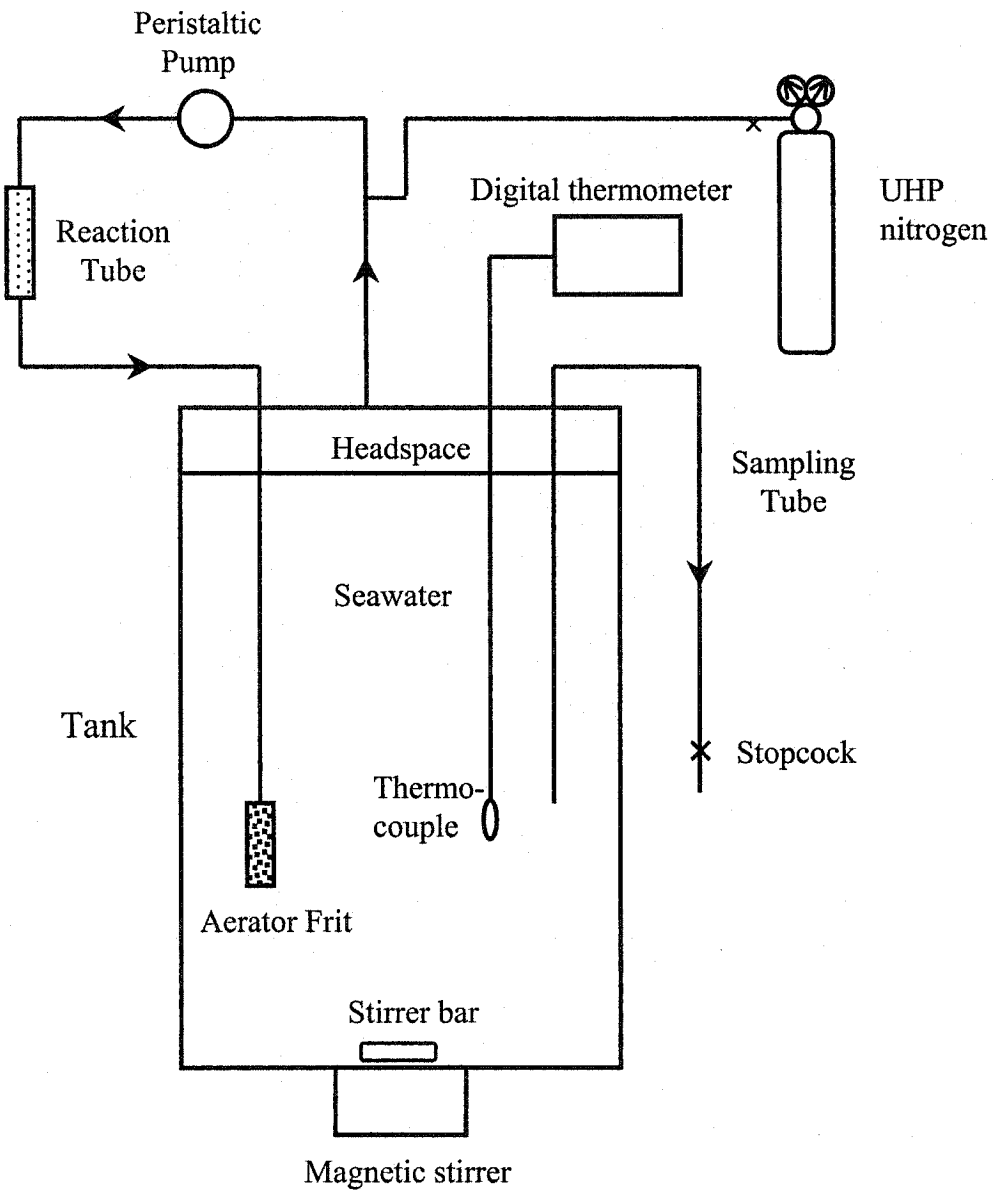

Figure 6.2. Schematic diagram of the sample vessel and associated equipment

draining. Four additional holes were drilled and tapped to accept Swagelock™ 12.5 mm tapered pipe thread male fittings. These fittings provided gas-tight openings for an equilibrator inlet tube terminating in a frit, a headspace outlet line, a sampling tube, and a sealed glass tube containing a thermocouple. All tubing entering the vessel was 0.25" o.d. thick-wall borosilicate glass chromatography tubing. The headspace pressure was maintained an about 1 atmosphere with UHP nitrogen.

6.2.3. Experimental procedure

Prior to each experiment, the inside of the sample vessel was cleaned by scrubbing with a soft bristled brush and distilled water, then rinsing, first with dilute hydrochloric acid, followed by distilled water. The vessel was then filled with seawater from the Aquatron intake pipe, leaving a headspace of approximately 10 cm. The seawater sample was filtered through an 8 μm pore-size Millipore membrane housed in an in-line filter cartridge. The purpose of filtering was to remove organic particles that could potentially develop anoxic micro-sites, and permit denitrification to occur in otherwise well-oxygenated seawater. Kaplan and Wofsy (1985) estimated that organic particles of around 100 μm diameter in a typical oxygen minimum zone could potentially develop internal anoxia. While their estimate has large uncertainties, the possibility of low oxygen niche formation should be much reduced in particles one order of magnitude smaller.

Six series of incubation experiments were conducted. For the first five, conducted in winter 2001/2002, seawater with an *in situ* temperature of around 2-4 °C was allowed to thermally equilibrate over a period of 2-3 days to the ambient laboratory temperature of

around 21°C. The incubation vessel was then insulated with 100 mm thick fibreglass to prevent short-term temperature fluctuations. In the case of Experiment Six, conducted in March/April 2003, the incubation temperature was maintained at the *in situ* temperature of around 4°C. This was achieved by flowing cold water from the Aquatron supply through 11 mm o.d. flexible laboratory tubing tightly coiled around the incubation vessel. As before, the vessel was surrounded by insulation over the cooling coil to reduce heat transfer from the room to the seawater sample. In all experiments, the insulation was supplemented by an outer layer of black polyethylene film to ensure that light was excluded from the sample, thus minimising nitrate and nitrite uptake by phytoplankton. The seawater samples were continually agitated with a large magnetic stirrer bar to inhibit the formation of flocculates.

Before starting the experiments, the seawater was analysed for nitrate and, if necessary, enriched to around 10 μmol L^{-1}. Glucose was also added to a final concentration of 10 μmols L^{-1} to provide a source of carbon for heterotrophic bacteria. In the absence of repeated ecological assessments of the captive microbial community, the maximum length of time that an experiment can run, while maintaining approximately natural conditions within the sample vessel, is a matter of conjecture. For these experiments, an upper time limit of about one month was imposed.

In the first five experiments, $^{15}N_2O$ production and degradation rates were determined by incubating syringes with 100 μmol L^{-1} $^{15}NO_3^-$ or ~10 nmol L^{-1} $^{15}N_2O$ respectively. As the 10 nM spike was of similar concentration to the background N_2O, the measured degradation rates in the spiked samples should reflect actual rates of N_2O loss. In the case of Experiment Six, the $^{15}NO_3^-$ treatment remained at 100 μmol L^{-1}, but the $^{15}N_2O$

spike was decreased by a factor of 10 to 1nM. The purpose of this change was to improve overall analytical precision in two ways. First, to ensure complete flushing of $^{15}N_2O$ from the purge and trap system, so that the subsequent sample should not be affected by small residual amounts of analyte, and second, to reduce the overall range of $^{15}N_2O$ concentrations that were measured, so that the detector gain could be better optimised for the samples low in ^{15}N concentration.

Samples for determination of nitrate and nitrite were collected from the 220 L container at the same time as incubation samples. The results provide a guide to the prevailing balance of nitrogen cycling in the container, but should be interpreted with caution, as there may be other sources and sinks processes apart from denitrification that affect the net concentrations of these compounds. For example, assimilative nitrate reduction by phytoplankton may occur, although the likelyhood of this occurring should be very low, as light was excluded from the container for several days prior to making measurements. On the other hand, dark incubation will allow nitrification to proceed, which represents a source of nitrate, and a source and sink for nitrite.

6.2.4. Manipulation of dissolved oxygen

Removal of dissolved oxygen in the contained seawater was achieved using the well-known reaction of metallic iron with oxygen in the presence of water (rusting).

$$4\,Fe_{(s)} + 3\,O_{2\,(g)} \rightarrow 2\,Fe_2O_{3\,(s)}$$

Air from the sealed headspace was pumped via a peristaltic pump through a 25 mm × 150 mm borosilicate glass reaction tube. The tube was packed with a mixture of iron powder and activated carbon granules, moistened with seawater. Carbon and salt water catalysed the highly exothermic iron oxidation. Oxygen-depleted air from the reaction

tube was then recirculated through the seawater via an aerator frit with a maximum flow rate of about 100 mL min^{-1}. Dissolved oxygen was determined periodically using the Winkler method. At oxygen levels below about 20 μmol L^{-1}, the Winkler method was supplemented by the spectrophotometric method described in Chapter Three. Adjusting the flow rate by means of a speed control on the peristaltic pump provided a degree of control over the rate of oxygen removal. The principal advantage of this method of oxygen removal, compared to purging the seawater with an inert gas, is that only the oxygen is removed. The concentrations of other dissolved gases including nitrous oxide and carbon dioxide remain unaffected.

6.3. Results

6.3.1 Experiment One

In this first experiment, dissolved oxygen concentration was reduced from about 250 to 34 μmol L^{-1} over the first two days. Thereafter, the peristaltic pump was turned off, and the oxygen level allowed to decline naturally due to organic matter degradation. The initial plan was to begin rate measurements at an oxygen concentration of around 10 μmol L^{-1} O_2, and then incrementally reduce the oxygen level for each consecutive set of measurements. Only $^{15}N_2O$ production measurements were made in this initial experiment. Incubations were conducted at 11.5, 10.2 and 8.1 μmol O_2 L^{-1} (Figure 6.3). Production rates were close to zero in each instance, being -2 ± 4, -4 ± 21 and 2 ± 7 pmol L^{-1} d^{-1} respectively. Nitrate and nitrite measurements showed little change, indicating that an oxygen level conducive to nitrate reduction had not yet been reached.

6.3.2. Experiment Two

Incubation measurements were made at 7.4, 2.7 and 2.4 μmol O_2 L^{-1} (Figure 6.4). Only N_2O production was measured in the first set of incubations, and the resulting rates were close to zero (mean = 4 ± 4 pmol L^{-1} d^{-1}). The second set of incubations gave a mean production rate of 246 ± 27 pmol L^{-1} d^{-1}, and a mean loss rate of –304 ± 121 pmol L^{-1} d^{-1}. The latter measurements were made at a lower oxygen level than originally intended, and the threshold for the onset of N_2O production and loss had clearly been crossed. It was a concern that the rate of change in oxygen may have outstripped the capacity of enzymatic processes to adjust to new redox conditions, so giving false results. To address this concern, it was decided to maintain the oxygen level as constant as possible over an extended period, and then repeat the measurements.

The oxygen reaction tube was replaced with a glass septum port. Over the next nine days, oxygen concentration was monitored and its removal by respiration was approximately balanced by injections of air into a flow of headspace gas through the equilibration frit. On the tenth day, the third set of incubation measurements returned mean $^{15}N_2O$ production and consumption rates of 186 ± 19, and –318 ± 65 pmol L^{-1} d^{-1} respectively. Nitrate concentration rose slightly between the first and second sets of measurements, and then fell by about 1 μmol L^{-1} in ten days. Nitrite showed a net accumulation of ~ 0.25 μmol L^{-1} during the same period.

6.3.3. Experiment Three

^{15}N incubations were conducted at oxygen concentrations of 4.4, 2.7, and 1.9 μmol L^{-1} (Figure 6.5). These measurements yielded corresponding mean $^{15}N_2O$ production rates of 29 ± 7, 74 ± 9 and 16 ± 2 pmol L^{-1} d^{-1}, and $^{15}N_2O$ loss rates of 26 ± 51, –133 ± 20 and

-332 ± 84 pmol L^{-1} d^{-1}. Nitrate concentration declined by 1.8 μmol L^{-1} over the three sets of measurements, with a corresponding increase in nitrite of 0.87 μmol L^{-1}.

6.3.4. Experiment Four

The process of oxygen reduction was slightly modified in this and the following experiment to provide a more gradual rate of decline akin to natural conditions. Following an initial rapid removal of oxygen, the air-circulating pump was stopped and oxygen allowed to decline due to respiration. In this case, there was a gradual decline from 10.1 to 5.3 μmol L^{-1} over 16 days (Figure 6.6).

Incubation experiments were conducted at oxygen concentrations of 7.1, 5.8 and 5.3 μmol L^{-1}. Corresponding production rates were 5 ± 7, 21 ± 24 and 30 ± 7, while no significant loss rates were observed. The ambient nitrate and nitrite concentrations were higher than in other samples. A decline in nitrate of 1.6 μmol L^{-1} over the course of the incubation measurements, together with a 0.3 μmol L^{-1} rise in nitrite, provided evidence of nitrate reduction in the range ~5 to 7 μmol O_2 L^{-1}.

6.3.5. Experiment Five

Water filtration for this experiment proceeded relatively slowly due to a rapid build-up of green-brown material on the filter membranes, seriously affecting the flow rate. An examination of this material under a microscope revealed it to be composed primarily of diatoms, with large numbers of dinoflagellates also present. The filtered seawater had a discernable green tint, indicating that a substantial proportion of the phytoplankton population had passed through the filter membrane.

$^{15}N_2O$ production and degradation measurements were conducted at oxygen concentrations of 6.6, 3.0, 2.3 and 1.6 μmol L^{-1} (Figure 6.7). Corresponding $^{15}N_2O$

production rates were 11 ± 4, 99 ± 8, 132 ± 3 and 114 ± 28 pmol L^{-1} d^{-1}, while loss rates were 95 ± 237, −17 ± 321, −884 ± 103 and −915 ± 315 pmol L^{-1} d^{-1}. Nitrate declined by 2.7 μmol L^{-1} while nitrite increased by 0.14μmol L^{-1}.

6.3.6. Compiled results

Figure 6.8 shows all mean $^{15}N_2O$ production rates and loss rates from the first five experiments plotted against oxygen concentration. The measured production rates are corrected for reductive losses at very low oxygen levels. Although the methodology was, as far as possible, identical for each experiment, this initial study spanned a period of six months including the transition from mid-winter to the start of the spring bloom. It is therefore possible that the data show variability associated with seasonal changes in both the density, and species composition, of the microbial community. With this caveat in mind, the measurements are nonetheless grouped together for interpretation.

In the case of samples incubated with labelled nitrate, $^{15}N_2O$ production commenced at around 7 μmol O_2 L^{-1}, increasing exponentially with declining oxygen. Although the exponential relationship between production rate and oxygen concentration shown in Figure 6.8a returns the best statistical fit, this best-fit curve is influenced by the very low production rate at 1.9 μmol O_2 L^{-1} from Experiment 3, and therefore may not be the most appropriate. In the case of samples incubated with labelled N_2O, there appears to be a well-defined threshold of about 3 μmol O_2 L^{-1} below which N_2O is consumed, with the rate of consumption increasing sharply with declining oxygen. The linear relationship between N_2O loss rate and dissolved oxygen shown in Figure 6.8b, where $O_2 = < 3$ μmol L^{-1} is perhaps the best choice given the scarcity of data.

The data shown in Figures 6.8a and 6.8b suggest that denitrification was a modest net source of N_2O over the relatively narrow range of oxygen concentrations from ~3 to 7 μmol L^{-1}, and becomes a net sink at lower levels of oxygen. This can be further illustrated by combining these two plots, giving the net result shown in Figure 6.8c.

6.3.7. Experiment Six

This experiment took place almost a year after the initial set of five experiments. Unlike the 2001/2002 experiments, the incubation temperature was maintained at the *in situ* temperature of 4 ± 1 °C. In this way, perturbations to enzymatic processes resulting from the ~ 18 °C rise in temperature, imposed on the first set of water samples, were avoided. The measured rates of N_2O production and loss at low oxygen levels may therefore be more comparable to the Bedford Basin study, described in Chapter Five, where temperatures in the range 2-6 °C were normally encountered.

This experiment ran from mid-March to mid-April, therefore the seasonal timing was similar to Experiment Five. As for Experiment Five, there was evidence of abundant phytoplankton in the form of a green-brown filtrate, and a green tint to the collected seawater. The results are shown in Figure 6.9. Seven sets of incubations were carried out, at oxygen levels of 9.9, 7.0, 4.2, 2.9, 2.1, 1.2 and 0.4 μmol L^{-1}. A comparison was made of oxygen measurements made using the Winkler method and the spectrophotometric method show that the Winkler results were consistently higher by 0.5-1.5 μmol O_2 L^{-1}. The series of production rate measurements made at 7.0 μmol O_2 L^{-1} were rejected because of an inconsistency attributable to a small degree of air contamination in the first few samples. This contamination did not appear great enough to visibly affect the $^{15}N_2O$-spiked degradation samples, and so those results are included.

$^{15}N_2O$ production rates were close to zero apart from a peak at 34 ± 9 pmol L^{-1} d^{-1} at 2.9 μmol O_2 L^{-1}, about half the rate of production seen at comparable oxygen concentrations in the 2001/2002 experiments. The degradation results were consistent with earlier experiments, in that no significant loss rates were seen above 2.9 μmol O_2 L^{-1}. Below this threshold, the measured loss rates were -94 ± 9, -62 ± 8, and -67 ± 26 pmol L^{-1} d^{-1} at oxygen concentrations of 2.1, 1.2 and 0.4 μmol L^{-1}. These loss rates equate to 9.6, 6.7 and 6.9% d^{-1}. In support of these findings, the record of ambient N_2O concentration shows a rapid decline in concentration after March 4th, when dissolved oxygen fell below 3 μmol O_2 L^{-1}. Net degradation rates calculated from the change in background N_2O concentrations with time are 8.0% d^{-1} (March 4th to 7th), 5.4% d^{-1} (March 7th to 9th) and 5.9% d^{-1}(March 9th to 11th), showing good agreement with the incubation results. Nitrate concentration showed little change from March 27th to April 7th, and then declined by about 1 μmol L^{-1} by the end of the experiment. In contrast, nitrite showed a consistent, albeit small, increase over the period March 27th to April 12th.

6.4. Discussion.

The results obtained from these low-oxygen experiments show clear evidence of three reductive steps in denitrification: nitrate reduction, nitrite reduction and nitrous oxide reduction. It also appears that the initiation of these processes is staggered under declining oxygen conditions. Nitrate reduction seems to be the most oxygen-tolerant process, as nitrate loss, together with nitrite accumulation, was clearly evident below about 8 μmol O_2 L^{-1}. It should be stressed however, that the nitrate and nitrite data only show net changes in nutrient concentration. The nitrification and denitrification pathways, rather than being precisely partitioned, may overlap over a range of oxygen

concentrations. Indeed, N_2O production from labelled ammonium was observed down to ~2.5 μmol O_2 L^{-1} in the Bedford Basin. Hence, it is easily conceivable that nitrate reduction could occur at oxygen concentrations higher than 8 μmol O_2 L^{-1}, and that the oxidation of nitrite to nitrate by nitrifying bacteria could balance the reductive process, resulting in no apparent change in the concentrations of these compounds over time. Furthermore, assimilatory nitrate reduction cannot be ruled out as a sink for nitrate, particularly in the samples that showed visible chlorophyll. The onset of nitrate reduction could certainly be better defined by monitoring the transfer of ^{15}N from the nitrate pool to the nitrite pool, but such work was beyond the scope of this study.

Figure 6.8a shows the appearance of ^{15}N-labelled N_2O below about 7 μmol O_2 L^{-1}, implying activation of the nitrite reductase enzyme. There did not appear to be a well-defined breakpoint, or single critical oxygen level, for the onset of nitrite reduction. Rather, there seemed to be a progressive increase in its rate as oxygen declined. It is interesting to note that nitrite accumulation occurred down to the lowest measured oxygen levels, suggesting that nitrite reduction is an overall rate-limiting stage of denitrification. This is in general agreement with high nitrite concentrations observed in zones of extreme oxygen depletion, e.g. the Arabian Sea (Naqvi and Noronha, 1991; Morrison *et al.*, 1998).

The onset of nitrous oxide reduction did seem to have a more dramatic, well-defined breakpoint of ~3 μmol O_2 L^{-1} (Figure 6.8b). This is substantially lower than some field measurements imply. For example, a comparison of oxygen and nitrous oxide data from the Baltic Sea (Rönner, 1983) indicated that N_2O increased as oxygen declined, until a critical point of about 9 μmol O_2 L^{-1} was reached, at which point N_2O concentrations

shifted from supersaturation to undersaturation. The rate of N_2O removal in the incubation experiments increased rapidly with a further decline in oxygen, to loss rates of up to about 10% d^{-1}. These loss rates were confirmed by a time-series of background N_2O measurements in Experiment Six, and most likely would have eventually led to almost complete N_2O depletion. This is interesting, as it implies that the capacity of the denitrifying community to reduce N_2O far exceeds the rate of supply from nitrite reduction. The experiments support the hypothesis that nitrous oxide reductase has a lower tolerance to oxygen inhibition than nitrite reductase, as opposed to a "spin-up" time for the induction of nitrous oxide reductase. Nitrous oxide loss was evident immediately whenever oxygen fell below 3 μmol O_2 L^{-1}, and in the case of Experiment Two, loss rates at ~ 2.5 μmol O_2 L^{-1}, remained similar even though the measurements were separated by ten days.

These results have important environmental implications. First, the potential for denitrification to contribute to net N_2O production in the water column may be limited to a very narrow range of oxygen concentrations. In addition, production rates seen here in this narrow range were at most ~ 1% d^{-1}. It is therefore difficult to imagine a comparable process being responsible for N_2O supersaturations of up to several thousand %, seen, for example, on the western Indian shelf (Naqvi *et al.*, 2000). Indeed, there has been a suspicion for some time, based on naturally occurring isotopic ratios, that such high levels of N_2O may arise from the reduction of one or more of the compounds produced by nitrification, the so called "nitrification-denitrification couple", rather than from "classical denitrification" studied here.

Second, seawater of below 3 μmol O_2 L^{-1} could form a highly active sink for N_2O. It was speculated in Chapter Five that the apparent nitrous oxide deficit, appearing in low oxygen conditions at the end of 2002, was due to an N_2O flux to anoxic, organic-rich sediments, or very low oxygen water overlying the sediments. Similarly, Naqvi and Noronha (1991) proposed that marginal sediments in contact with low-oxygen, but not denitrifying, waters in the Arabian Sea could be a sink for N_2O. These results tend to support these hypotheses, given that a small shift in oxygen concentration can result in a comparatively large sink term.

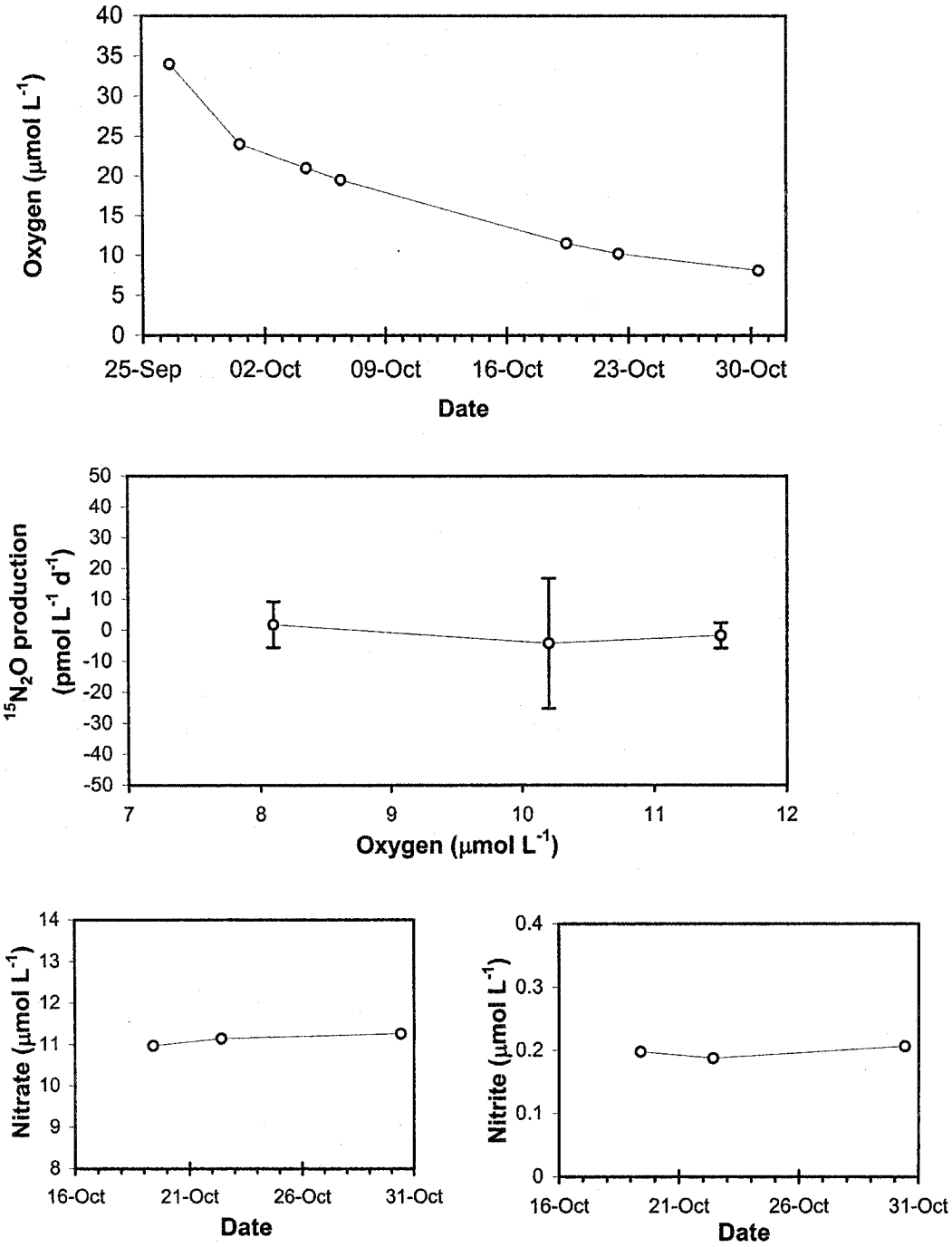

Figure 6.3. Results from Experiment 1. Oxygen concentration (top), N_2O production rates (middle), and nitrate and nitrite concentrations (bottom).

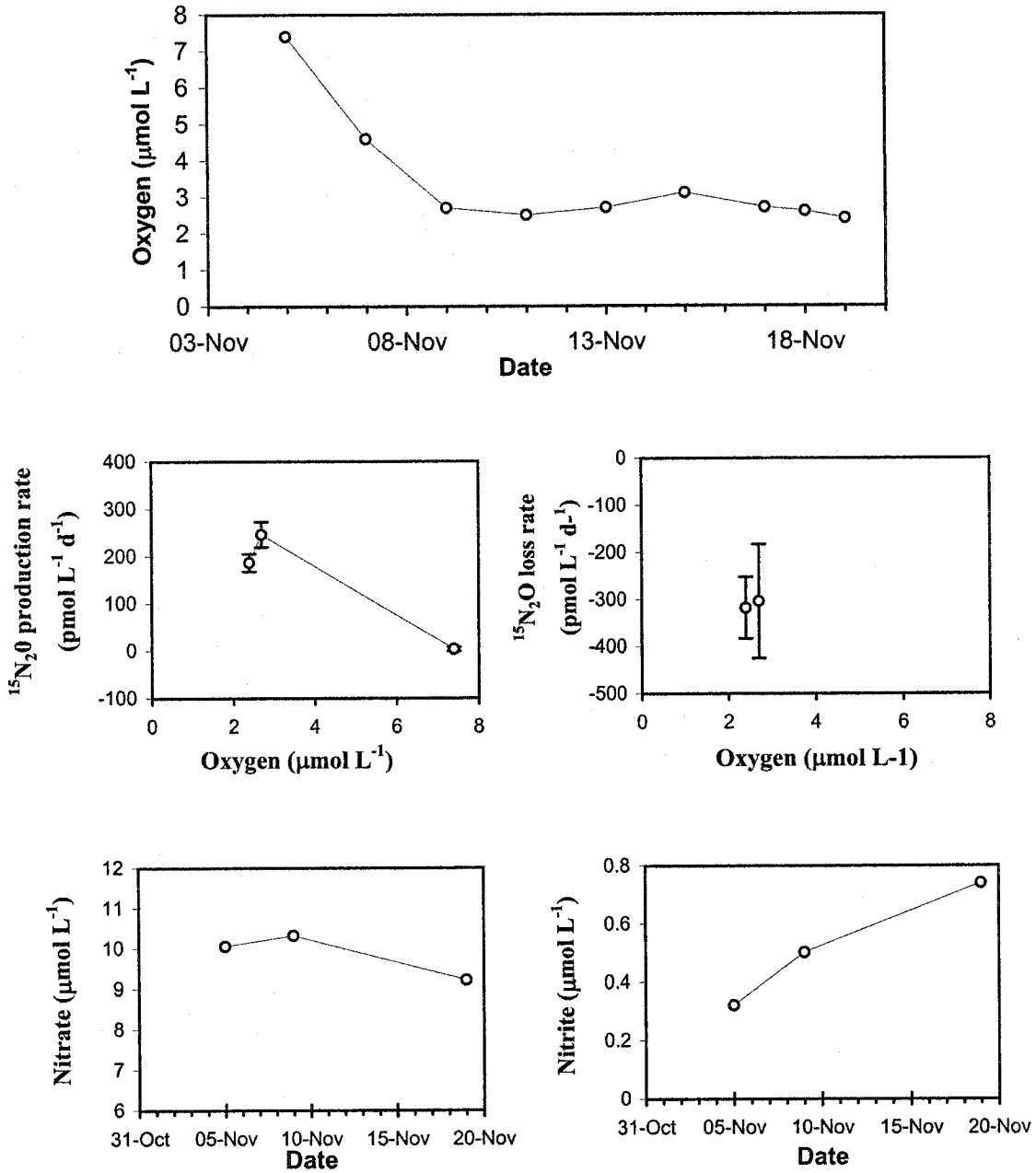

Figure 6.4. Results from Experiment 2. Top: oxygen concentration. Middle: $^{15}N_2O$ production and loss rates. Bottom: Nitrate and nitrite concentrations.

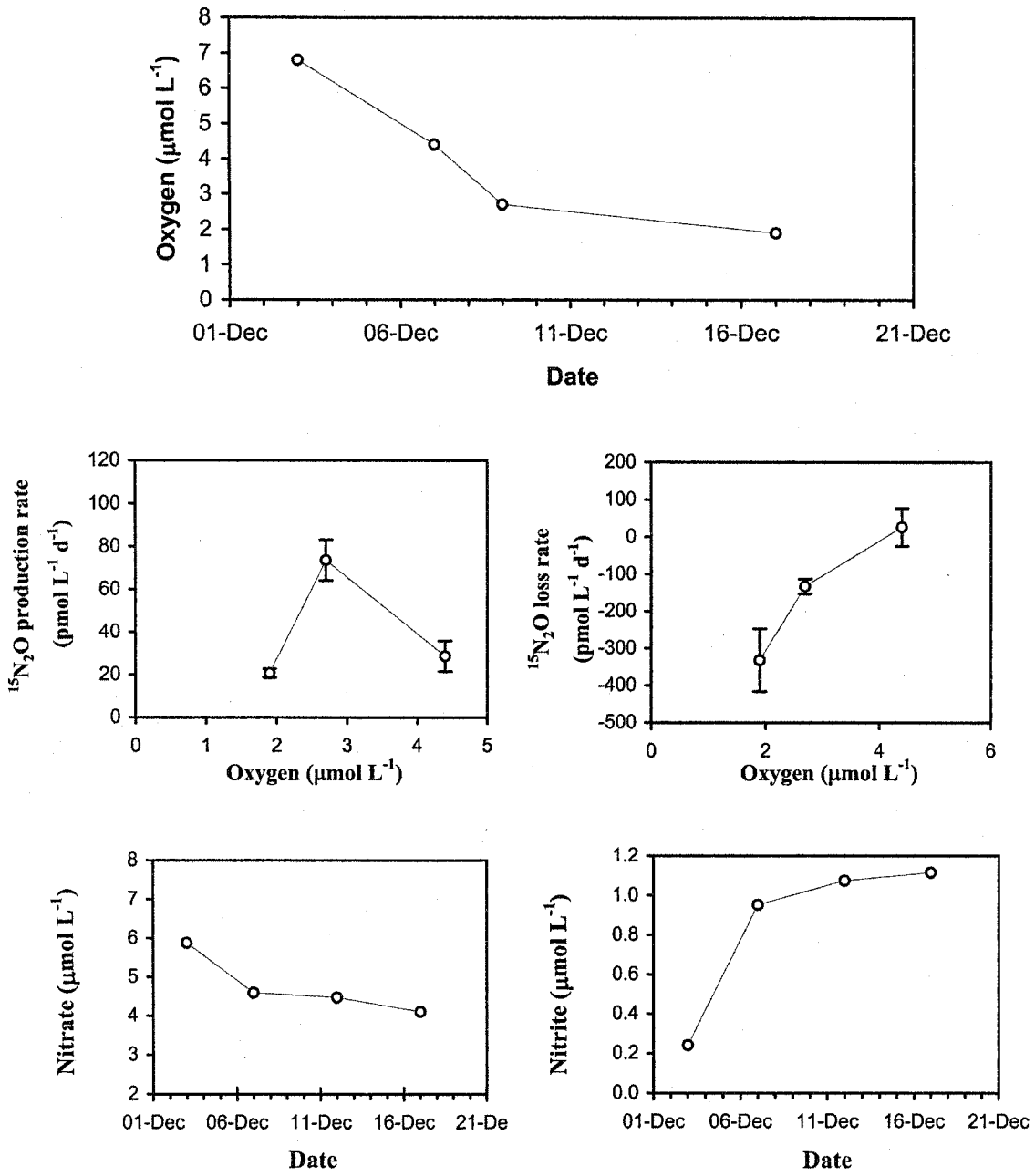

Figure 6.5. Results from Experiment 3. Top: oxygen concentration. Middle: $^{15}N_2O$ production and loss rates. Bottom: Nitrate and nitrite concentrations.

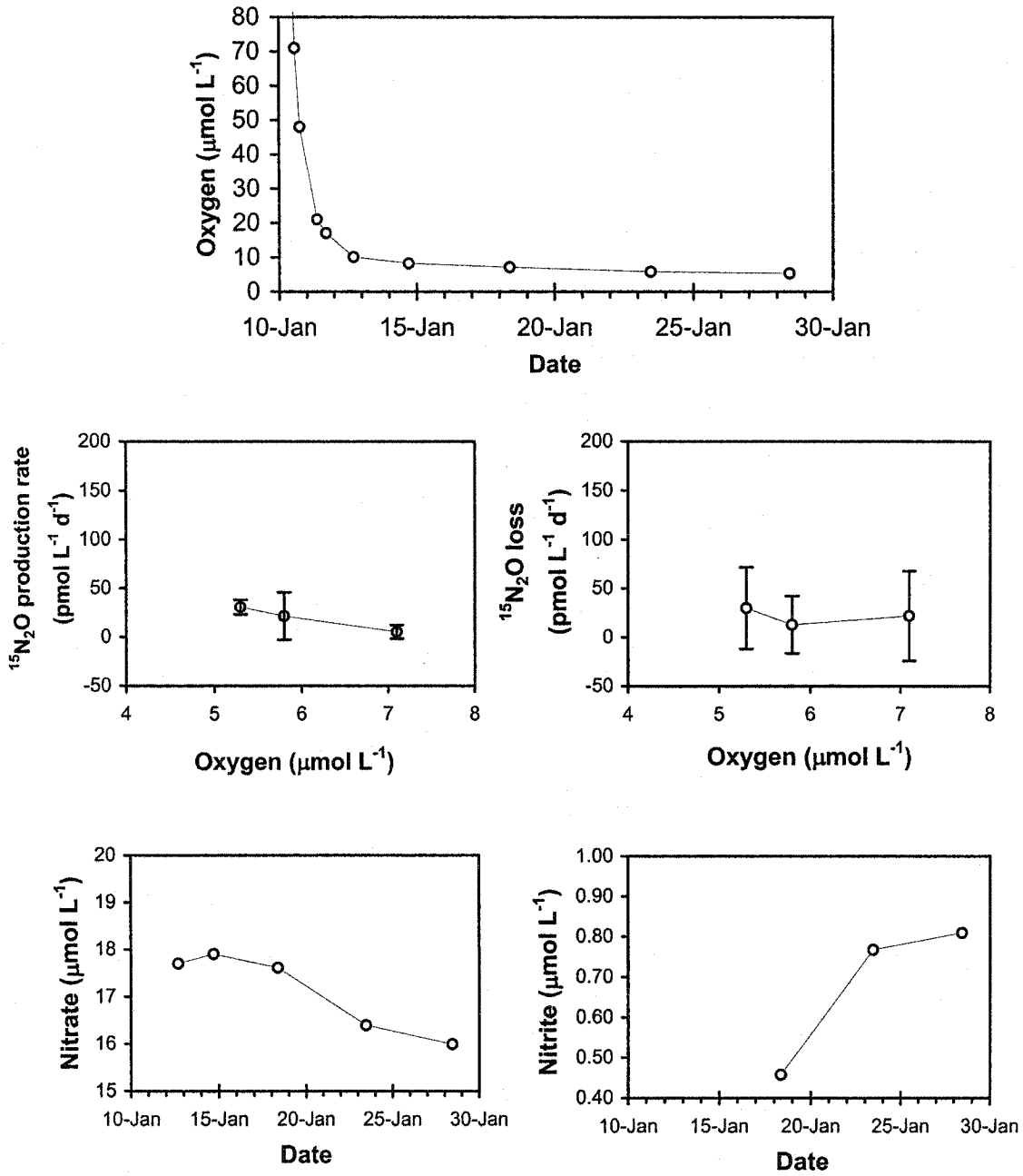

Figure 6.6. Results from Experiment 4. Top: oxygen concentration. Middle: $^{15}N_2O$ production and loss rates. Bottom: Nitrate and nitrite concentrations.

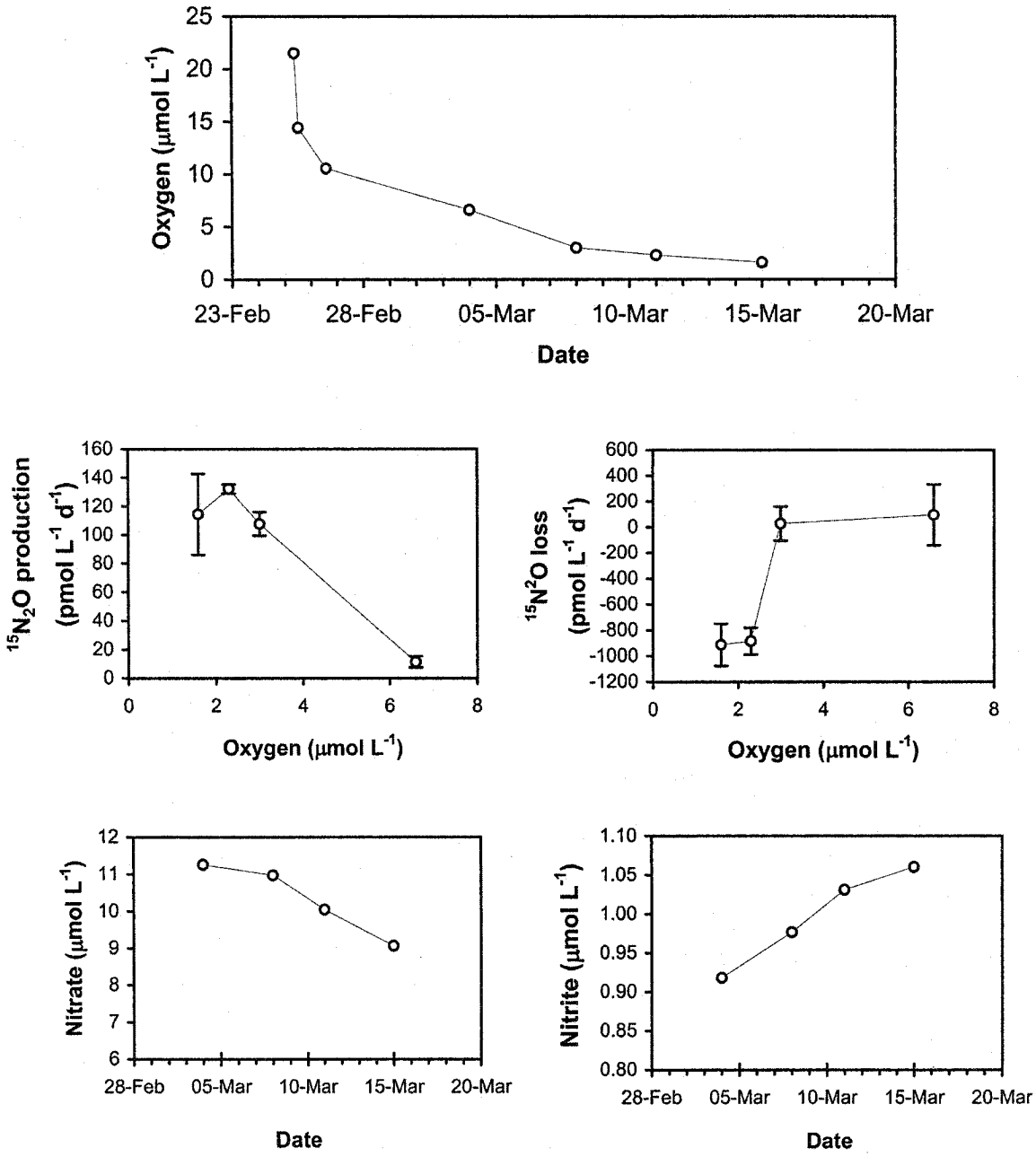

Figure 6.7. Results from Experiment 5. Top: oxygen concentration. Middle: $^{15}N_2O$ production and loss rates. Bottom: Nitrate and nitrite concentrations.

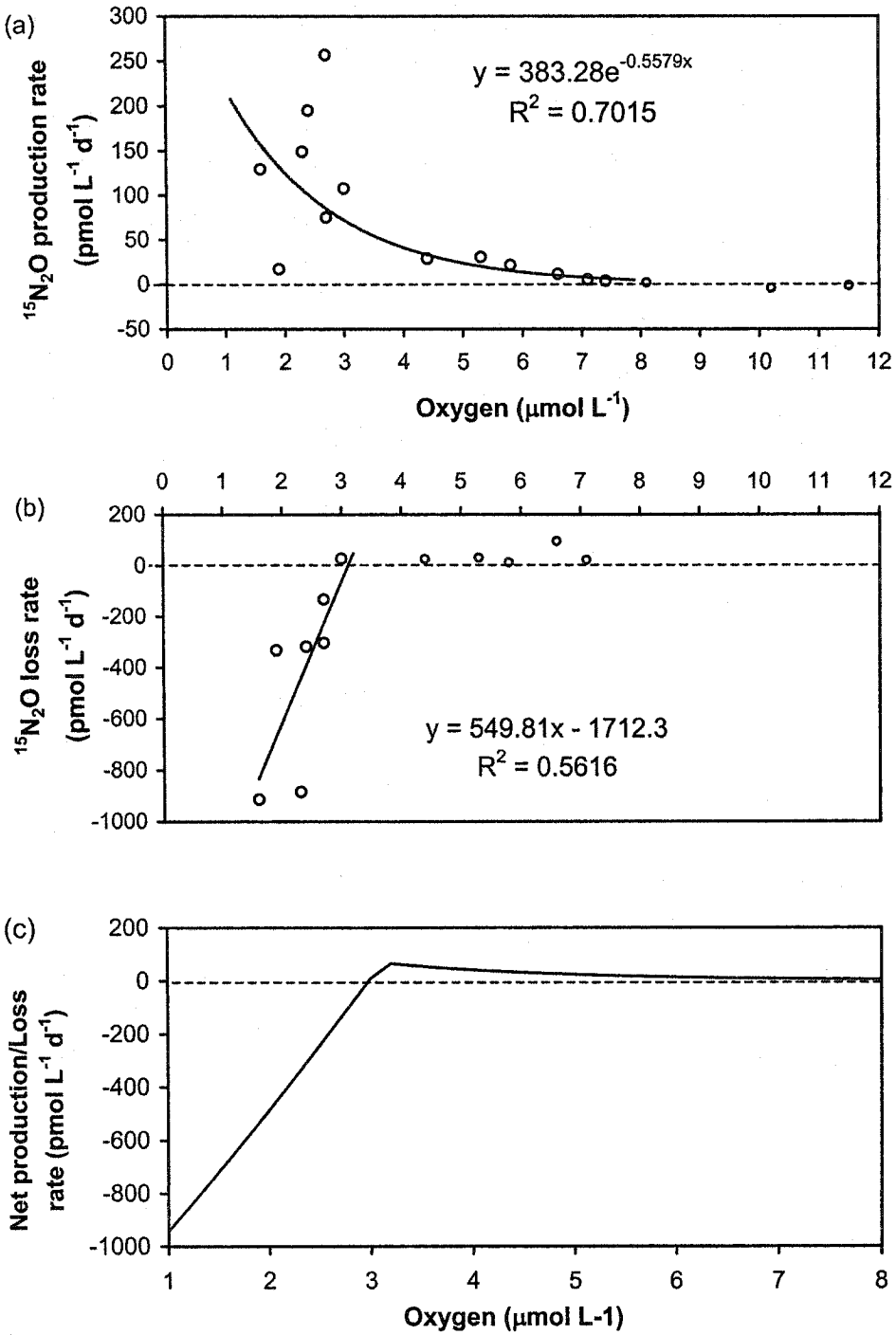

Figure 6.8. (a) $^{15}N_2O$ production rates, and (b), $^{15}N_2O$ loss rates, compiled from Experiments 1-5. (c) Net rates derived from (a) and (b).

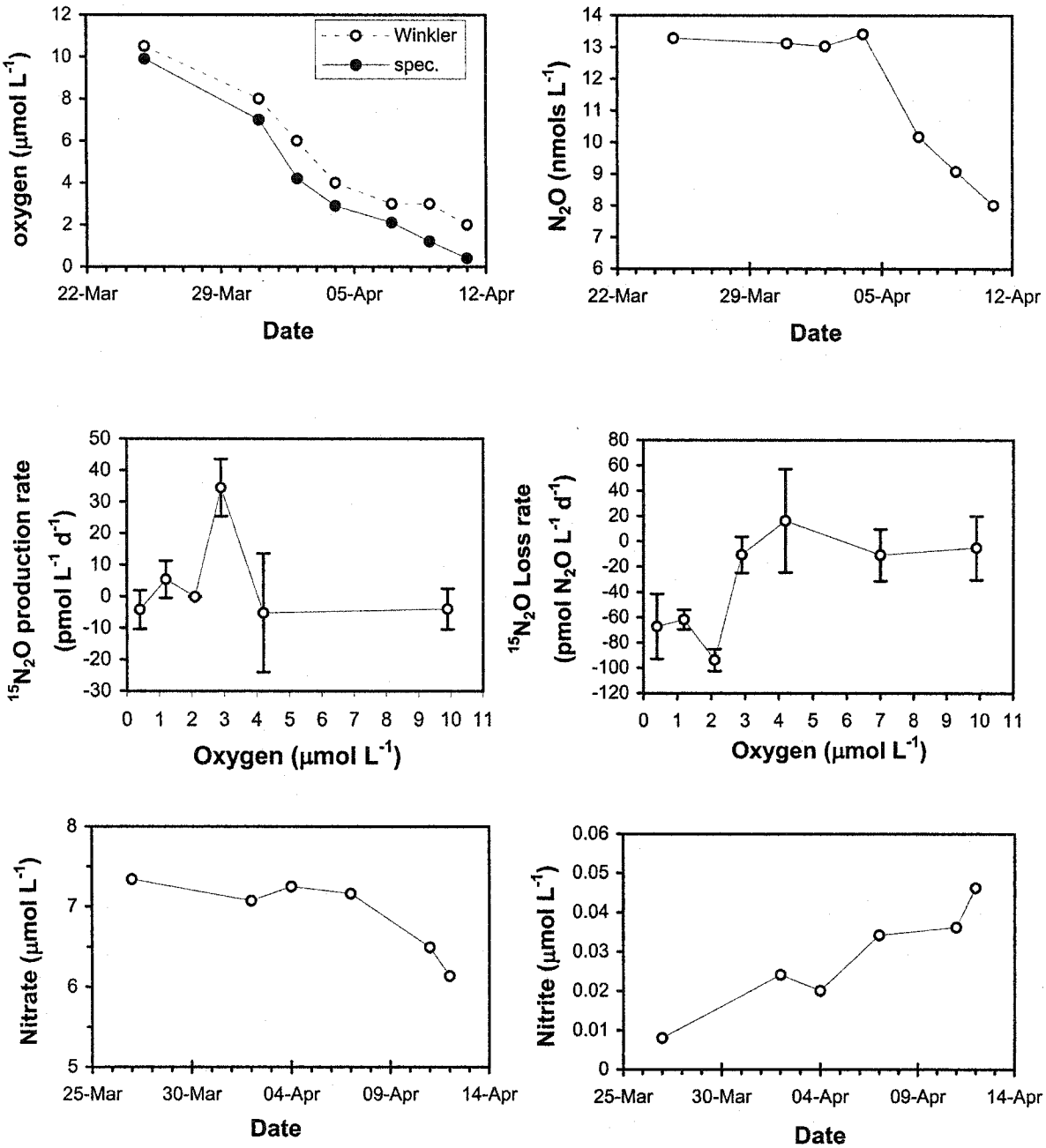

Figure 6.9. Results from Experiment 6. Top left: oxygen concentration. Solid line shows measurements made using the Winkler method, dashed line, spectrophotometric method. Top right: N_2O concentration. Middle: $^{15}N_2O$ production and loss rates. Bottom: Nitrate and nitrite concentrations.

Chapter 7

Conclusions and Recommendations for Future Work

7.1. Conclusions

This study addressed some fundamental questions concerning marine N_2O cycling by means of a ^{15}N tracer method. The importance of two bacterial pathways, ammonium oxidation and dissimilative nitrate reduction, were examined in relation to water column N_2O production and loss. In particular, the role of oxygen in controlling the rates of these processes was studied. The coastal margin provided the focus of interest, as this part of the ocean is of disproportionately high importance in the global marine N_2O flux, and is the region most affected by anthropogenic perturbation to the marine nitrogen cycle. In addition, a short cruise to the Labrador Sea presented the opportunity to obtain N_2O measurements in a sub-polar sea. The major conclusions are summarised below.

7.1.1. Analytical method

The combination of purge and trap/gas chromatography with a compact quadrupole mass-analyser can provide a relatively low-cost method of applying stable isotope techniques to marine N_2O studies. The equipment is portable enough for ship-borne operation, enabling ^{15}N tracer investigations of N_2O cycling to be conducted in remote areas of special interest. Previously, this would have entailed poison-terminated incubations and the possibly lengthy storage of samples awaiting laboratory analysis. N_2O is highly suited to small sample-volume purge-and-trap phase separation and preconcentration, and front-cut chromatography allows for multiple analyses without the need for frequent column or detector baking. The use of fully labelled N_2O as an internal standard can return the level of analytical precision necessary for kinetic studies.

The purity of the internal standard used in these studies was limited by the isotopic enrichment of the reagents used in its synthesis, particularly with regard to the ^{18}O-labelled sodium nitrate (95% enriched). As a consequence, the fully labelled N_2O product was contaminated by a small fraction of $^{15}N_2{}^{16}O$, which is also the principle analyte. This is not an ideal situation, and future researchers adopting this technique may well be able to reduce contamination by obtaining reagents of greater isotopic purity than those used here, or possibly by obtaining $^{15}N_2{}^{18}O$ of greater isotopic enrichment from a commercial source, although none was available at the time of this study.

The ion-fragment analysis method used in these studies has provided a solution to CO_2 interference while returning adequate sensitivity where rates of N_2O cycling are high, such as in eutrophic estuarine waters. This approach is however a compromise between sensitivity and analytical turn-around time for the instrumental set up described. With the relatively small background signal of the NO^+ fragment ion, the signal to noise ratio is lower than for the N_2O^+ parent ion. On the other hand, total chromatographic separation of the N_2O peak from that of CO_2 would require a sub-ambient oven temperature and/or longer chromatographic column, with a corresponding increase in the retention time and therefore sample turn-around time.

In ocean regions where N_2O production/consumption rates are low, two modifications to the method could be applied to enhance rate measurement. First, parent-ion analysis may further improve the precision of $^{15}N_2O$ production rates by giving a higher signal to noise ratio for the $^{15}N_2O$ peak, so reducing errors in baseline determination. Second, incubation times could be extended to make low $^{15}N_2O$ production and loss rates easier to determine. It is probably unrealistic to incubate sample of less than 100 mL for much

past 24 hours and expect the *in vitro* rates to reflect those in the natural environment. For extended incubation times, it would therefore be desirable to have larger incubation vessels offering a higher volume:surface area ratio, but that also allow subsamples to be drawn without the introduction of air. One option is to use larger borosilicate syringes, and 250 mL versions, although expensive, may be worth considering.

7.1.2. Labrador Sea cruise

The surface waters of the Scotian Shelf, Gulf of Saint Lawrence and Labrador Sea were found to be slightly supersaturated with nitrous oxide at a level similar to most of the global ocean. Consequently, this region constituted a modest source of N_2O to the atmosphere at the time of this study. Flux estimates, ranging from 0 – 4.2 μmol N_2O m^{-2} d^{-1}, were highly dependent on the estimated windspeed. A greater number of measurements combined with long-term average windspeed data may help to improve the reliability of these estimates.

The mechanism of N_2O production in the region at the time of this study probably comprised two synchronous components. First, ammonium oxidation was seen to provide a source of N_2O at some of the stations where incubations were carried out. Second, solar heating of the sub-polar Atlantic basin surface water in the spring and summer is likely to result in apparent N_2O production by progressively reducing the solubility coefficient in the mixed layer, resulting in an efflux of N_2O as equilibration across the sea/air interface proceeds. An N_2O flux from the Labrador Sea during early summer, whether originating from ammonium oxidation, or sea surface warming, may only be one facet of the overall cycle in ocean-atmosphere N_2O exchange. Seasonal cooling of the surface water in fall and winter will result in increased N_2O solubility,

reversing the direction of the flux. Given that this enhanced solubility is accompanied by winter deep-water formation in this region, the Labrador Sea may be a sink for N_2O in the winter, with long-term sequestration to the North Atlantic Deep Water.

7.1.3. The Bedford Basin study

Nitrous oxide production rate measurements, extending over a period of eighteen months in the deep water of the Bedford Basin, showed that nitrification was the predominant source of N_2O in the water column. In contrast, denitrification appeared to be a relatively minor source of N_2O, as for the most part, N_2O production from the reduction of labelled nitrate was not detectable. Under low oxygen conditions, N_2O measurements were consistent with a large in situ sink, presumable by denitrification in anoxic water.

The efficiency of ammonium conversion to N_2O displayed a negative relationship with dissolved oxygen, and increased exponentially as oxygen declined. N_2O yields (100 mol N_2O/mol NH_4^+) ranged from around 0.01 to 0.11% with the highest yields occurring in conditions approaching sub-oxia. Plots of background N_2O versus AOU and nitrate agreed with the non-linear nature of this relationship. The factors governing nitrification were not obvious, and ammonium oxidation rates showed no correlation to substrate concentration. Both ammonium oxidation rates and N_2O production rates were suppressed after mixing events. In the case of N_2O production, this observation can be at least partly explained by the very low N_2O yields at high oxygen concentrations. For ammonium oxidation, variations in the biomass of active bacteria caused by water mass movement may have played a role. No bacteria counts were performed in this work, but

the role of microbial ecology in coastal N_2O production may prove to be a fruitful avenue for future studies.

Given the similarity of the N_2O:AOU relationship for July 2001 to March 2002 in the Bedford Basin, to that found in upper 500 m of the Northwest Indian Ocean by Upstill-Goddard *et al.* (1999), it is tempting to conclude that N_2O is formed by a similar process in these otherwise disparate regions. Therefore, applying Occam's Razor, enhanced N_2O production at low oxygen levels, found in regions such as the Northwest Indian Ocean, may be explained most simply by nitrification alone, rather than invoking an additional process such as denitrification in anoxic micro sites.

7.1.4. Laboratory incubation experiments

Incubations of sub-oxic filtered seawater with ^{15}N-labelled nitrate revealed that $^{15}N_2O$ production occurred at oxygen levels below around 8 μmol L^{-1}, progressively increasing as oxygen declined. Below around 3 μmol O_2 L^{-1}, N_2O consumption dominated, resulting in a net loss of this compound, presumably by reduction to dinitrogen. This latter observation lends some weight to the argument for a substantial *in situ* N_2O sink in the near anoxic water of the Bedford Basin.

These experiments were relatively simplistic, and provided no information on the nature of the denitrifying populations. Nevertheless, the results do support the hypothesis that the distribution of N_2O across suboxic/anoxic gradients results from nitrous oxide reductase being more sensitive to oxygen inhibition than nitrite reductase, rather than being an effect of a hysteresis in nitrous oxide reductase synthesis.

7.2. Suggestions for future work

With respect to the N_2O yield from nitrification during the latter half of the Bedford Basin study, the cause of the apparent fall in yield as oxygen levels neared anoxia remains unresolved. There is a need to acquire more data to better constrain the N_2O yield:O_2 relationship proposed in Chapter Five. Ideally, further measurements should be made under controlled conditions to reduce the likelihood of ecological variability affecting the results, as may be the case in a study that encompasses a number of seasons. It would be therefore beneficial to conduct a series of experiments similar to those described in Chapter Six, but with large seawater samples collected from a natural, nitrifying environment. Measurements of ammonium oxidation and N_2O production rates would be obtained under a range of oxygen levels.

The biochemical pathway or pathways responsible for nitrous oxide production via ammonium oxidation needs to be investigated. This study raises the question of why the apparent efficiency of ammonium conversion to N_2O increases as oxygen declines. A number of possibilities may be considered. One is that N_2O is formed by a single pathway with NH_2OH or NO as the precursor, and this process is favoured at low oxygen levels. Another possibility is that two pathways are involved. The efficiency of the primary pathway remains relatively unchanged, but the N_2O so produced is increasingly supplemented by another, presumably reductive, process as oxygen declines. This latter hypothesis, coupled nitrification-denitrification, has been considered as an N_2O production mechanism for the last ~15 years. The reduction of nitrite to N_2O by nitrifiers has been suggested to explain the isotopic composition of N_2O in low oxygen waters of the northwestern Arabian Sea (Yoshinari *et al.*, 1997). This pathway could be consistent

with the Bedford Basin results if ^{15}N-labelled nitrite produced by the oxidation of $^{15}NH_4^+$ were reduced to $^{15}N_2O$ at low oxygen levels, supplementing the 'normal' N_2O source. However, anaerobic reduction of nitrite by denitrifiers seems unlikely, given that $^{15}NO_3^-$ reduction to $^{15}N_2O$ was not observed over most of the range of oxygen concentrations where N_2O yield was enhanced.

An explanation to this conundrum may be that nitrite reduction took place but was not mediated by facultative anaerobes. Instead, an intracellular pathway within the ammonium oxidising bacterium could be responsible. Poth and Focht (1985) demonstrated the production of N_2O from nitrite by the ubiquitous marine ammonium oxidiser *Nitrosomonas europaea*. The possibility of this process occurring in natural waters could be investigated by conducting further $^{15}N_2O$ production rate measurements under low oxygen concentrations, with additional measurements of samples treated with $^{15}NO_2^-$.

A long-term goal for ship-borne ^{15}N tracer studies could be an investigation of N_2O cycling in the persistent low-oxygen, upwelling zones encountered off western continental shelves and in the northwestern Indian Ocean. These regions undoubtedly form an important component of the ocean N_2O source (e.g. Codispoti *et al.*, 1993), yet it may well also be the case that the associated anoxic core zones are important in-situ sinks for N_2O, so mitigating the net efflux from these regions. If this is the case, then the magnitude of the N_2O source from upwelling zones may be highly sensitive to the supply of particulate organic carbon from primary production, as the experiments described in Chapter Six suggest that the balance between net N_2O production and consumption by denitrification is critically dependent on oxygen concentration. Primary productivity in

the eastern tropical South Pacific is greatly influenced by the well-known En Niño/La Niña Southern Oscillation, and the frequency of this cycle may be increasing as a result of climate change. It is therefore important to quantify N_2O turnover in low-oxygen regions underlying areas of high primary productivity, and assess the sensitivity of this turnover to changes in circulation and stratification resulting from anthropogenic climate perturbation.

7.3. Summary

These studies showed that oxygen is a highly important control on the production of nitrous oxide by the microbial pathways of nitrification and denitrification. Nitrification was found to be the predominant source of N_2O in coastal seawater. The net production of N_2O by denitrification appears to be restricted to a narrow range of suboxia, but could potentially be important where such conditions persist. Denitrification in anoxic regions is likely to be a comparatively large N_2O sink. The empirical relationship between the yield of N_2O from ammonium oxidation and dissolved oxygen, found in the course of this work, will aid in modelling N_2O emissions from the sea.

Development and expansion of seasonal suboxia in coastal margins, a likely result of the current increasing trend in eutrophication, may enhance an already important global source of N_2O. Conversely, an increase in the incidence of anoxia could act to mitigate N_2O fluxes. The net effects of oxygen depletion on the coastal N_2O source strength should be considered in future modelled projections of atmospheric nitrous oxide accumulation.

References

Amouroux, D., Roberts, G., Rapsomanikis, S. and Andreae, M. O., 2002. Biogenic gas (CH_4, N_2O, DMS) emission to the atmosphere from near-shore and shelf waters of the north-western Black Sea. *Estuarine, Coastal and Shelf Science*, 54: 575-587.

Andersson, A., Laurent, P., Kihn, A., Prevost, M. and Servais, P., 2001. Impact of temperature on nitrification in biological activated carbon (BAC) filters used for drinking water treatment. *Water Research*, 35: 2923-2934.

Bange, H. W., Rapsomanikis, S. and Andreae, M. O., 1996a. Nitrous oxide in coastal waters. *Global Biogeochemical Cycles*, 10: 197-207.

Bange, H. W., Rapsomanikis, S. and Andreae, M. O., 1996b. The Aegean Sea as a source of atmospheric nitrous oxide and methane. *Marine Chemistry*, 53: 41-49.

Barnes, J. and Owens, N. J. P., 1999. Denitrification and nitrous oxide concentrations in the Humber estuary, UK, and adjacent coastal zones. *Marine Pollution Bulletin*, 37: 247-260.

Barsdate, R. J. and Dugdale, R. C., 1965. Rapid conversion of organic nitrogen to N_2 for mass spectrometry: an automated Dumas procedure. *Analytical Biochemistry*, 13: 1-5.

Battle, M., Bender, M., Sowers, T., Tans, P. P., Butler, J. H., Elkins, J. W., Ellis, J. T., Conway, T., Zhang, N., Lang, P. and Clarke, A. D., 1996. Atmospheric gas concentrations over the past century measured in air from firn at the South Pole. *Nature*, 383: 231-235.

Bengtsson, G. and Annadotta, H., 1989. Nitrate reduction in a ground water microcosm determined by ^{15}N gas chromatography-mass spectrometry. *Applied and Environmental Microbiology*, 55: 2861-2870.

Berounsky, V. M. and Nixon, S. W., 1990. Temperature and the annual cycle of nitrification in waters of Narragansett Bay. *Limnology and Oceanography*, 35: 1610-1617.

Berounsky, V. M. and Nixon, S. W., 1993. Rates of nitrification along an estuarine gradient in Narragansett Bay. *Estuaries*, 16: 718-730.

Bianchi, M., Fosset, C. and Conan, P., 1999. Nitrification rates in the NW Mediterranean Sea. *Aquatic Microbial Ecology*, 17: 267-278.

Billen, G., 1976. Evaluation of nitrifying activity in the sediments by dark ^{14}C-bicarbonate incorporation. *Water Research*, 10: 51-57.

Bock, E., 1965. Vergleichende untersuchung über die wirkung sichtbaren Lichtes auf *Nitrosomonas europaea* und *Nitrobacter winogradskyi*. *Archiv für Mikrobiologie*, 51: 18-41.

Bock, E., Koops, H.-P. and Harms, H., 1986. Cell biology of nitrifying bacteria, In: Prosser, I. (Editor), Nitrification. IRL Press, Oxford, pp. 17-38.

Bonin, P., Tamburini, C. and Michotey, V., 2002. Determination of the bacterial processes which are sources of nitrous oxide production in marine samples. *Water Research*, 36: 722-732.

Bouillot, P., Roustan, J. L., Albagnac, G. and Cadet, J. L., 1992. Biological nitrification kinetics at low temperature in a drinking-water production plant. *Water Supply*, 10: 137-153.

Bouwman, A. F., Van der Hoek, K. W. and Olivier, J. G. J., 1995. Uncertainties in the global source distribution of nitrous oxide. *Journal of Geophysical Research*, 100: 2785-2800.

Brenninkmeijer, C. A. M. and Röckmann, T., 1999. Mass spectrometry of the intramolecular nitrogen isotope distribution of environmental nitrous oxide using fragment-ion analysis. *Rapid Communications in Mass Spectrometry*, 13: 2028-2033.

Broecker, W. S., 1991. The Great Ocean Conveyor. *Oceanography*, 4: 79-89.

Broenkow, W. W. and Cline, J. D., 1969. Colorimetric determination of dissolved oxygen at low concentrations. *Limnology and Oceanography*, 14: 450-454.

Butler, J. H. and Elkins, J. W., 1991. An automated technique for the measurement of dissolved N_2O in natural waters. *Marine Chemistry*, 34: 47-61.

Butler, J. H., Elkins, J. W. and Thompson, T. M., 1989. Tropospheric and dissolved N_2O of the west Pacific and east Indian Oceans during the El Nino Southern Oscillation event of 1987. *Journal of Geophysical Research*, 94: 14865-14877.

Capone, D. G., 2000. The marine microbial nitrogen cycle, In: Kirchman, D. L. (Editor), Microbial Ecology of the Ocean. Wiley-Liss, New York, pp. 455-493.

Cavigelli, M. A. and Robertson, G. P., 2000. The functional significance of denitrifier community composition in a terrestrial ecosystem. *Ecology*, 81: 1402-1414.

Chan, Y. K. and Campbell, N. E. R., 1980. Denitrification in Lake 227 during summer stratification. *Canadian Journal of Fisheries and Aquatic Sciences*, 37: 506-512.

Cline, J. D. and Richards, F. A., 1972. Oxygen deficient conditions and nitrate reduction in the eastern tropical north Pacific Ocean. *Limnology and Oceanography*, 17: 885-900.

Codispoti, L. A., Brandes, J. A., Christensen, J. P., Devol, A. H., Naqvi, S. W. A., Paerl, H. W. and Yoshinari, T., 2001. The oceanic fixed nitrogen and nitrous oxide budgets: Moving targets as we enter the anthropocene? *Scientia Marina*, 65: 85-105.

Codispoti, L. A., Elkins, J. W., Yoshinari, T., Friederich, G. E., Sakamoto, C. M., and Packard, T. T., 1993. On the nitrous oxide flux from productive regions that contain low oxygen waters, In: Desai, B. N. (Editor), Oceanography of the Indian Ocean. A. A. Balkema, Rotterdam, pp. 271-284.

Cohen, Y., 1978. Consumption of dissolved nitrous oxide in an anoxic basin, Saanich Inlet, British Columbia. *Nature*, 272: 235-237.

Cohen, Y. and Gordon, L. I., 1978. Nitrous oxide in the oxygen minimum of the eastern tropical North Pacific: evidence for its consumption during denitrification and possible mechanisms for its production. *Deep-Sea Research*, 25: 509-524.

Craig, H. and Gordon, L. I., 1963. Nitrous oxide in the ocean and marine atmosphere. *Geochimica et Cosmochimica Acta*, 27: 949-955.

Crutzen, P. J. and Andreae, M. O., 1990. Biomass burning in the tropics: impact on atmospheric chemistry and biogeochemical cycles. *Science*, 250: 1669-1678.

Crutzen, P. J. and Ramanathan, V., 2000. The ascent of atmospheric sciences. *Science*, 290: 299-304.

Dalsgaard, T., Canfield, D. E., Petersen, J., Thamdrup, B., and Acuña-González, J., 2003. N_2 production by the anammox reaction in the anoxic water column of Golfo Dulce, Costa Rica. *Nature*, 422: 606-608.

de Bie, M. J. M., Middelburg, J. J., Starink, M. and Laanbroek, H. J., 2002. Factors controlling nitrous oxide at the microbial community and estuarine scale. *Marine Ecology Progress Series*, 240: 1-9.

de Vries, H. J. M., Olivier, J. G. J., Van den Wijngaart, R. A., Kreileman, G. J. J. and Toet, A. M. C., 1994. Model for calculating regional energy use, industrial production and greenhouse gas emissions for evaluating global climate scenarios. *Water, Air and Soil Pollution*, 76: 79-131.

de Wilde, H. P. J. and de Bie, M. J. M., 2000. Nitrous oxide in the Schelde estuary: production by nitrification and emission to the atmosphere. *Marine Chemistry*, 69: 203-216.

de Wilde, H. P. J. and Helder, W., 1997. Nitrous oxide in the Somali Basin: the role of upwelling. *Deep-Sea Research 2: Topical Studies in Oceanography*, 44: 1319-1340.

Dendooven, L. and Anderson, J. M., 1994. Dynamics of reduction enzymes involved in the denitrification process in Pasture Soil. *Soil Biology and Biochemistry*, 26: 1501-1506.

Dibb, J. E., Rasmussen, R. A., Mayewski, P. A. and Holdsworth, G., 1993. Northern Hemisphere concentrations of methane and nitrous oxide since 1800: Results from the Mt. Logan and 20D ice cores. *Chemosphere*, 27: 2413-2423.

Dore, J. E. and Karl, D. M., 1996. Nitrification in the euphotic zone as a source for nitrite, nitrate, and nitrous oxide at Station ALOHA. *Limnology and Oceanography*, 41: 1619-1628.

Dore, J. E., Popp, B. N., Karl, D. M. and Sansone, F. J., 1998. A large source of atmospheric nitrous oxide from subtropical North Pacific surface waters. *Nature*, 396: 63-66.

Elkins, J. W., Wofsy, S. C., McElroy, M. B., Kolb, C. E. and Kaplan, W. A., 1978. Aquatic sources and sinks for nitrous oxide. *Nature*, 275: 602-606.

Etheridge, D. M., Pearman, G. I. and deSilva, F., 1988. Atmospheric trace-gas variations as revealed by air trapped in an ice core from Law Dome, Antarctica. *Annals Glaciology*, 10: 28-33.

Everett, J. T. and Fitzharris, B. B., 1998. The Arctic and the Antarctic. In: Watson, R. T., Zinyowera, M. C., Moss, R. H. and Dokken, D. J. (Editors), The Regional Impacts of Climate Change. An Assessment of Vulnerability. A Special Report of IPCC Working Group II for the Intergovernmental Panel of Climate Change. Cambridge University Press, Cambridge, United Kingdom, pp. 85-103.

Falkowski, P. G., Scholes, R. J., Boyle, E., Canadell, J., Canfield, D., Elser, J., Gruber, N., Hibbard, K., Hogberg, P., Linder, S., Mackenzie, F. T., Moore, B., Pedersen, T., Rosenthal, Y., Seitzinger, S., Smetacek, V. and Steffen, W., 2000. The global carbon cycle: A test of our knowledge of earth as a system. *Science*, 290: 291-296.

Feliatra, F. and Bianchi, M., 1993. Rates of nitrification and carbon uptake in the Rhone river plume (Northwestern Mediterranean Sea). *Microbial Ecology*, 26: 21-28.

Firth, J. R. and Edwards, C., 2000. Denitrification by indigenous microbial populations of river water measured using membrane inlet mass spectrometry. *Journal of Applied Microbiology*, 89: 123-129.

Firestone, M. K., and Tiedje, J. M., 1979. Temporal change in nitrous oxide and dinitrogen from denitrification following onset of anaerobiosis. *Applied Environmental Microbiology*, 38: 673-679.

Flückiger, J., Dallenbach, A., Blunier, T., Stauffer, B., Stocker, T. F., Raynaud, D. and Barnola, J. M., 1999. Variations in atmospheric N_2O concentration during abrupt climate changes. *Science*, 285: 227-230.

Freidman, L. and Bigeleisen, J., 1950. Oxygen and nitrogen isotope effects in the decomposition of ammonium nitrate. *Journal of Chemical Physics*, 18: 1325-1331.

Galloway, J. N., Schlesinger, W. H., Levy II, H., Michaels, A. and Schnoor, J. L., 1995. Nitrogen Fixation: Anthropogenic enhancement - environmental response. *Global Biogeochemical Cycles*, 9: 235-252.

Goering, J. J., 1968. Denitrification in the oxygen minimum layer of the eastern tropical Pacific Ocean. *Deep-Sea Research*, 15: 157-164.

Goreau, T. J., Kaplan, W. A., Wofsy, J. C., McElroy, M. B., Valois, F. W. and Watson, S. W., 1980. Production of NO_2^- and N_2O by nitrifying bacteria at reduced concentrations of oxygen. *Applied Environmental Microbiology*, 40: 526-532.

Gregory, D., 1973. A physical oceanographic study of the Northwest Arm of Halifax Harbour: M.Sc. thesis, Dalhousie University, 83 p.

Guerrero, M. A. and Jones, R. D., 1996a. Photoinhibition of marine nitrifying bacteria. 1. Wavelength-dependent response. *Marine Ecology Progress Series*, 141: 183-192.

Guerrero, M. A. and Jones, R. D., 1996b. Photoinhibition of marine nitrifying bacteria. 2. Dark recovery after monochromatic or polychromatic irradiation. *Marine Ecology Progress Series*, 141: 193-198.

Hansen, H. P. and Koroleff, F., 1999. Determination of nutrients. In: Grasshoff, K., Kremling, K., and Ehrhardt, M. (Editors), Methods of Seawater Analysis. Wiley-VCH, New York, pp.159-228.

Hashimoto, L. K., Kaplan, W. A., Wofsy, S. C. and McElroy, M. B., 1983. Transformations of fixed nitrogen and N_2O in the Cariaco Trench. *Deep-Sea Research*, 30: 575-590.

Hochstein, L. I., Betlach, M. and Kritikos, G., 1984. The effect of oxygen on denitrification during steady-state growth of *Paracoccus halodenitrificans*. *Archives of Microbiology*, 137: 74-78.

Horrigan, S. G., Carlucci, A. F. and Williams, P. M., 1981. Light inhibition of nitrification in sea-surface films. *Journal of Marine Research*, 39: 557-565.

Horrigan, S. G., Montoya, J. P., Nevins, J. L., McCarthy, J. J., Ducklow, H., Goericke, R. and Malone, T., 1990. Nitrogenous nutrient transformations in the spring and fall in Chesapeake Bay. *Estuarine, Coastal and Shelf Science*, 30: 369-391.

Howarth, R. W., Billen, G., Swaney, D., Townsend, A., Jarworski, N., Lajtha, K., Downing, J. A., Elmgren, R., Caraco, N., Jordan, T., Berendse, F., Freney, J., Kudeyarov, V., Murdoch, P. and Zhao-Liang, Z., 1996. Regional nitrogen budgets and riverine N & P fluxes for the drainages to the North Atlantic Ocean: Natural and human influences, In: Howarth, R. W. (Editor), Nitrogen Cycling in the North Atlantic Ocean and its Watersheds. Kluwer Academic Publishers, London, pp. 75-139.

Hynes, R. K. and Knowles, R., 1983. Inhibition of chemoautotrophic nitrification by sodium chlorate and sodium chlorite: a re-examination. *Applied and Environmental Microbiology*, 45: 1178-1182.

IPCC, 1990. Climate Change: The IPCC Scientific Assessment. Houghton, J. T., Jenkins, G. J. and Ephraums, J. J. (Editors). Cambridge University Press, Cambridge, UK .

IPCC, 2001. Climate change 2001: The scientific basis. Contribution of working group 1 to the third assessment report of the Intergovernmental Panel on Climate Change. Cambridge University Press, UK.

Iriarte, A., Daneri, G., Garcia, M. T., Purdie, D. A. and Crawford, D. W., 1991. Plankton community respiration and its relationship to chlorophyll *a* concentration in marine coastal waters. *Oceanologica Acta*, 14: 379-388.

Jensen, B. B. and Burris, R. H., 1986. N_2O as a substrate and as a competitive inhibitor of nitrogenase. *Biochemistry*, 25: 1083-1088.

Kaplan, W. A. and Wofsy, S. C., 1985. The biogeochemistry of nitrous oxide: a review. *Advances in Aquatic Microbiology*, 3: 181-206.

Karl, D. M. and Dore, J. E., 2001. Microbial ecology at sea: Sampling, subsampling and incubation experiments, In: Paul, J. H. (Editor), Methods in Microbiology. Academic Press, New York, pp. 13-39.

Kawamiya, M., Kishi, M. J., Yamanaka, Y. and Suginohara, N., 1995. An ecological-physical coupled model applied to Station Papa. *Journal of Oceanography*, 51: 635-664.

Kennish, M. J., 1997. Estuarine and Marine Pollution. CRC Press, Boca Raton, 524 pp.

Khalil, M. A. K. and Rasmussen, R. A., 1988. Nitrous oxide: trends and global mass balance over the last 3000 years. *Annals Glaciology*, 10: 73-79.

Khalil, M. A. K. and Rasmussen, R. A., 1992. The global sources of nitrous oxide. *Journal of Geophysical Research*, 97: 14651-14660.

Khalil, M. A. K., Rasmussen, R. A. and Shearer, M. J., 2002. Atmospheric nitrous oxide: patterns of global change during recent decades and centuries. *Chemosphere*, 47: 807-821.

Kim, K. R. and Craig, H., 1990. Two-isotope characterisation of N_2O in the Pacific Ocean and constraints on its origin in deep water. *Nature*, 347: 58-61.

King, D. B. and Saltzman, E. S., 1997. Removal of methyl bromide in coastal seawater: Chemical and biological rates. *Journal of Geophysical Research*, 102: 18715-18721.

Kroeze, C., 1994. Nitrous oxide and global warming. *The Science of the Total Environment*, 143: 193-209.

Kroeze, C. and Seitzinger, S. P., 1998. Nitrogen inputs to rivers, estuaries and continental shelves and related nitrous oxide emissions in 1990 and 2050: a global model. *Nutrient Cycling in Agreosystems*, 52: 195-212.

Kuypers, M. M. M., Sliekers, A. O., Lavik, G., Schmid, M., Jørgensen, B. B., Kuenen, J. G., Damsté, J. S. S., Strous, M., and Jetten, M. S. M., 2003. Anaerobic ammonium oxidation by anammox bacteria in the Black Sea. *Nature*, 422: 608-611.

Lashof, D. A. and Ahuja, D., 1990. Relative contributions of greenhouse gas emissions to the global warming. *Nature*, 344: 529-531.

Law, C. S. and Owens, N. J. P., 1990. Significant flux of atmospheric nitrous oxide from the northwest Indian Ocean. *Nature*, 346: 826-828.

Law, C. S., Rees, A. P. and Owens, N. J. P., 1992. Nitrous oxide: Estuarine sources and atmospheric flux. *Estuarine, Coastal and Shelf Science*, 35: 301-314.

Leuenberger, M. and Siegenthaler, U., 1992. Ice-age atmospheric concentration of nitrous oxide from an Antarctic ice core. *Nature*, 360: 449-451.

Li, W. K. W., Dickie, P. M. and Spry, J. A., 1998. Plankton monitoring programme in the Bedford Basin, 1991-1997, 342 pp.

Lipschultz, F., Wofsy, S. C., Ward, B. B., Codispoti, L. A., Friederich, G. and Elkins, J. W., 1990. Bacterial transformations of inorganic nitrogen in the oxygen deficient waters of the eastern tropical south Pacific Ocean. *Deep-Sea Research*, 37: 1513-1541.

Liss, P. S. and Merlivat, L., 1986. Air-sea gas exchange rates: Introduction and synthesis, In: Buat-Menard, P. (Editor), The Role of Air-Sea Exchange in Geochemical Cycling. Dordrecht: Reidel, pp.113-127.

Livingston, R. J., 2001. Eutrophication processes in coastal systems. CRC Press, Boca Raton, 327 pp.

Longhurst, A. R., 1998. Ecological geography of the sea. Academic Press, San Diego, 398 pp.

Machida, T., Nakazawa, T., Fujii, Y., Aoki, S. and Watanabe, O., 1995. Increase in the atmospheric nitrous oxide concentration during the last 250 years. *Geophysical Research Letters*, 22: 2921-2924.

McElroy, M. B. and McConnell, J. C., 1971. Nitrous oxide: A natural source of stratospheric NO. *Journal of Atmospheric Science*, 28: 1095-1098.

Miller, J. C. and Miller, J. N., 1993. Statistics for Analytical Chemistry. Ellis Horwood Limited, Chichester, UK, 233 pp.

Mitchell, M. R., 1990. The influence of local wind forcing on the low-frequency variations of chlorophyll a in a small marine basin. *Continental Shelf Research*, 11: 53-66.

Moore, R. M. and Groszko, W., 1999. Methyl iodide distribution in the ocean and fluxes to the atmosphere. *Journal of Geophysical Research-Oceans*, 104: 11163-11171.

Moore, R. M., Groszko, W. and Niven, S., 1996. Ocean-atmosphere exchange of methyl chloride: results from N.W. Atlantic and Pacific Ocean studies. *Journal of Geophysical Research*, 101: 28529-28538.

Morrison, J. M., Codispoti, L. A., Gaurin, S., Jones, B., Manghnani, V. and Zheng, Z., 1998. Seasonal variations of hydrographic and nutrient fields during the US JGOFS Arabian Sea process study. *Deep-Sea Research Part II*, 45: 2053-2101.

Müller-Nuglück, M. and Engle, H., 1961. Photoinaktivierung von Nitrobacter winogradskyi Buch. *Archives of Microbiology*, 39: 130-138.

Muzio, L. J. and Kramlich, J. C., 1988. An artifact in the measurement of N_2O from combustion sources. *Geophysical Research Letters*, 15: 1369-1372.

Muzio, L. J., Teague, M. E., Kramlich, J. C., Cole, J. A., McCarthy, J. M. and Lyon, R. K., 1989. Errors in grab sample measurements of N_2O from combustion sources. *Journal of the Air Pollution Control Association*, 39: 287-293.

Naqvi, S. W. A., Jayakumar, D. A., Narvekar, P. V., Nalk, H., Sarma, V. V. S. S., D'Souza, W., Joseph, S. and George, M. D., 2000. Increased marine production of N_2O due to intensifying anoxia on the Indian continental shelf. *Nature*, 408: 346-349.

Naqvi, S. W. A. and Noronha, R. J., 1991. Nitrous oxide in the Arabian Sea. *Deep-Sea Research*, 38: 871-890.

Naqvi, S. W. A., Yoshinari, T., Jayakumar, D. A., Altabet, M. A., Narvekar, P. V., Devol, A. H., Brandes, J. A. and Codispoti, L. A., 1998. Budgetary and biogeochemical implications of N_2O isotope signatures in the Arabian Sea. *Nature*, 394: 462-464.

Nevison, C. and Holland, E., 1997. A re-examination of the impact of anthropogenically fixed nitrogen on atmospheric N_2O and the stratospheric O_3 layer. *Journal of Geophysical Research*, 102: 25,519-25,536.

Nevison, C. D., Weiss, R. F. and Erickson III, D. J., 1995. Global oceanic emissions of nitrous oxide. *Journal of Geophysical Research*, 100: 15809-15820.

Olson, R. J., 1981a. ^{15}N tracer studies of the primary nitrite maximum. *Journal of Marine Research*, 39: 203-226.

Olson, R. J., 1981b. Differential photoinhibition of marine nitrifying bacteria: A possible mechanism for the formation of the primary nitrite maximum. *Journal of Marine Research*, 39: 227-238.

Ostrom, N. A., Russ, M. E., Popp, B., Rust, T. M. and Karl, D. M., 2000. Mechanisms of nitrous oxide production in the subtropical North Pacific based on determinations of the isotopic abundances of nitrous oxide and di-oxygen. *Global Change Science*, 2: 281-290.

Oudot, C., Andrie, C. and Montel, Y., 1990. Nitrous oxide production in the tropical Atlantic Ocean. *Deep-Sea Research*, 37: 183-202.

Owens, N. J. P., 1986. Estuarine nitrification: A naturally occurring fluidised bed reaction? *Estuarine, Coastal and Shelf Science*, 22: 31-44.

Pakulski, J. D., Benner, R., Amon, R., Eadie, B. and Whitledge, T., 1995. Community metabolism and nutrient cycling in the Mississippi River plume - Evidence for intense nitrification at intermediate salinities. *Marine Ecology Progress Series*, 117: 207-218.

Parsons, T. R., Maita, Y. and Lalli, C. M., 1984. A manual of chemical and biological methods for seawater analysis. Pergamon Press, Oxford, 173 pp.

Petrie, B., Topless, B. J. and Wright, D. G., 1987. Coastal upwelling and eddy development off Nova Scotia. *Journal of Geophysical Research*, 29: 979-991.

Pierotti, D. and Rasmussen, R. A., 1980. Nitrous oxide measurements in the eastern tropical Pacific Ocean. *Tellus*, 32: 56-72.

Pimentel, D., Harman, R., Pacenza, M., Pecarsky, J. and Pimentel, M., 1994. Natural resources and an optimum human population. *Population and Environment*, 15: 347-369.

Platt, T., and Conover, R. J., 1975. The ecology of St. Margarets Bay and other inlets on the Atlantic coast of Nova Scotia, In: Cameron, T. W., and Billengsley, L. W. (Editors), Energy flow-its biological dimension. Royal Society of Canada, Ottawa, pp. 249-259.

Platt, T., Conover, R. J., Loucks, R., Mann, K. H., Peer, D. L., Prakash, A. and Sameoto, D. D., 1970. Study of a eutrophicated marine basin.: FAO Technical Conference on Marine Pollution and its Effect on Living Resources and Fishing, p. 10.

Platt, T., Prakash, A. and Irwin, B., 1972. Phytoplankton nutrients and flushing of inlets on the coast of Nova Scotia. *Le Naturaliste Canadien*, 99: 253-261.

Pomeroy, L. R. and Peters, F., 1995. Limits to growth and respiration of bacterioplankton in the Gulf of Mexico. *Marine Ecology Progress Series*, 117: 259-268.

Pomeroy, L. R., Sheldon, J. E. and Sheldon, W. M., 1994. Changes in bacterial numbers and leucine assimilation during estimations of microbial respiratory rates in seawater by the precision Winkler method. *Applied Environmental Microbiology*, 60: 328-332.

Poth, M., 1986. Dinitrogen production from nitrite by a *Nitrosomonas* isolate. *Applied Environmental Microbiology*, 52: 957-959.

Prather, M., Derwent, R., Ehhalt, D., Fraser, P., Sanhueza, E. and Zhou, X., 1995. Radiative forcing of climate change, In: Houghton, J. T., Meira Filho, L. G., Callander, B. A., Harris, N., Kattenberg, A., and Maskell, K.(Editors), Climate Change 1995. The Science of Climate Change. Contribution of Working Group 1 to the Second Assessment of the Intergovernmental Panel on Climate Change. Cambridge University Press, Cambridge, UK, pp. 65-131.

Rees, A. P., Owens, N. J. P. and Upstill-Goddard, R. C., 1997. Nitrous oxide in the Bellinghausen Sea and Drake Passage. *Journal of Geophysical Research*, 102: 3383-3391.

Rivera-Ortiz, J. M. and Burris, R. H., 1975. Interactions among substrates and inhibitors of nitrogenase. *Journal of Bacteriology*, 123: 537-545.

Robertson, L. A. and Kuenen, J. G., 1991. Physiology of nitrifying and denitrifying bacteria, In: Rodgers, J. E., and Whitman, W. B. (Editors), Microbial Production and Consumption of Greenhouse Gases: Methane, Nitrogen Oxides and Halomethanes. American Society for Microbiology, Washington D.C., pp. 189-199.

Ronen, D., Magaritz, M. and Almon, E., 1988. Contaminated aquifers are a forgotten component in the global N_2O budget. *Nature*, 335: 57-59.

Rönner, U., 1983. Distribution, production and consumption of nitrous oxide in the Baltic Sea. *Geochimica et Cosmochimica Acta*, 47: 2179-2188.

Saino, T. H., Wada, E. and Hattori, A., 1983. Subsurface ammonium maximum in the northern North Pacific and the Bering Sea in summer. *Deep-Sea Research*, 30: 1157-1171.

Sandstrom, H., 1980. On the wind induced sea level changes on the Scotian Shelf. *Journal of Geophysical Research*, 85: 461-468.

Seitzinger, S. P. and Kroeze, C., 1998. Global distribution of nitrous oxide production and N inputs in freshwater and coastal marine ecosystems. *Global Biogeochemical Cycles*, 12: 93-113.

Smith, R. E. H., Harrison, W. G., Irwin, B. and Platt, T. P., 1986. Metabolism and carbon exchange in microplankton of the Grand Banks (Newfoundland). *Marine Ecology Progress Series*, 34: 171-183.

Solórzano, L., 1969. Determination of ammonia in natural waters by the phenolhypochlorite method. *Limnology and Oceanography*, 14: 799-801.

Solomon, S. and Srinivasan, J., 1995. Radiative forcing. In: Houghton, J.T., Meira Filho, L.G., Callander, B.A., Harris, N., Kattenberg, A. and Maskell, K. (Editors), Climate Change 1995. The Science of Climate Change. Contribution of Working Group 1 to the Second Assessment of the Intergovernmental Panel on Climate Change. Cambridge University Press, Cambridge, UK, pp. 108-118.

Somville, M., 1978. A method for the measurement of nitrification rates in water. *Water Research*, 12: 843-848.

Spindel, W., 1962. Nitrogen-15. In: Herber, R. H. (Editor), Inorganic Isotopic Synthesis. W A Benjamin Inc, New York, pp. 102.

Stehr, G., Böttcher, B., Dittberner, P., Rath, G. and Koops, H., 1995. The ammonia-oxidizing nitrifying population of the River Elbe estuary. *FEMS Microbiology Ecology*, 17: 177-186.

Stuven, R., Vollmer, M. and Bock, E., 1992. The impact of organic matter on nitric oxide formation by *Nitrosomonas europaea*. *Archives of Microbiology*, 158: 439-443.

Suntharalingam, P., 1997. Modeling the global oceanic nitrous oxide distribution.: Ph.D thesis, Princeton University, 236 p.

Suntharalingam, P. and Sarmiento, J. L., 1995, Modeling global air-sea N_2O fluxes: a sensitivity analysis of the gas-exchange formulation: Third International Symposium on Air-Water Gas Transfer.

Suntharalingam, P. and Sarmiento, J. L., 2000. Factors governing the oceanic nitrous oxide distribution: Simulations with an ocean general circulation model. *Global Biogeochemical Cycles*, 14: 429-454.

Tait, V. K., Gershey, R. M. and Jones, E. P., 2000. Inorganic carbon in the Labrador Sea: Estimation of the anthropogenic component. *Deep-Sea Research (Part I, Oceanographic Research Papers)*, 2: 295-308.

Tiedje, J. M., 1988. Ecology of denitrification and dissimilatory nitrate reduction to ammonium, In: Zehnder, A. J. B. (Editor), Environmental Microbiology of Anaerobes. John Wiley and Sons, New York, pp.179-244.

Tokarczyk, R. and Saltzman, E. S., 2001. Methyl bromide loss rates in surface waters of the North Atlantic Ocean, Caribbean Sea and eastern Pacific (8°N-45°N). *Journal of Geophysical Research*, 106: 9843-9851.

Tokarczyk, R., Saltzman, E. S., Moore, R. M. and Yvon-Lewis, S. A., 2003. Biological degradation of methyl chloride in coastal seawater. *Global Biogeochemical Cycles*, 17.

Upstill-Goddard, R. C., Barnes, J. and Owens, N. J. P., 1999. Nitrous oxide and methane during the 1994 SW monsoon in the Arabian Sea/northwestern Indian Ocean. *Journal of Geophysical Research*, 104: 30,067-30,084.

Upstill-Goddard, R. C., Rees, A. P. and Owens, N. J. P., 1996. Simultaneous high-precison measurements of methane and nitrous oxide in water and seawater by single-phase equilibration gas chromatography. *Deep Sea Research*, 43: 1669-1682.

Wada, E. and Hattori, A., 1972. Nitrite distribution and nitrate reduction in deep sea waters. *Deep-Sea Research*, 19: 123-132.

Wanninkhof, R., 1992. Relationship between wind speed and gas exchange over the ocean. *Journal of Geophysical Research*, 97: 7373-7382.

Ward, B. B., 1985. Light and substrate concentration relationships with marine ammonium assimilation and oxidation rates. *Marine Chemistry*, 16: 301-316.

Ward, B. B., 1987. Nitrogen transformations in the Southern California Bight. *Deep-Sea Research*, 34: 785-805.

Ward, B. B., 2000. Nitrification and the marine nitrogen cycle, In: Kirchman, D. L. (Editors), Microbial Ecology of the Ocean. Wiley-Liss, New York, pp. 427-453.

Ward, B. B. and Kilpatrick, K. A., 1990. Relationship between substrate concentration and oxidation of ammonium and methane in a stratified water column. *Continental Shelf Research*, 10: 1193-1208.

Ward, B. B., Olson, R. J. and Perry, M. J., 1982. Microbial nitrification rates in the primary nitrite maximum off Southern California. *Deep-Sea Research*, 29: 247-255.

Ward, B. B., Talbot, M. C., and Perry, M. J., 1984. Contributions of phytoplankton and nitrifying bacteria to ammonium and nitrite dynamics in coastal waters. *Continental Shelf Research*, 3: 383-398.

Ward, B. B. and Zafiriou, O. C., 1988. Nitrification and nitric oxide in the oxygen minimum of the eastern tropical North Pacific. *Deep-Sea Research*, 35: 1127-1142.

Weiss, R. F., 1978. Nitrous oxide in the surface water and marine atmosphere of the North Atlantic and Indian Oceans. *EOS, Transactions of the American Geophysical Union*, 59: 1101-1102.

Weiss, R. F. and Price, B. A., 1980. Nitrous oxide solubility in water and seawater. *Marine Chemistry*, 8: 347-359.

Williams, P. J., 1984. A review of measurements of respiration rates of marine plankton populations, In: Hobbie, J. E., and Williams, P. J. (Editors), Heterotrophic activity in the sea. Plenum Press, pp.357-389.

Wood, E. D., Armstrong, F. A. J. and Richards, F. A., 1967. Determination of nitrate in sea-water by cadmium-copper reduction to nitrite. *Journal of the Marine Biological Association of the United Kingdom*, 47: 23-31.

Yoshida, N., 1988. ^{15}N depleted N_2O as a product of nitrification. *Nature*, 335: 528-529.

Yoshida, N., Morimoto, H., Hirano, M., Koike, I., Matsuo, S., Wada, E., Saino, T. and Hattori, A., 1989. Nitrification rates and ^{15}N abundances of N_2O and NO_3^- in the Western North Pacific. *Nature*, 342: 895-897.

Yoshida, N. and Toyoda, S., 2000. Constraining the atmospheric N_2O budget from intramolecular site preference in N_2O isotopomers. *Nature*, 405: 330-333.

Yoshinari, T., 1976. Nitrous oxide in the sea. *Marine Chemistry*, 4: 189-202.

Yoshinari, T., Altabet, M. A., Naqvi, S. W. A., Codispoti, L., Jayakumar, A., Kuhland, M. and Devol, A., 1997. Nitrogen and oxygen isotopic composition of N_2O from suboxic waters of the eastern tropical North Pacific and the Arabian Sea - measurement by continuous-flow isotope-ratio monitoring. *Marine Chemistry*, 56: 253-264.

Zardini, D., Raynaud, D., Scharffe, D. and Seiler, W., 1989. N_2O measurements of air extracted from Antarctic ice cores: implication on atmospheric N_2O back to the last glacial-interglacial transition. *Journal of Atmospheric Chemistry*, 8: 189-201.

APPENDIX 1 - Statistical equations in Microsoft Excel

1. Linear Regression

The slope m of the regression is calculated according to the sum of least squares method

$$m = \frac{N\sum x_i y_i - \sum x_i \sum y_i}{N\sum x_i^2 - \left(\sum x_i\right)^2}$$

Where N = number of x,y data points

2. Rate Error

For each rate derived from a linear regression, the estimated error is reported as the standard deviation of the slope S_m

$$S_m = \sqrt{\frac{(S_r)^2}{S_{xx}}}$$

Where S_r is the standard deviation about the regression line

$$S_r = \sqrt{\frac{S_{yy} - m^2 S_{xx}}{N-2}}$$

S_{xx} is the sums of squares of the deviations of x from the mean x

$$S_{xx} = \sum x_i^2 - \frac{\left(\sum x_i\right)^2}{N}$$

Similarly, S_{yy} is the sum of squares of the deviations of y from the mean y

$$S_{yy} = \sum y_i^2 - \frac{\left(\sum y_i\right)^2}{N}$$

Test of zero slope coefficient

The significance of a regression is given by its p-value at the 95% confidence level. The null hypothesis is tested as P(t > t-stat), where

$$\text{t-stat} = \frac{m}{S_m}$$

and t is a t-distributed random variable with n-2 degrees of freedom, where n is the number of data points.